West Pakistan

Water and Power Development Authority

OUTLET GATES FOR TUNNELS 3 AND 4 HYDRAULIC MODEL STUDY

TARBELA DAM PROJECT
INDUS RIVER
WEST PAKISTAN

Civil Engineering Department

ENGINEERING RESEARCH CENTER

COLORADO STATE UNIVERSITY

FORT COLLINS, COLORADO

Prepared for

Tippetts-Abbett-McCarthy-Stratton

New York, New York

April 1970

CER69-70 SK28

FINAL REPORT OF THE MODEL STUDIES OF THE OUTLET GATES FOR TUNNELS 3 AND 4

TARBELA DAM PROJECT
INDUS RIVER
WEST PAKISTAN

Stratton

. Tullis

April 1970

TABLE OF CONTENTS

LIST OF FIGURES

LIST OF FIGURES - continued

LIST OF FIGURES - continued

LIST OF FIGURES - continued

LIST OF TABLES

FINAL REPORT OF THE MODEL STUDIES OF THE OUTLET GATES FOR TUNNELS 3 and 4 TARBELA DAM PROJECT, INDUS RIVER, WEST PAKISTAN

SUMMARY

Hydraulic model studies of the radial gate and appurtenant works for tunnels 3 and 4 of the Tarbela project were performed at Colorado State University under contract with Tippetts-Abbett-McCarthy-Stratton of New York. The radial gates in size and operational detail establish many new precedents in hydraulic equipment practice.

There are two radial gates each at the ends of tunnels 3 and 4 to regulate irrigation releases. The gates may be set at any required opening between closed and nominally half-open positions. The heads against the gate may vary from 183 feet at low reservoir level to 433 feet at full reservoir. With these large heads, standard seals for radial gates located on the edge of the skin plate would be inadequate; therefore, caisson-type seals were placed on the face of the skin plate in the form of a picture frame. This arrangement of the seals made it necessary to provide a seating surface at the tunnel portal. The seating surface along the bottom was made possible by a step in the floor; the seating surface along the sides necessitated recesses in the side walls; and the seating surface for the top seal was cylindrical in shape, extending from elevations 1129 to 1146. The side and bottom seating surfaces created questions on how to treat certain structural and geometric details so that large-velocity flows could be discharged efficiently.

The major modification resulting from this study was to the geometry of the side walls of the gate structure. The modification consisted of replacing the original curved triangular side-wall recesses with straight wall offsets displaced 16 inches laterally from the transition side walls. With the addition of side-wall deflectors, the entire outlet works is hydraulically satisfactory for all conditions of flow. Other details are discussed in this report.

I. INTRODUCTION

Tarbela Dam Project - General Description

Although complete and comprehensive descriptions of the Tarbela Dam project may be found in other reports (cf. Ref. 1), a brief description of the project follows. The purpose of the project description is to provide reference background for the reader. The entire Tarbela project, in many aspects, establishes new precedents for hydraulic structures and hydromachinery in terms of size, capacity, and operational details.

The dam, shown in figure 1, is an earth embankment across the Indus River valley with a crest length of approximately 9,000 feet and a height of about 450 feet. Two auxiliary embankment dams complete the closure of the upstream end of the side valley. Two saddle spillways cut through the left bank, discharge into a side valley and back again into the main river.

Tarbela reservoir will have an ultimate gross acre-feet storage capacity of 11.1 millions (MAF) with reservoir elevation at 1550 feet, and a capacity of 1.8 MAF at maximum drawdown to elevation 1300 ft. This leaves a net usable capacity of 9.3 MAF. The Indus River at the site of the project has an annual average unregulated flow of 64 MAF.

The two saddle spillways will have conventional overflow crests with radial gate controls and will discharge into channels leading to the large excavated channel along the natural side valley, the Dal Darra. The joint capacity of the spillways will be about 1,400,000 cfs.

The four tunnels, each about one-half mile long, will follow curved alignments through the rock of the right abutment. The location and relative positions of the tunnels are shown with more detail in figure 2. Initially, during construction of the dam, they will serve for river diversion, and finally for power generation and irrigation releases. The four tunnels are numbered in numerical order beginning with the one closest to the river. Tunnels 1 and 2 will serve river diversion initially. Directly upon closure of these two tunnels, tunnels 3 and 4 will carry the diversion flows. After closure of tunnel 1, a manifold will be connected to the outlet which will lead

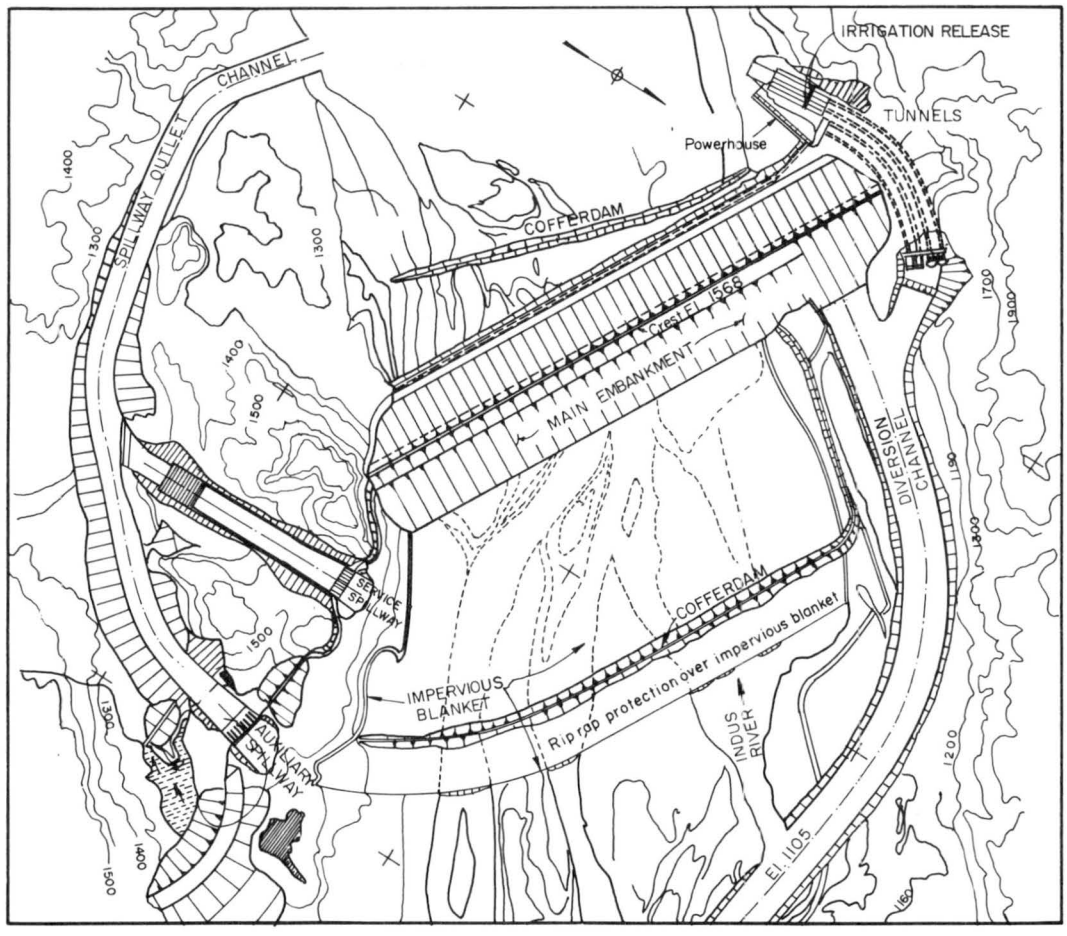

Figure 1. General plan of the Tarbela project.

to the first four power generation units. As need for more electrical power arises, tunnel 2 will also be connected to four additional turbine-generator units. Tunnels 3 and 4 will be regulated by the subject radial gates at the outlet during both diversion and irrigation releases. Each tunnel will terminate with a bifurcation leading to passages 24 feet high and 16 feet wide. The radial gates will be placed at the terminals of these passages. This report is concerned with the hydraulic effect on the operational and certain structural details associated with these gates. Ultimately, tunnel 3 is scheduled to be converted to serve four additional units for power generation, making up, in total, 12 units capable of developing 2,100 MW.

The tunnels are circular in cross-sectional shape, and vary somewhat in diameter. Tunnels 1, 2, and 3 are 45 feet in diameter upstream from approximately centrally located service gates and 43.5 feet in diameter downstream. Tunnel 4 is 45 feet in diameter upstream and 36 feet in diameter downstream from the gates.

With full reservoir at elevation 1550 feet, the maximum discharge expected through one side of the bifurcation of tunnel 3 is about 54,000 cfs. At minimum reservoir elevation of 1300 feet, the discharge will be 34,500 cfs. Discharges through the gates of tunnel 4 will be approximately 5 percent less because of the smaller size tunnel. Both gates of each tunnel will discharge into a common stilling basin (i.e., a separate stilling basin for each tunnel) and because of this, simultaneous, symmetrical operation of the gates will normally prevail. Another pertinent reason for insisting on simultaneous, symmetrical gate operation is to prevent cavitation at the bifurcation and unsymmetrical pressure forces on the splitter wall of the bifurcation.

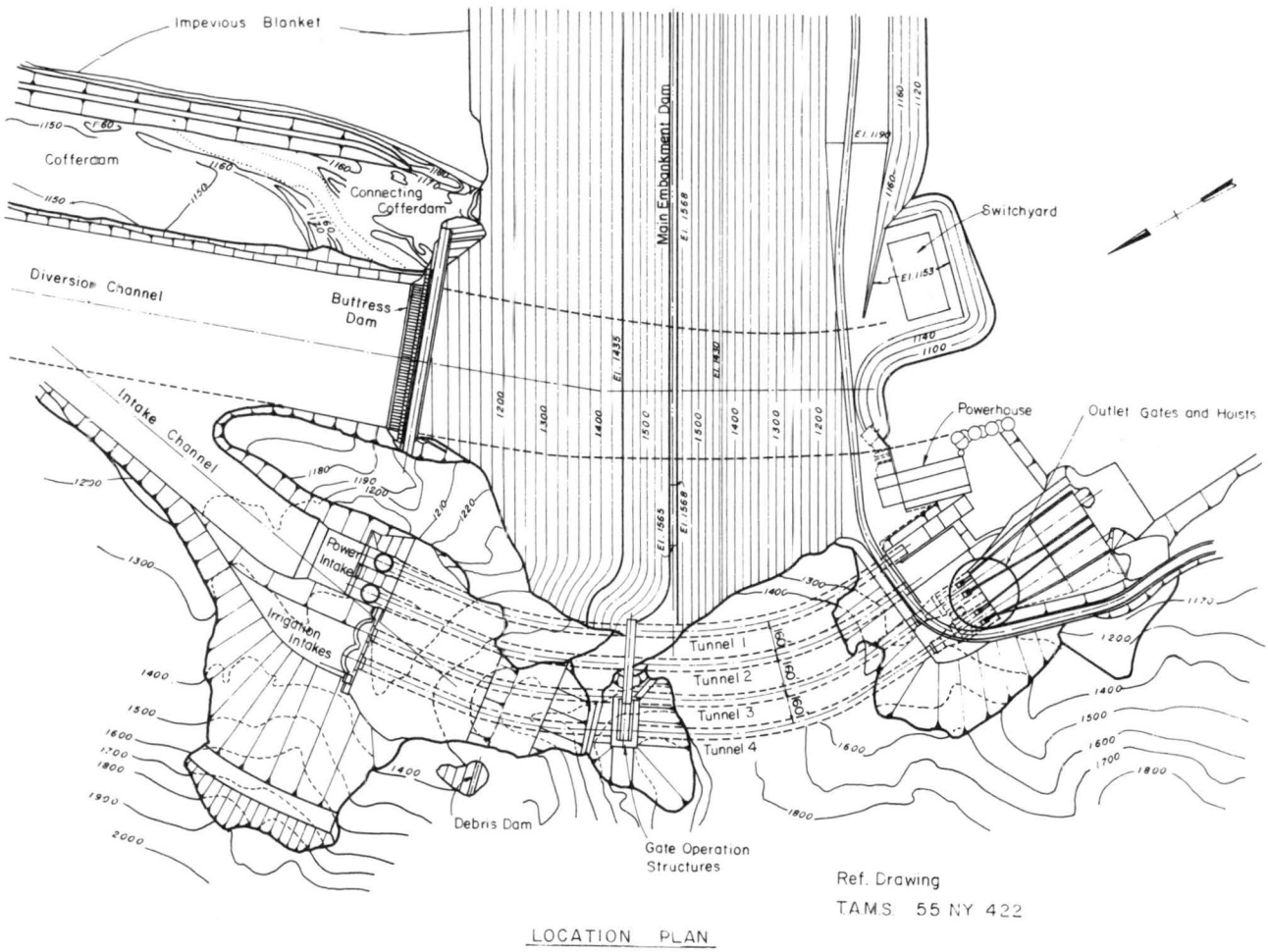

LOCATION PLAN

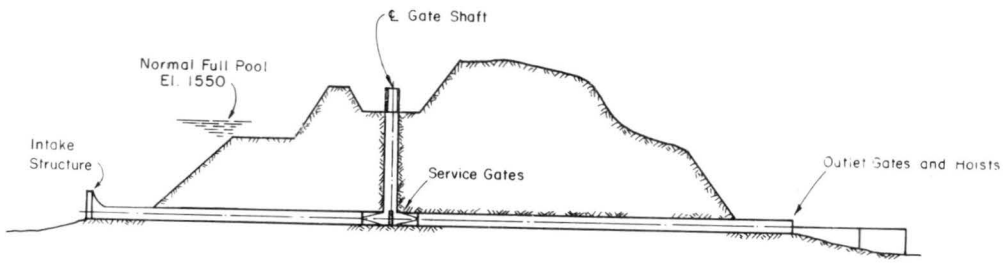

TUNNEL 4 PROFILE

TUNNEL 3 SIMILAR

Not to scale

Figure 2. Tunnels and outlet works.

Radial Gates - Design Features

The choice of radial gates at the outlets of tunnels 3 and 4 was dictated by the need to regulate a large range of discharges. The heads under which the gates would normally operate are large. Based upon the maximum and minimum reservoir elevations, static heads on the gate would be about 433 and 183 feet, respectively, measured from the centerline of the conduit. Wheel gates were considered unsatisfactory because vibrations could result at partial openings. Designing appropriate seals for wheel-type gates is also a major problem in that the gates must be sufficiently free to slide, yet tight enough to effect a seal. Since the gates are meant to regulate irrigation releases in conjunction with power plant discharges, frequent adjustments of gate openings would be necessary.

Large valves were also considered. Certainly, the large operating heads would not be unusual for valves, but the expected silt and trash loads through the tunnels would be a problem for any practically sized valves. Also, a large number of valves would be required to pass the needed flows.

Use of radial gates will permit passage of large discharges. The arrangement of the radial gates is shown in figure 3. The major problem is with the seals on the gates. Normal seals which are placed along the perimeter of the gates for low-head installations would not be satisfactory for the high heads in the Tarbela tunnels. Therefore, the seals were placed on the upstream face of the skin plate, as shown in figure 4, and a tight seal can be effected by pressing the entire gate forward (upstream). Before the gate can be moved vertically, the pressure on the seals must be relieved by backing the gate away from the seats (downstream motion). This upstream-downstream motion of the gate is accomplished by mounting the arms of the radial gates on an eccentric trunnion. Rotation of the trunnion thus causes sealing and unsealing of the gate. The force required to rotate the shaft will be applied at the end of a central lever by means of a hydraulic cylinder. Attached to the same lever will be a weight arranged to produce a constant sealing force on the gate of approximately 2,000,000 pounds in excess of the hydrodynamic force on the gate. As the hydrodynamic force

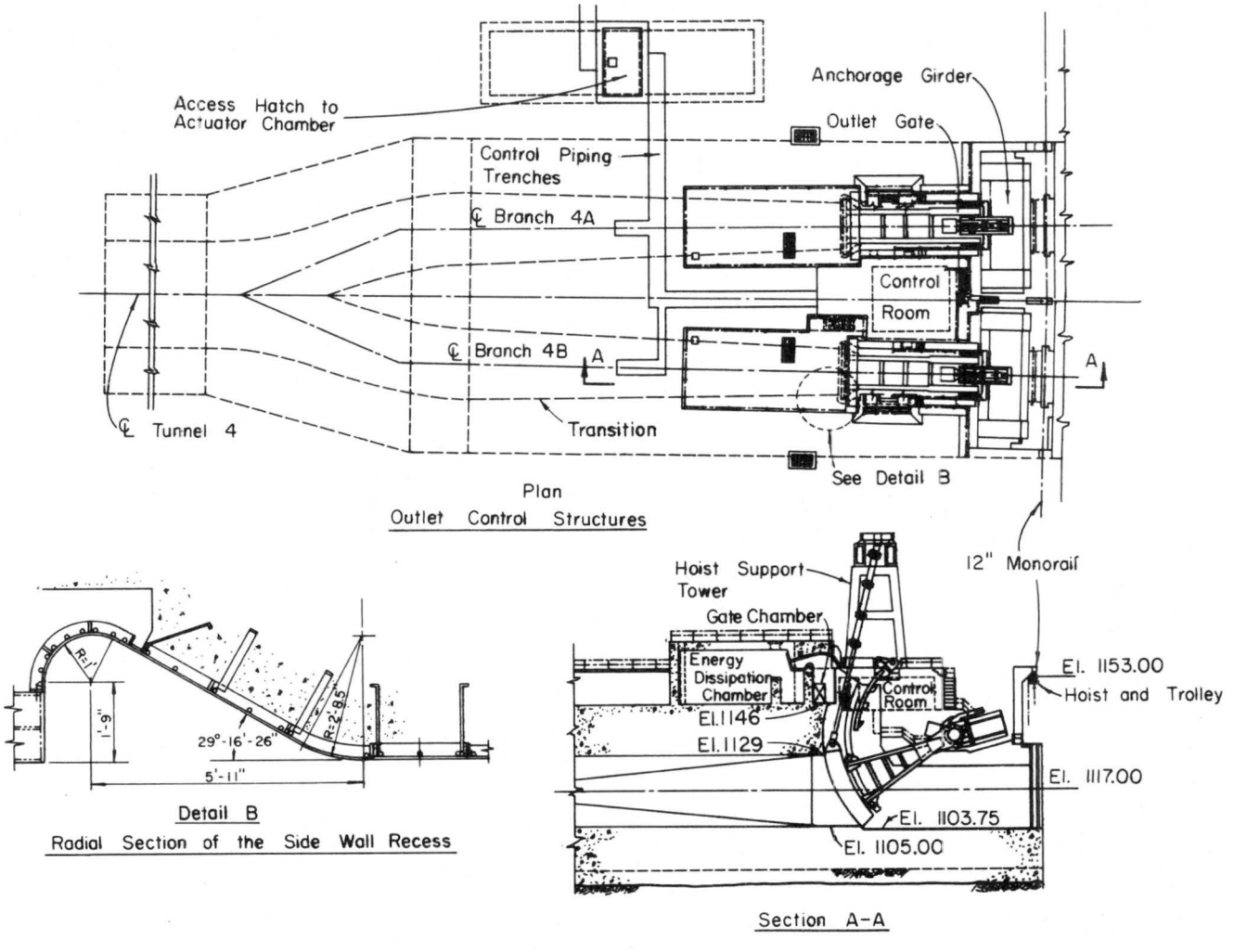

Figure 5-2 Radial gates for tunnels 3 and 4.

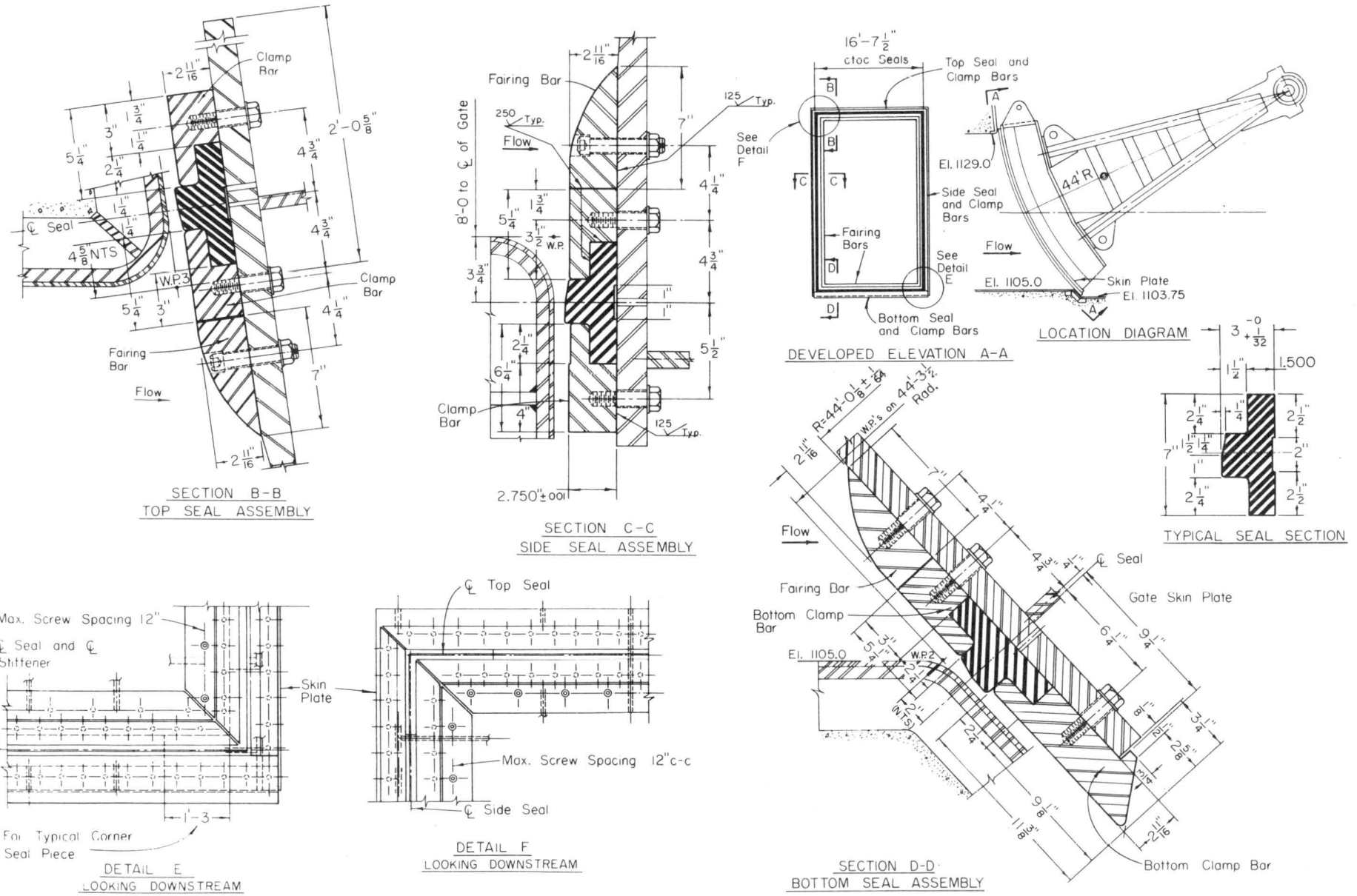

Figure 4. Radial gate seals

on the gate is directly proportional to the reservoir level, and the pressure within the tunnel, say 60 ft upstream of the gate, is proportional to reservoir level and gate opening, then, by using the pressure head in the tunnel and a differential piston to drive the hydraulic cylinder which rotates the eccentric trunnion, it is possible to arrange a constant differential sealing force.

The placement of the seals on the face of the skin plate necessitated seating surfaces which were created by recesses in the side walls, as shown in Detail B of figure 3, and a sloping step drop in the floor of the gate structure from the floor level of the transition. The seating surface for the top seal was created by a cylindrical surface extending from elevation 1129 to 1146, as shown in figure 3. This extensive top seating surface would allow the gate to be sealed at any position of the gate from closed to nominally half open. A regulatory position of the gate above half open is not planned.

There are two sets of hydraulic problems which arise from the particular placement of the seals just described. The first set of problems concerns the cavitation of the gate structure walls downstream from the recesses, the air requirement to ventilate the jet at the step in the floor and the spray in the gate structure which undoubtedly will arise because of the discontinuity in the walls at the recesses. These problems are associated with long term usage of the gates. The second set of problems arises when the gate is retracted prior to vertical movement of the gate. When the gate is retracted, under operating conditions, the gap between the seal and the seat will vary between 0.5 and 0.8 inch. The total flow through the gap can then be as large as 1010 cfs with an average velocity of about 162 feet per second. The seal clamp bars were designed to avoid cavitation with the jet discharging past the seals and to prevent extrusion of the seals under unbalanced hydraulic pressures. Provisions for the large quantities of flow past the seals are required.

The flow past the top seal can be effectively stopped by a jet arrestor along the skin plate above the top seal, as shown in figure 5. The jet arrestor is basically a flap which is thrust in contact with the cylindrical seating surface by hydraulic cylinders. They remain in contact with the seating surface even with the gate retracted and is depended upon to maintain a reasonably tight seal. To provide for gate openings greater than 12 feet (which will occur while the gate is being raised to the full-open position), an intermediate jet arrestor is provided to become effective as the upper jet arrestor rises above the seating surface at elevation 1146.

A collector-energy dissipator basin is provided as a safeguard in case wear or damage should at some time impair the effectiveness of the jet arrestor. In that event, the water jet past the top seal would be directed upward along the cylindrical seating surface. The jet will be deflected into the collector-energy dissipating basin. The water in the basin will then be piped out to a downstream point beyond the gate structure. When the gate opening exceeds 14 feet, the top seal will clear the cylindrical seating surface and the jet thickness would increase to about 3 inches. The pressure in the tunnel will be less because of the larger discharge and the jet will not reach the deflector but will flow into the chamber above and the water will flow over and around the portion of the gate extending above elevation 1146.

In the original design, water flow past the side seals is redirected back into the channel by the virtual shape of the recesses. It was planned that some arrangement of baffles mounted on the radial gate arms would direct the flow downstream in line with the channel.

Variations in the width of the gap at the side seals and consequent variations in the thickness of the jet could occur because of imperfections of fabrication and erection or because of temperature shrinkage or expansion of the steel members of the radial gate. Nonuniformity in the jets could cause sidewise loads on the radial gate with the possibility of setting up vibrations. To provide for this possibility, hydraulically operated rams or dashpots will be located on both the upper and lower arms of the gate on both sides and will thrust against the channel walls with sufficient force to deter any sidewise motion.

The gate hoist for vertical movement will be a hydraulic cylinder (oil as the fluid) of approximately 28 ft-stroke and 25 in.-bore. The raising speed will be about one foot per minute and the closure speed will be about 5 feet per minute. The length of the hoist cylinder will permit the gate to be raised to the full-open position in continuous motion. To raise the gate to higher positions for maintenance purposes, it will be necessary to disconnect the hoist and reconnect it to a bracket on the upstream face of the skin plate. Dogging supports are provided on both gate arms with latches to support the gate during the change of hoist positions.

These radial gates of the Tarbela project establish new precedents of combined size and head and require new concepts in design and operation. Many more interesting details are described in the design report (Ref. 1). The foregoing brief description has provided some of the essential details which sets the background for the hydraulic study described in this report.

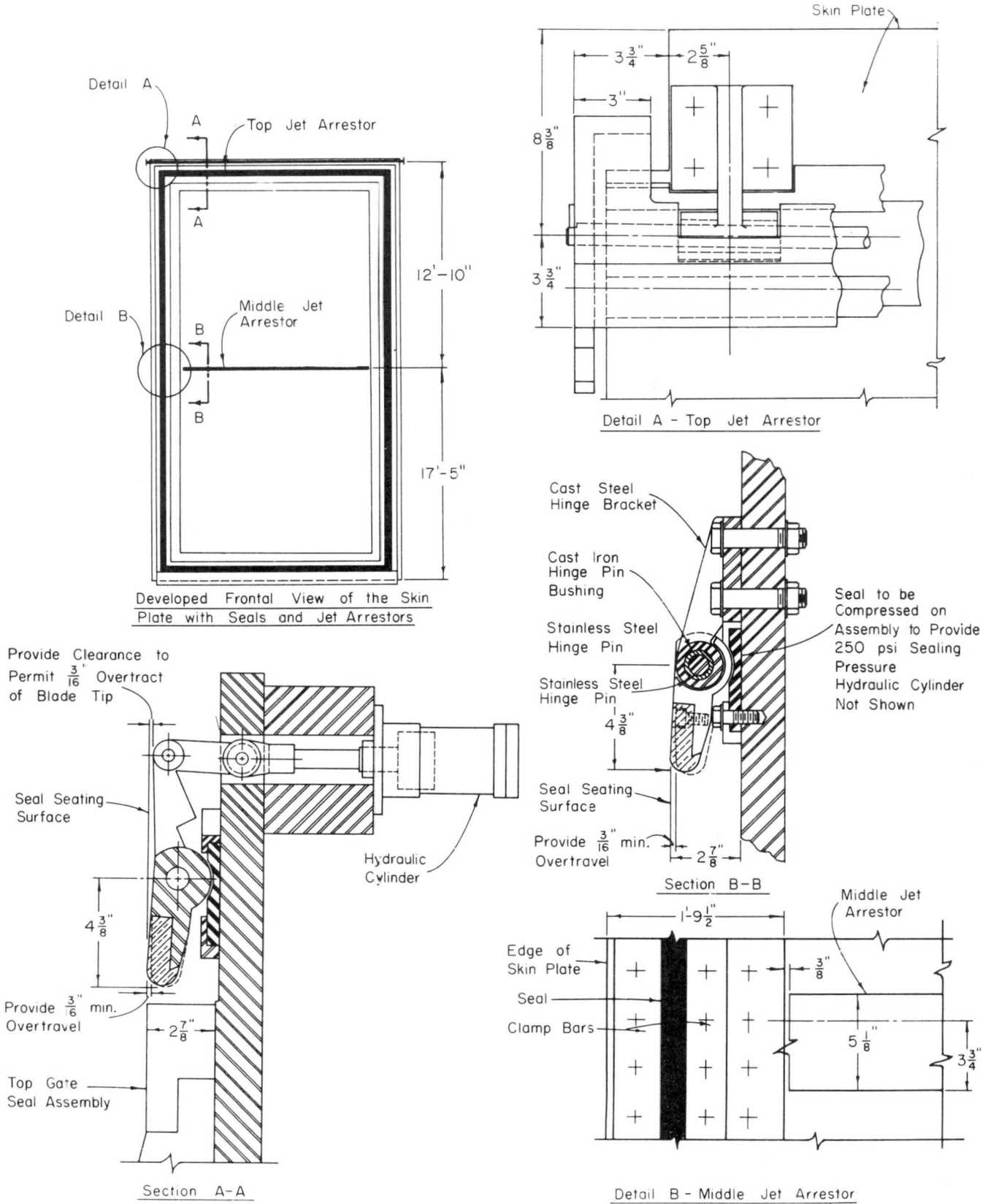

Figure 5.4 Jet arrestors on the radial gates.

Scope of the Model Study

A number of problems arise in the design of the gates which cannot be solved analytically with satisfactory confidence. The majority of these relate to the hydraulics of the flow under the gate and through the gap between the seal and seat when the gate is retracted. Specific questions which the model studies were designed to answer can be listed as follows:

(a) With the large-velocity flow past the seals, are the provisions adequate to prevent cavitation?

(b) Will the deflector hood at elevation 1158 intercept the jet issuing from the top seal and direct it into the collector-dissipator basin in case of failure of the jet arrestors to function as intended, and is the basin adequate in size and arrangement to dissipate the energy?

(c) Are pressures in the vicinity of the sidewall recesses above the cavitation range under all conditions of operation?

(d) What provisions need to be made to contain the jets from the side seals within the waterway channel?

(e) In the event that the original design of the gate recesses requires modification, what arrangement is satisfactory in terms of the hydraulics of the flow?

(f) Are corrections necessary in the assumed pressure distribution used for computing the hydraulic load on the gate?

(g) What is the coefficient of discharge at each gate opening?

(h) What ventilation arrangement is needed at the step in the floor?

To answer these questions, three models of different scales were utilized. One was a model with a geometric scale of 1:4, model to prototype, designed to investigate details of the flow past the top seal and into the collector-dissipator basin. This model was also used to observe the flow past the side seals and side wall recesses. The model was a two-dimensional representation of a 36-in. prototype length of the seal and skin plate and is referred herein as the sectional model. The second was a geometric scale model of 1:12 which included the entire gate, upstream transition, and a portion of the downstream channel chute to the stilling basin. The third was a 1:70 scale model of the transition and gate structure which was used to provide qualitative answers related to the effectiveness of changes in the geometry of the side wall recesses.

II. SECTIONAL MODEL

Similitude

In order to relate phenomena observed on the model to the prototype, it is necessary to know the appropriate scale relationships. There are four important events related to the sectional models and these are: cavitation, friction losses, air entrainment and jet dispersion. To reproduce the cavitation characteristics of the prototype in the model, the piezometric heads must be identical for model and prototype. In this way the cavitation numbers will be the same. In the sectional models we are concerned, not so much with the cavitation characteristics as with cavitation potential, with the aim of improving geometric features to avoid or eliminate cavitation. Therefore, if the model is operated at large heads, regions of significant low pressure can be identified. The effects of fluid friction and turbulence relate with the Reynolds number. If the same fluid is used for model and prototype, the model velocity, hence the head, must be greater than the prototype head to achieve equality of Reynolds numbers (Re). We note, however, that the drag, or friction coefficient is relatively insensitive to change in Re at large Reynolds numbers. Thus, the characteristic model Re (i.e., Reynolds number based on flow velocity and gap width) should be large. Energy losses due to fluid friction will, in general, be slightly larger in the model than the prototype when based on the Froude scale. Air entrainment depends upon the shear at the interface and turbulent intensities, hence upon the magnitude of velocity and the Reynolds number. If the velocity is large in the model, then the air entrainment will be fairly well reproduced.

In view of the foregoing, it was decided that the size of the sectional model should be as large as possible and a geometric model scale of 1:4, model to prototype, was selected for the sectional model. By using Froude number similitude, as we must to reproduce the jet trajectories, the model velocity would be one-half the prototype velocity and Re would be one-eighth of that corresponding to the prototype. Characteristic $(Re)_p$ (subscript p refers to prototype) for flow through the seal gap is of the order of 10^6. This means that in the model Re is of order 10^5, which is large enough to avoid serious scale effects.

Description of the Side Seal Model

The sectional model was constructed to reproduce two configurations, the top seal and the side seal. The side seal configuration is shown schematically in figure 6 with the seal, skin plate, and recess shown with more detail in figure 7. Photographs of the completed model are shown in figures 8 and 9. The flow past the side seal in the model is upward. Although this is not the prototype flow direction, this orientation was dopted so that the model could be readily converted for the top seal study. Because the gravitational forces are small in comparison with the inertial forces (momentum of the flow), the orientation has negligible effect on the geometry of the jet for the side seal study. Proper orientation is, however, important for the top seal configuration.

The position of the skin plate was made adjustable with respect to the seating face to permit a variable gap width between the seal and the seat from zero to 0.8 in. or more in prototype dimensions. The rubber seal of the prototype was modeled with aluminum, machined to the dimensions of the undistorted rubber seal of the prototype, because rubber or other elastic material with appropriately scaled elastic properties was not readily available.

Some extrusion of the rubber seal due to unbalanced hydraulic forces can be expected in the prototype. Excepting for small distortion in shape, this was considered to be a mechanical rather than a hydraulic problem and was adequately provided for in the design of the prototype seal clamp bars. It was not considered essential to provide an elastic seal in this model. Piezometer taps were located on the seating surface of the recess, as shown in figure 7, to measure the pressure heads mainly as a means of predicting the possibility of cavitation.

Discharge through the model was regulated by the gate valves shown in the figures, and the flow rate was determined by orifices in the line upstream of the valves. Pressure in the tunnel was measured with a gauge located in the square conduit upstream of the skin plate.

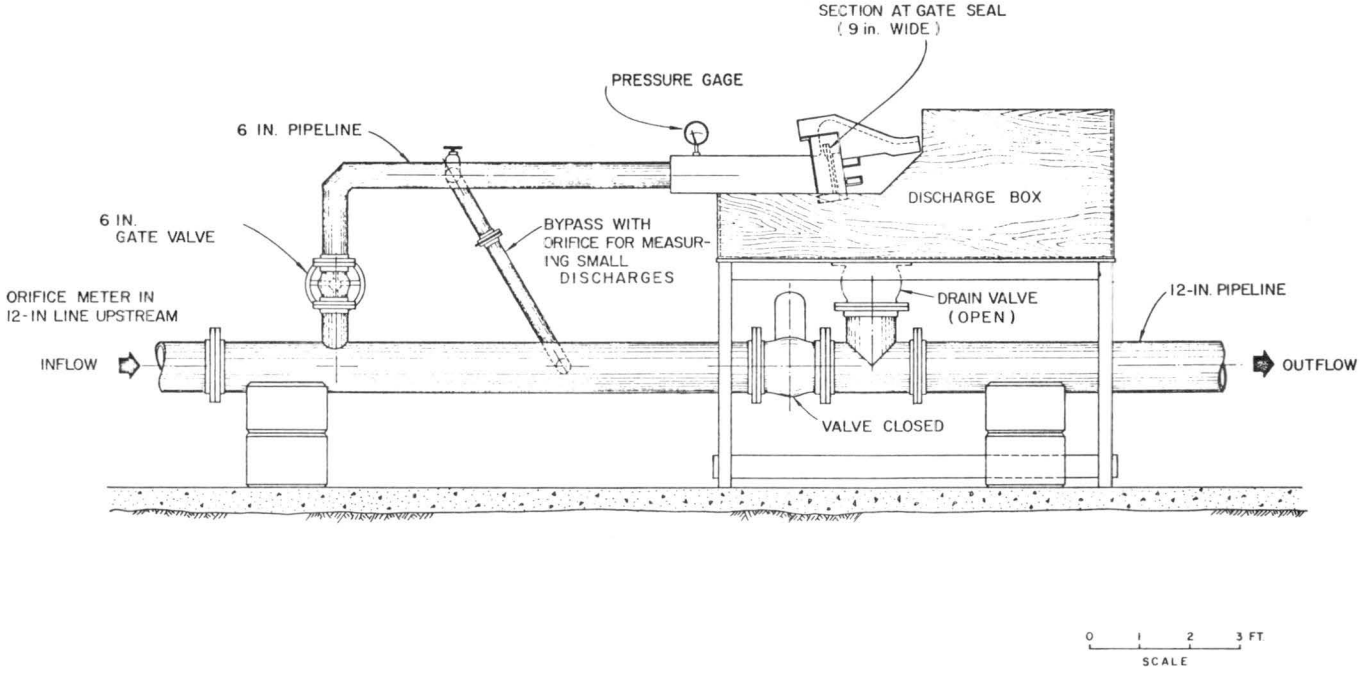

Figure 6. 1:4-scale side-seal sectional model.

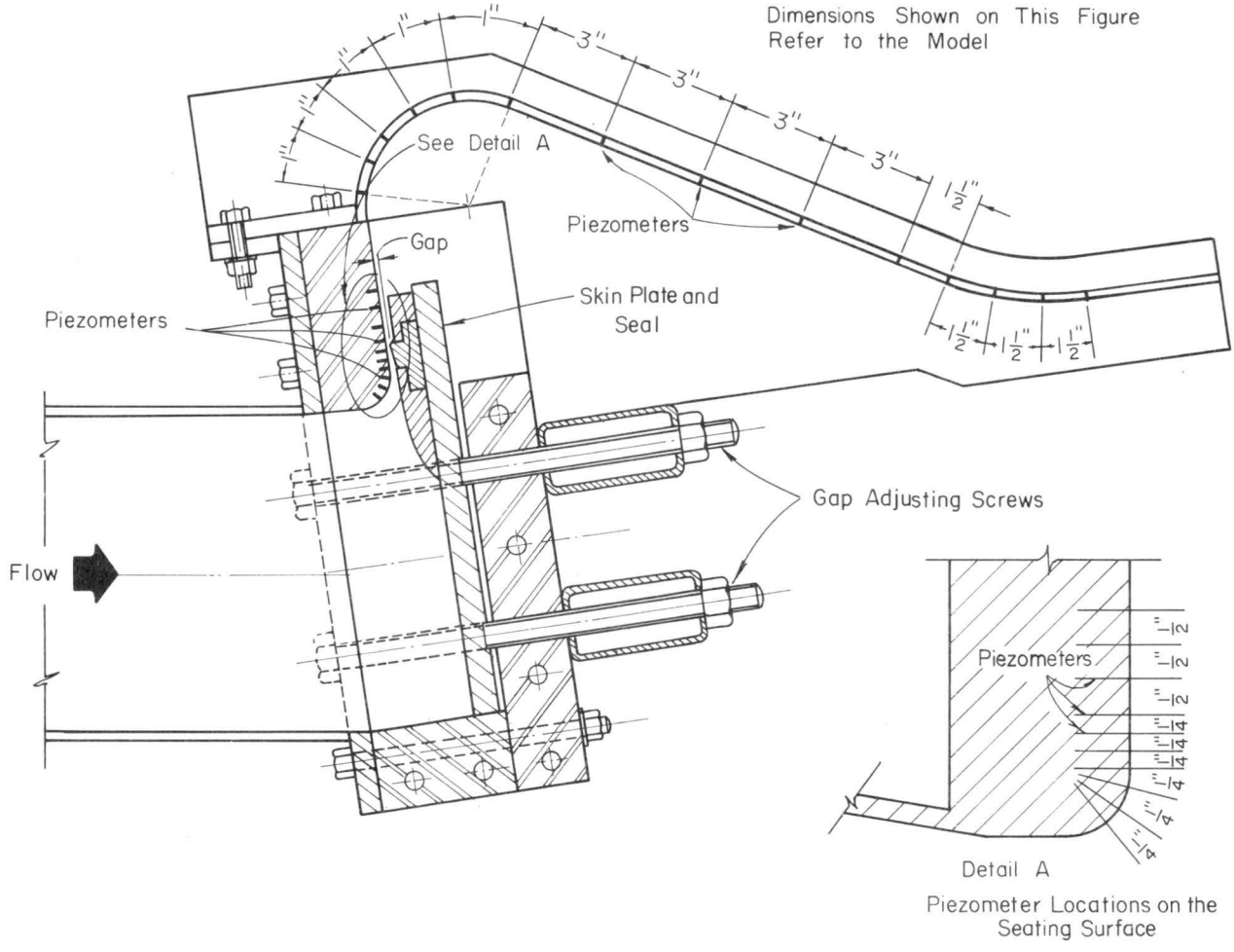

Figure 7. Details of the side-seal recess.

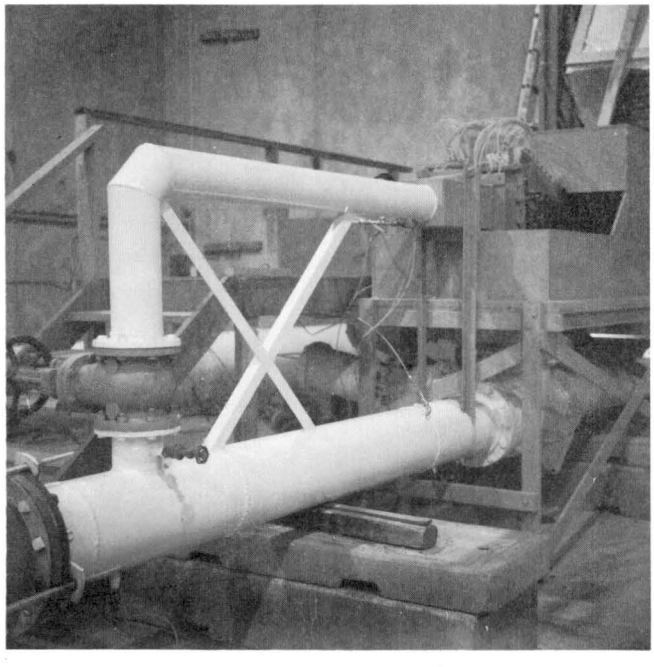

Figure 8. General arrangement for the 1:4-scale side-seal configuration.

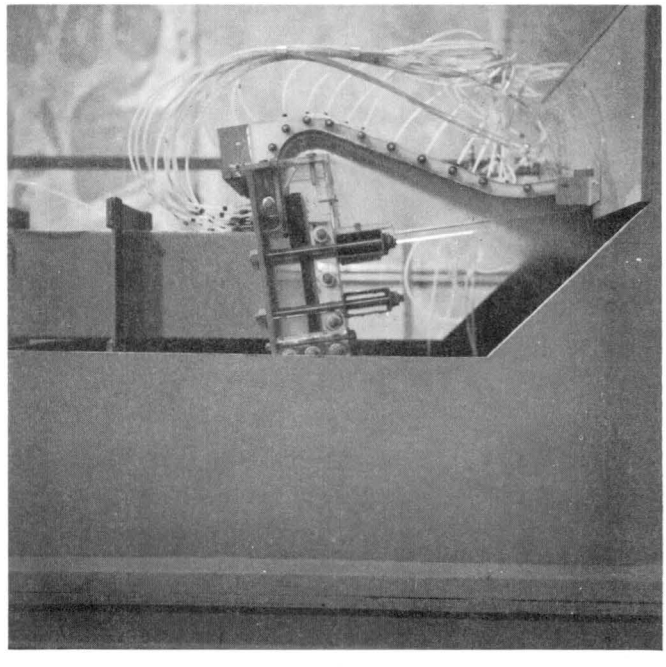

Figure 9. Details of the side-seal recess model.

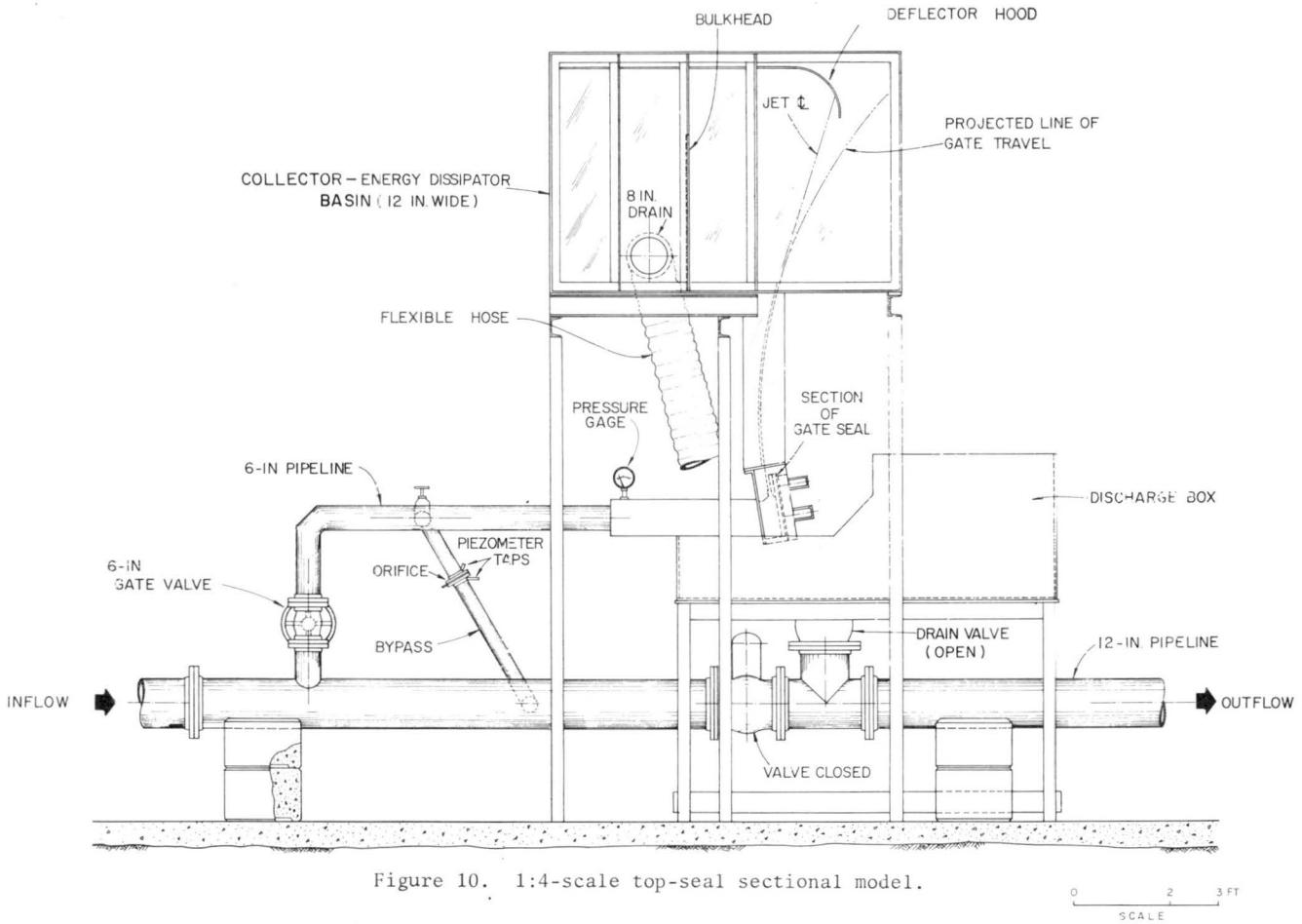

Figure 10. 1:4-scale top-seal sectional model.

Description of the Top Seal Model

The top seal sectional model is shown schematically in figure 10 with details of the seal in figure 11. The only difference in the seal detail was that the skin plate was extended to represent to scale the upper portion of the prototype skin plate. The jet arrestor was not modeled, however, as the jet would develop only if the arrestor were not in place. The cylindrical sealing surface was reproduced in the model as well as a sectional slice of the deflector hood and collector-dissipator basin. The sectional width of the sealing surface was 3 feet wide (9 inches in the model), but the hood and the collector-dissipator section was 4 feet wide to compensate for the fact that the basin and hood were wider than the gate in the prototype. The important effect, so far as this model was concerned, was that distortions on both sides of the upward jet were not introduced by frictional drag on the walls above elevation 1146. A photograph of the finished model is shown in figure 12.

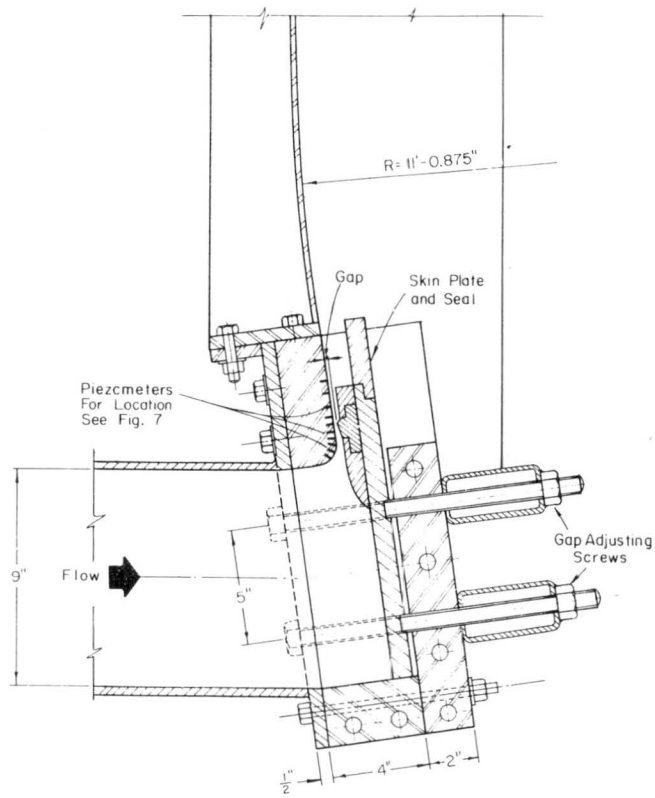

Figure 11. Detail of top-seal model.

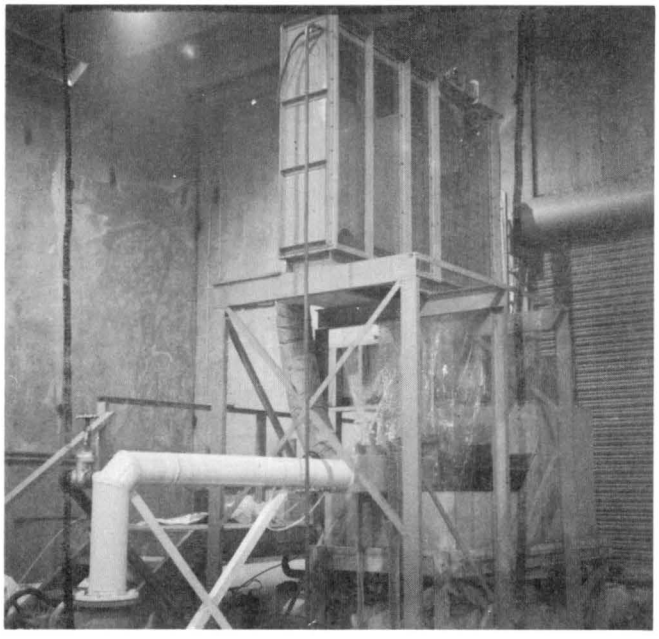

Figure 12. 1:4-scale top-seal sectional model.

Side-Seal Model Results

Two gap widths were tested in the model with steady-state flows. One gap width was 0.05 in. (representing 0.20 in. prototype) and the other was 0.2 in. (0.8 in. prototype). Head-discharge relationships for the wider gap are presented in figure 13. Different curves relate head to discharge for increasing discharge than for decreasing discharge because of the effect of jet ventilation. If the head in the tunnel is greater than, say 70 feet, and the gate is retracted, the curves in figure 13 indicate that the jet ventilated and cavitation will not occur at the seals. The momentum of the jet is sufficient to cause the jet to spring free of the skin plate and the jet becomes well ventilated. Recall that in the section on similitude we mentioned that for similarity in cavitation characteristics, the piezometric heads must be identical. This means that for all heads in the tunnel (reasonably near the portal) greater than 70 feet, there should be no problem with cavitation at the seals. If on the other hand the piezometric head should drop to less than 50 feet, cavitation might occur.

If the radial gate is closed, and retracted, the minimum head on the gate will be about 180 feet. The only possible way heads less than 70 feet can be encountered is if the gate is partially open. A check of the rating curves for the gates in the Design Report, (Ref. 1, figure 7-1), indicates that at nominal half-open position and minimum reservoir level at 1300 ft, the pressure head in the tunnel 60-ft upstream from the gate is about 155 feet. As the gate will not be held partially open above 12 feet, it seems clear that cavitation will not occur in the vicinity of the seals. Perhaps this statement could be modified in the following way: If cavitation occurs, it will occur when the gate is so nearly fully open that the head in the tunnel will be less than 50 feet. According to figure 13, however, even for this transitory (gate moving) condition the upper curve indicated as "ventilated" should apply, and therefore, cavitation should not be a problem at any time.

Pressure heads, h_p, were measured along the gate seat and are shown in non-dimensional form in figure 14. The head ratio, h_p/h_t, is plotted perpendicular to the surface at the location of the piezometer, where h_t is the total head measured in the square conduit. Piezometer locations are dimensioned on figure 7. Negative pressure heads were recorded near the downstream edge of the gate seal for the unventilated flows. When the jet was ventilated, the pressure heads increased so that only a very small negative head resulted for a total model head, h_t, of 33.4 ft. For the purpose of converting model heads to the prototype, a geometric scale of 4 may be used so that the head corresponds to about 134 ft. At larger heads it should be noted that the pressure heads were all positive.

The spread or dispersion of the jet after it leaves the seal gap and flows along the contour of the side recess is shown in figure 15. The photograph is a time exposure (relative to fluid velocity) so that the flow shown represents a maximum envelope of the spreading jet. There is very little dispersion of the jet until it leaves the P.T. of the circular curve and begins to flow along the hypotenuse of the seal recess. The measured jet profile is presented in figure 16 for a total model head of 92.8 ft and model gap width of 0.2 in. (0.8 in. prototype). The line drawn is a subjective estimate of the envelope which includes the majority of the flow. Some spray extends beyond the line. The magnitude of the spray can be judged qualitatively in figure 15. At the transition from the side recess to the vertical sidewall of the gate structure, the flow spreads considerably. Part of the flow follows the curve and the balance proceeds along the tangential direction. The pressure heads measured along the flow line are also shown on figure 16 in terms of the piezometric-to-total head ratio. Slight negative pressure heads were evident along the circular arc at the vertical side wall. Elsewhere the pressure heads were positive or zero as expected.

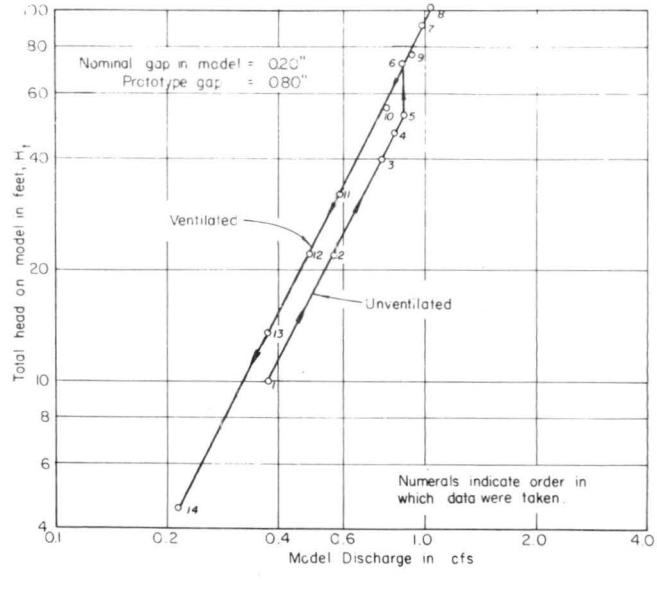

Figure 13. Effect of ventilation on discharge through the side-seal gap.

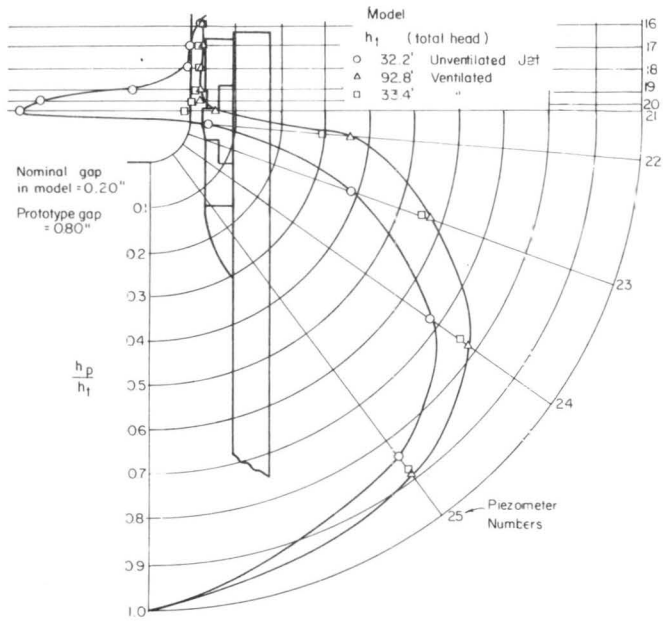

Figure 14. Effect of jet ventilation on piezometric head in the vicinity of the side-seal gap.

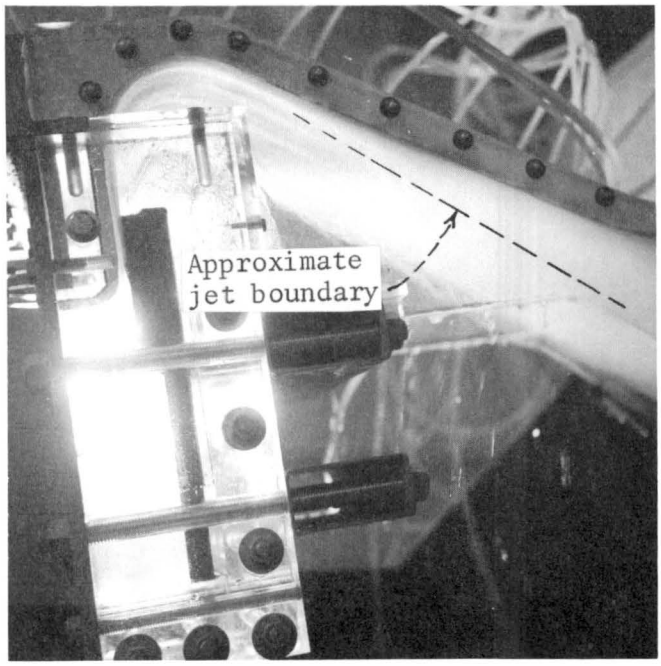

Figure 15. The dispersion of the jet through the side-seal gap at 0.8-in. gap width and 280-ft head.

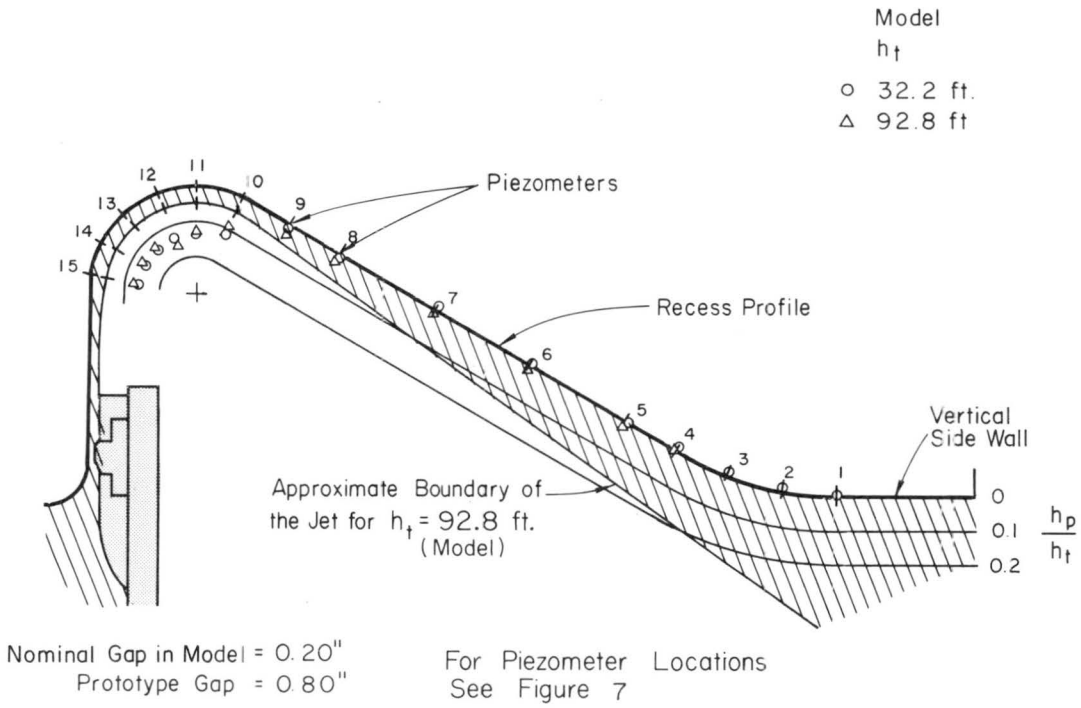

Figure 16. Piezometric head and jet profile in side-seal recess.

Ventilation of the Jet

One modification that was tested in the model was to add ventilation slots along the periphery of the outside seal clamp bar, in an effort to provide more air to the vicinity of the seal gap. The modification tested is shown in figure 17 with a photograph of the actual modification shown in figure 18. The ventilation slots did seem to improve the ventilation, and the piezometric head curve in figure 19 indicates the improvement in terms of the pressure heads at the gap. The results compare directly with figure 14. There is only a single relationship between head and discharge as the jet is always ventilated. As was previously discussed, the possibility of cavitation is remote, and the merit of this modification is therefore questionable.

Top-Seal Model Results

Flow characteristics through the top seal gap was the same as that previously described for the side seal model. The geometry was identical excepting for a short extension of the skin plate to accommodate the jet arrestor. The jet arrestor was not modeled as these tests were to simulate conditions without the jet arrestor. The extension did not affect ventilation of the jet at the seal; therefore, cavitation of the top seal should not occur.

A photograph of the jet along the cylindrical surface of the top gate seat, deflector hood and into the collector basin is shown in figure 20. The jet pictured represents a condition where the gate is closed, retracted 0.8 in. (prototype) and the head in the tunnel is 370 feet. There is little dispersion of the jet along the cylindrical seating surface. The centrifugal force assists in keeping the jet well contained. Once the jet leaves the seating surface at elevation 1146, surface drag with the air causes a small amount of spreading of the jet.

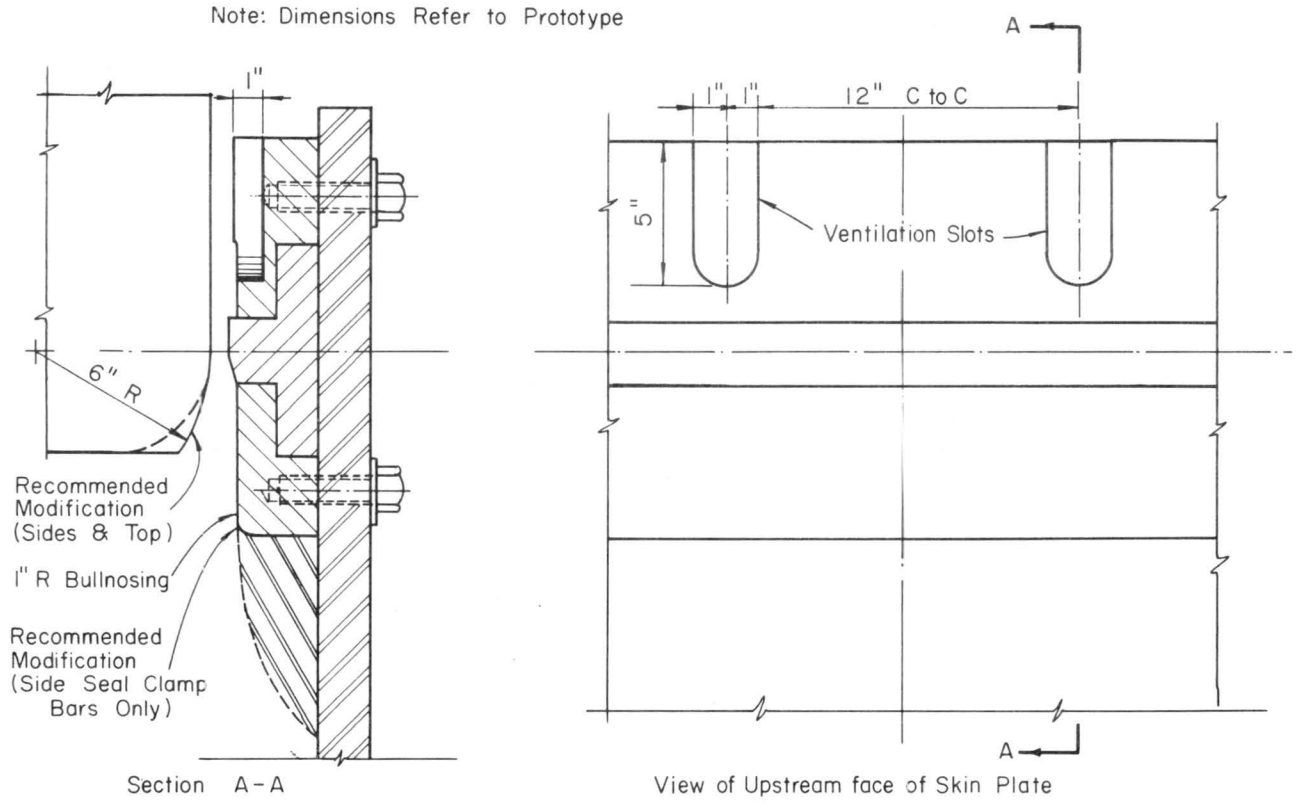

Figure 17. Proposed changes to side-seal geometry.

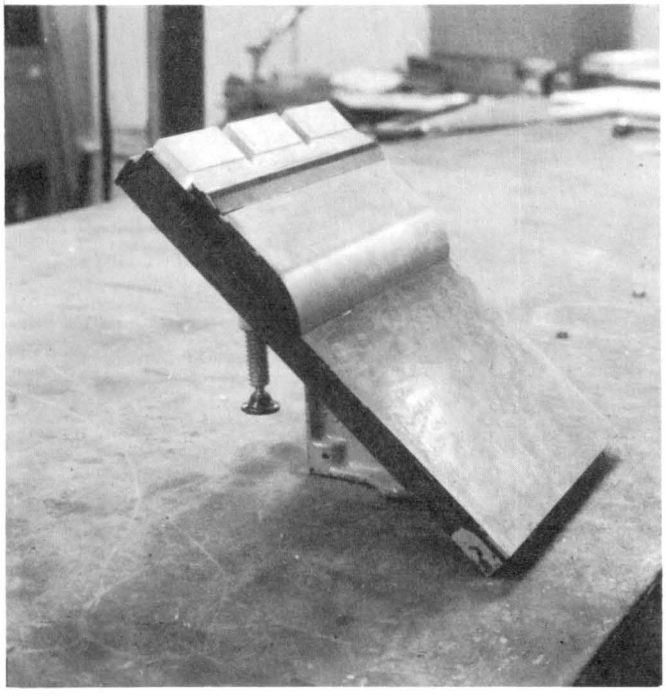

Figure 18. Ventilation slots in the seal clamp bar.

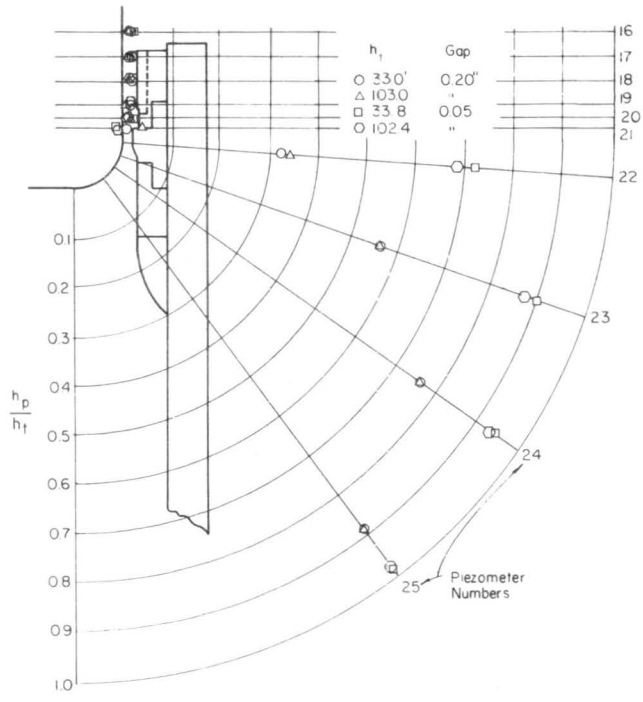

Figure 19. Piezometric heads in vicinity of side-seal gap with ventilation slots.

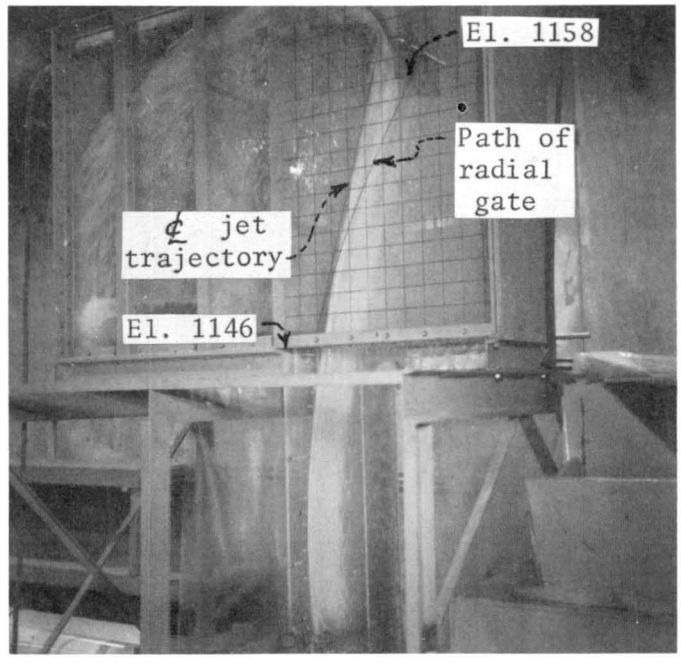

Figure 20. Top-seal sectional model with 0.8-in. gap and 370-ft head.

The deflector at elevation 1158 is very effective in directing the jet into the collector-dissipator basin. The water impinges on the end wall of the basin but this should cause no trouble to the concrete face of the prototype, especially since the duration of the flow is short. It should be noted that the length of the basin in this model was much shorter than the original design of the prototype. Whereas the original basin was designed to be about 55 feet in length, measured from the tip of the deflector, the model length corresponding to the prototype was 23 feet. There will be more discussion concerning the basin length in the discussion of the 1:12 general model results. For gap widths of 0.8 in., prototype, the deflector directs all of the flow into the basin for heads greater than 180 feet. At heads between 180 and 100 ft, part of the jet is deflected into the basin, part is deflected into the gate chamber and part of the spray is not intercepted by the deflector at all. When the head is less than 100 ft, the jet just reaches the deflector and the water falls back on itself and into the gate structure. These conditions are depicted in the photographs of figures 21 and 22.

A smaller seal gap of 0.2 in. (prototype) causes greater energy loss of the jet due to frictional drag with the air. The result is that with total head in the tunnel less than 250 ft, the deflector does not direct all the flow into the basin; and at 120 ft head, the jet barely reaches the deflector and the resulting disintegration of the jet appears similar to figures 21 and 22.

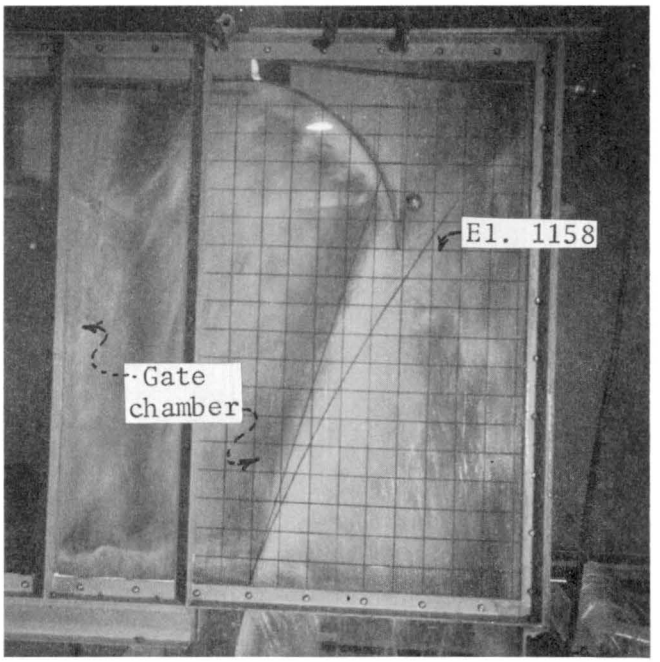

Figure 21. Gap width is 0.8 in. and H_a is 180 ft. Note that the water falls into the gate chamber and part of the jet misses the deflector.

Recommendations

It is recommended that the geometry of tne upstream edge of the gate seat be modified at the top and side seals, as shown in figure 17. This change would provide a distinct separation point for the flow through the tunnel when the gate is fully open, and will help to prevent local regions of small negative pressures around the circular arc. A second modification also shown in figure 17 is a reduction in the fairing of the inner seal clamp bar for the side seals only. Only a small amount of rounding is necessary to prevent a sharp corner and possible flow separation. The top and bottom seal clamp bars should not be altered because of the large velocities which may occur in the vicinity of the seals.

It is recommended that the length of the original collector-dissipator basin be reduced. Unless there are other reasons which may supercede the hydraulic conditions, the height of the deflector may be lowered by 3 feet to elevation 1155. Consequently, the height of the basin may be correspondingly reduced. The location of the beginning of the deflector with respect to the gate arc is satisfactory, even though some of the flow passes by the deflector at low heads. It has already been noted that circumstances for low head prevail only when the gate is being raised from one-half open to full open so the splash time should be minimal although the quantity of flow may be substantial (about 100 cfs). These comments are also tempered by the fact that the jet arrestors above the top seal and at nominal mid-position should prevent any upward spray from forming.

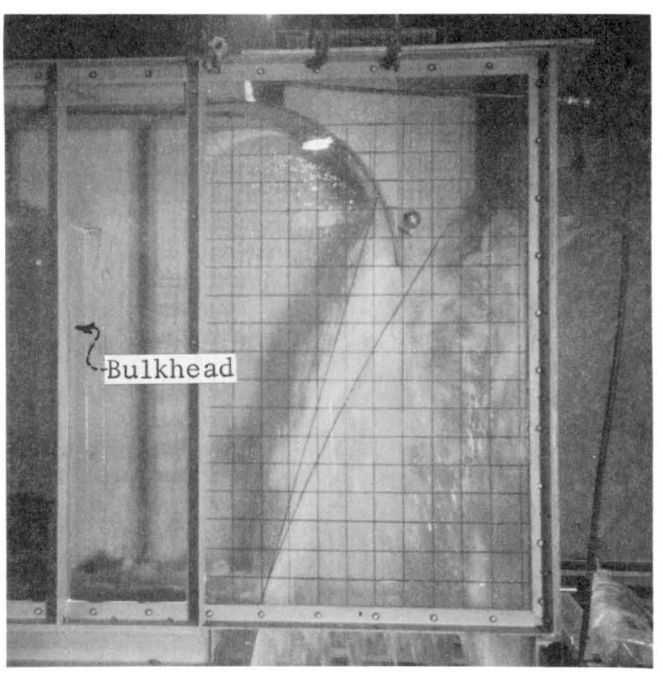

Figure 22. Gap width is 0.8 in. and H_a is 100 ft. There is no flow into the basin. The water just reaches the deflector.

III. THE RADIAL GATE MODEL

The outlet gates will be top-seal type radial gates set in the gate chambers of the outlet control structures, as shown in figure 3. The radius of each gate is 44.0 ft, measured from the trunnion to the face of the skin plate. The trunnion pin embodies an eccentric and can be rotated independently to effect an upstream-downstream (sealing and unsealing) motion of the gate at any setting. The pressure for the hydraulic system, which is used to apply torque to the eccentric trunnion pin to seat the gate, is supplied from the water within the tunnel. The location of the pressure source is nominally midway along the transition from the Y-branch to the sealing face, about 60 feet upstream of the gate face. When the hydraulic pressure is released, the gate is unseated by the hydrostatic force acting on the skin plate.

The regulation range of the gate is from closed to half-open, a vertical distance of 12 feet. Above that range, the gate will be operated only in the fully-open position.

The entire transition from the Y-branch to the seating face will be lined with steel. The gate chambers and gate structure down to the stop-log slots will also be steel lined.

Model Construction

The radial gate model was constructed to a geometric scale of 1:12, model to prototype, and includes the entire transition from the Y-branch, the gate structure and gate, and a portion of the chute leading to the stilling basin. The initial arrangement of the model included only a modest length of the chute, as shown in figure 23. Later, 66 feet of chute length was added downstream from the gate structure.

The transition for the model was constructed from ¼-inch steel plate with several steel collars at intermediate positions to maintain proper shape. Piezometric taps were located at mid-length of the transition to obtain pressure heads which relate to prototype pressures needed to operate the hydraulic system for the eccentric trunnion.

When the radial gate is retracted, a considerable quantity of flow will pass the periphery of the skin plate and will be directed against the arms of the gate. Thus, it seemed desirable to scale the dimensions of the structural members of the gate as closely as possible. The construction details of the model gate are shown in figure 24. The major difference from the prototype is that tubular 1½-in. square sections were used for the radial arms of the model instead of the 14-in. wide flange beams of the prototype.

The trunnion was machined from a 4½-in. diameter solid steel shaft. The ends of the trunnion were machined with a ¼-in. eccentricity to a diameter of 4 inches. The trunnion was supported by two 1-in. thick plates, which were bolted to the main supporting members shown in figure 23. A handle was fastened to one end of the trunnion to rotate the shaft to effect the upstream-downstream motion of the gate axis. The gate was attached to the trunnion with brackets which allowed the gate to rotate independently of the trunnion. Because of the close tolerance required in the retracting motion in this 1:12 scale model, friction bearings with thin silicon-base lubricant were used in favor of roller or ball bearings.

A ½-in. thick aluminum plate was rolled to form the skin plate. The seals were fabricated from strips of aluminum. As in the case of the sectional model, it was considered important to scale the seal gap width and the close model tolerance required for the entire gate seal precluded use of an elastic material for the seal.

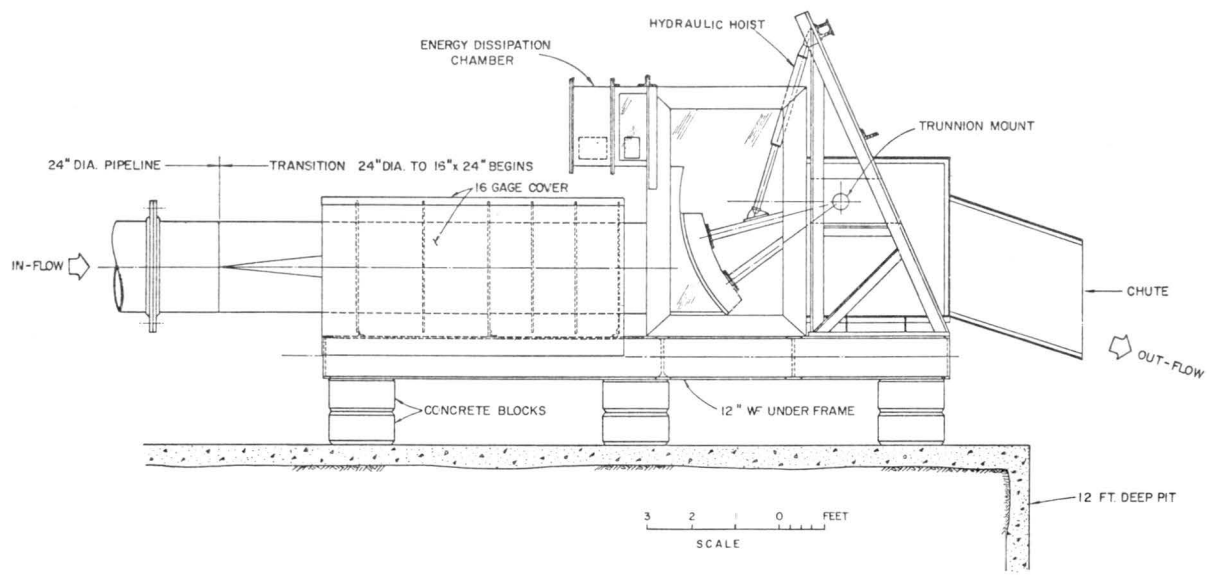

Figure 23. 1:12-scale general model of the radial gate structure and transition.

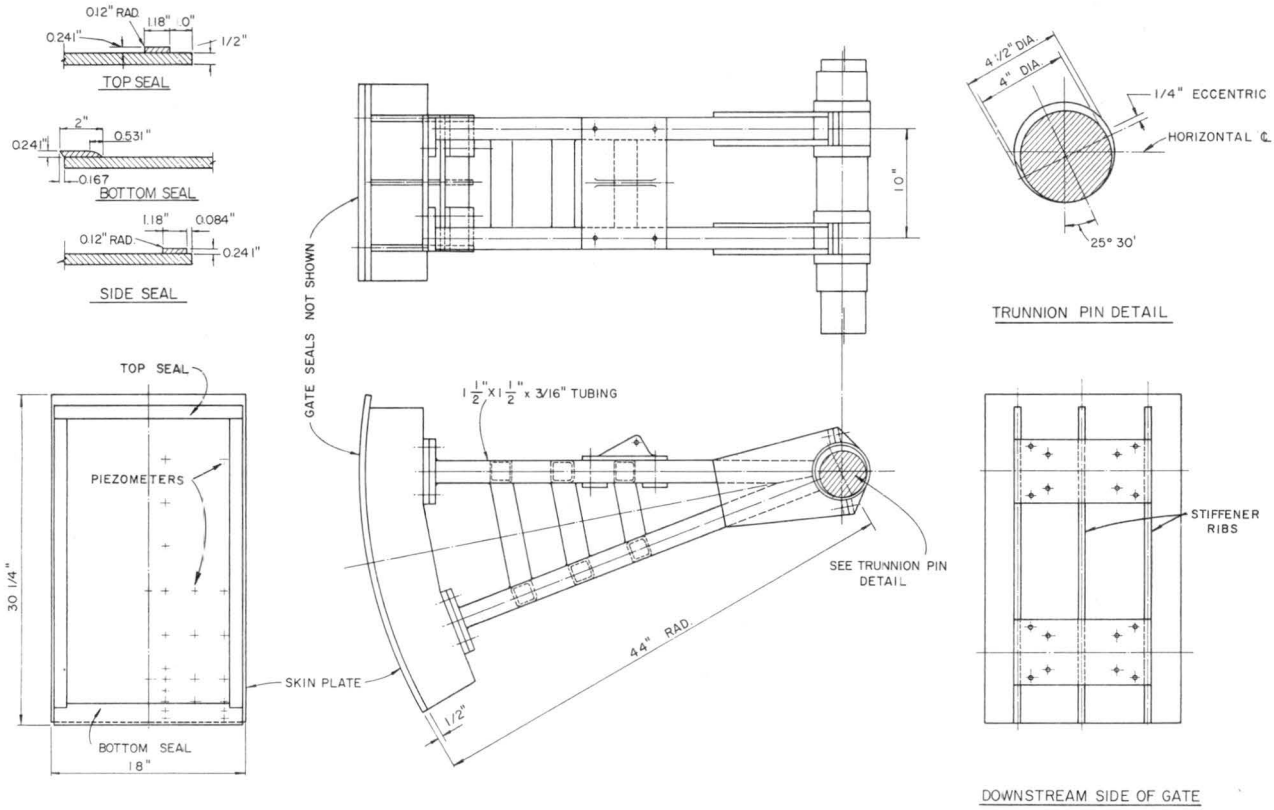

Figure 24. Details of the radial gate, 1:12 model.

An important dimension for this model was the radius from the trunnion to the surface of the seal. To obtain the necessary precision, the gate was first completely assembled and attached to the trunnion. With the trunnion in a horizontal position, the seal surfaces were then machined, using a rotary motion of the gate about the trunnion. The assembly and machining procedure is shown in figure 25. The resulting maximum variation in the radial length to the seal surface was measured to be 0.003 in.

The hoisting link for the model gate did not correspond to the prototype. The change in position of the connecting point with the hydraulic cylinder does not affect the gate in any way, and the change was made in the model to adapt to an available hydraulic cylinder. The side buffers were not included on the model gate.

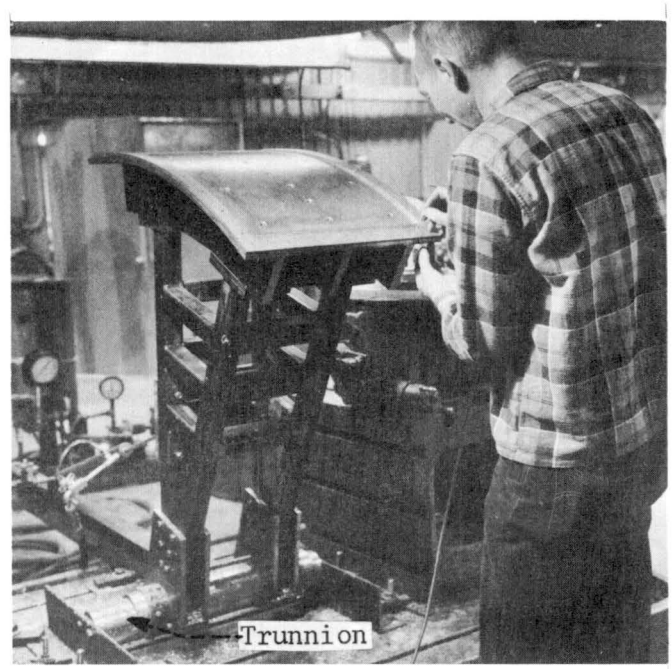

Figure 25. Machining the gate seals.

Plastic sides - It was considered extremely important, in the tests to be performed with this model, that visualization of the flow in the gate structure be possible. This required either observation windows in the sides, or plexiglas walls. Ultimately, plexiglas walls were selected. This necessitated use of 4-in. thick plexiglas to permit machining of the side wall recess.

One difficulty in machining the recess rested with the thermal expansion of the plexiglas. If the grooves were cut at normal room temperature, the radius to the gate seat would be incorrect when the plexiglas cooled to the temperature of the water during the experiments. This problem was overcome by maintaining the plexiglas at constant temperature with a flow of cold water and performing the entire machining operation under water. The machining procedure is depicted photographically in figures 26, 27, and 28. Final sanding and polishing was by hand.

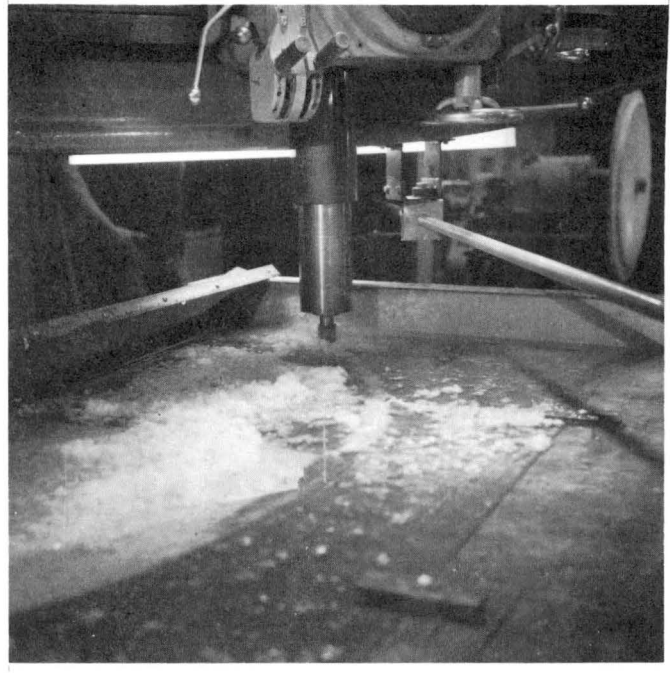

Figure 26. Milling the side-seal recess under water.

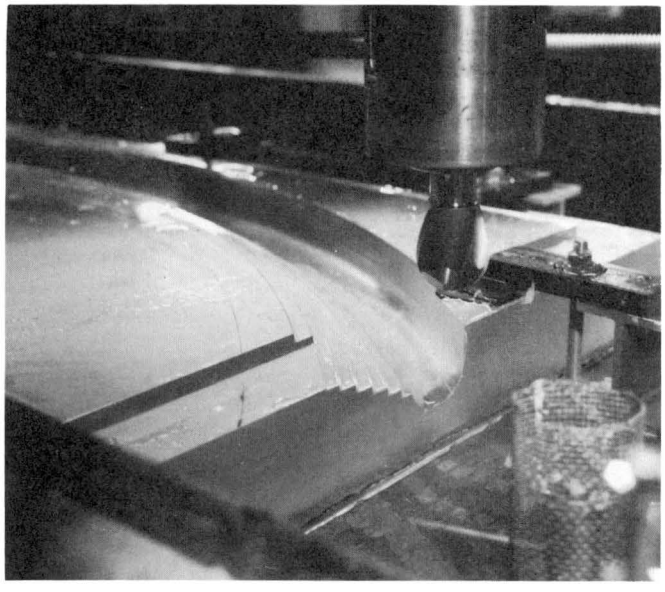

Figure 27. Milling the side seal was accomplished in steps (water drained for photography)

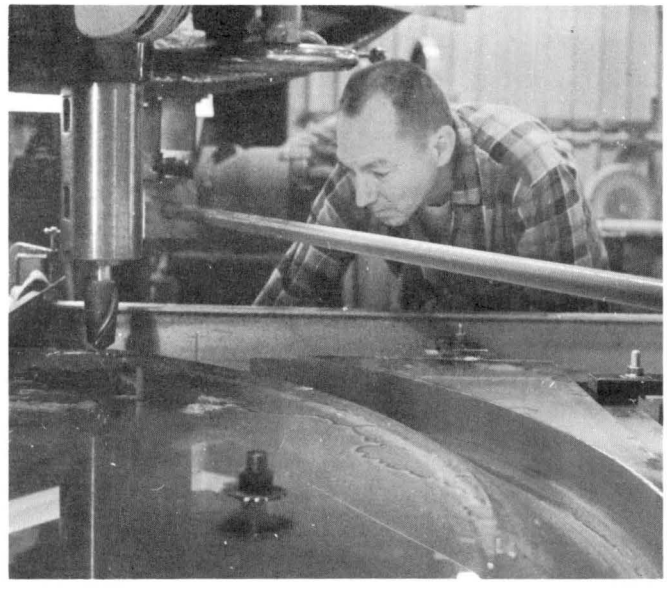

Figure 28. Final milling of the side-seal recess (water drained for photography).

Ventilation system - The bottom sealing arrangement for the gate necessitated an offset in the floor of the gate structure from the floor level of elevation 1105 of the transition to elevation 1103.75 in the gate structure. Cavitation, always suspected at such an offset, can be effectively eliminated by adequate ventilation.

The ventilation system for the model was slightly different from that suggested in the original design. The first difference was in the cross-sectional shape of the air supply conduit, which was altered for ease of machining. This difference would have no effect in determining the adequacy of the ventilation system. The second difference involved addition of an independent system of vents to the sloping face of the offset below the lower sealing surface. It was thought that at small gate openings, the downward component of flow momentum created by the curved face of the gate would prevent the jet from springing clear beyond the primary ventilation system, while ventilation may be required beneath the jet. Hereinafter, the ventilation system on the sloping surface will be referred to as the secondary system, while the one along the floor will be referred to as the primary system.

The offset ventilation systems and a section of the gate structure floor are shown in figure 29. Construction was of plexiglas, as shown in figure 30. Separate air inlets were provided to the two systems.

Collector-dissipator basin - It was discussed in Section I that jet arrestors will be placed above the top seal and at an intermediate position on the prototype gate skin plate. When these arrestors are functioning, the flow of water in the upward direction should be negligible. In the event that the arrestors should suffer even partial failure, it was considered necessary to provide a deflector to direct the upward jet into a stilling basin. Studies with the sectional model indicated that the deflector could be lowered 3 feet so that the leading edge of the deflector could be placed at elevation 1155. The length of the basin could be reduced by about one half, and a change of shape of the front wall (bulkhead) of the basin was suggested. These changes were included in the model and are shown on the drawing of figure 31.

Water supply - The radial gate model was installed in the Hydro Machinery Laboratory where large discharges and heads were available. A schematic drawing of the model arrangement is shown in figure 32. The flow system consisted of two throttling valves, a 24-in. ball valve as the upstream control, and a 20-in. butterfly valve 56 feet upstream of the transition. Downstream from the 20-in. valve, the line was expanded to 24-in. diameter pipe. The two valves in series made it possible to reduce the 90 psi supply pressure to about 10 psi while preventing serious cavitation damage to the valves. An 8-in. pressure-relief valve was installed to protect the plexiglas walls of the model from damage if large pressures were inadvertently applied.

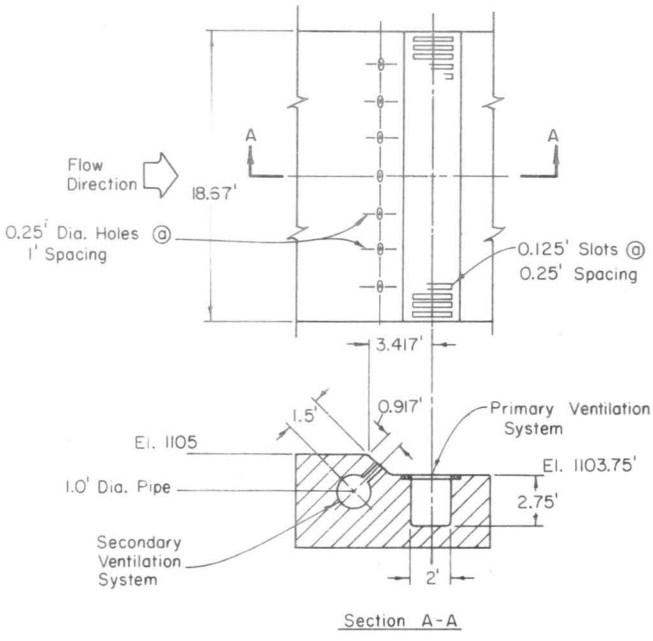

Figure 29. The offset ventilation systems.

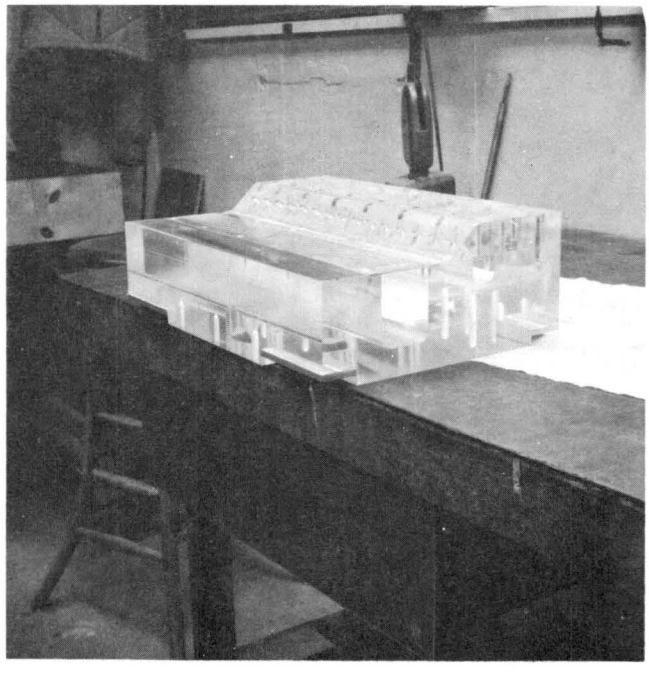

Figure 30. The step in the floor and ventilation systems were constructed from a plexiglas block.

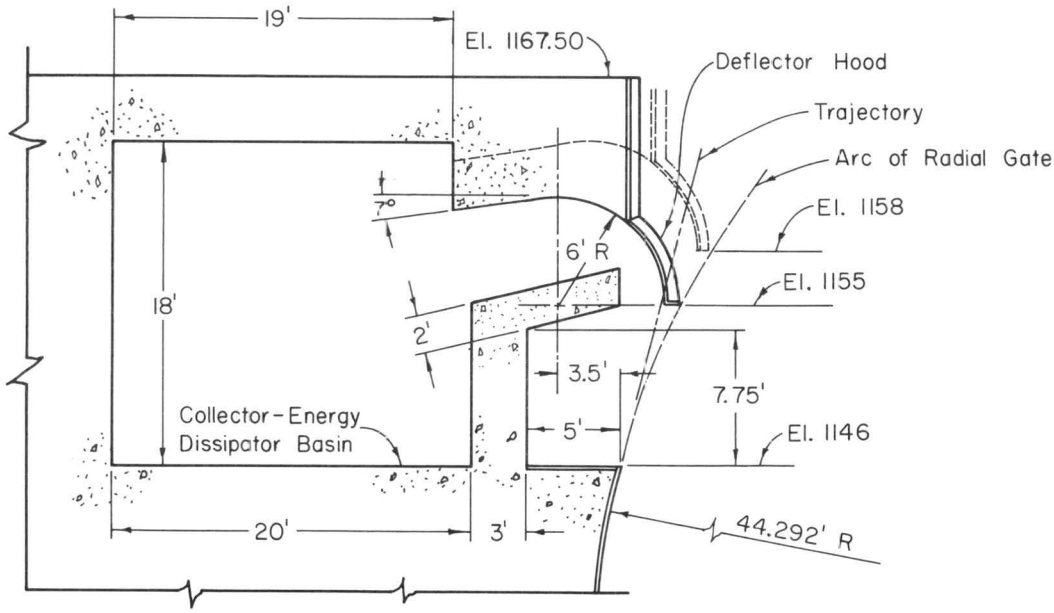

Figure 31. Sectional view of the collector-energy dissipator in the 1:12-scale model.

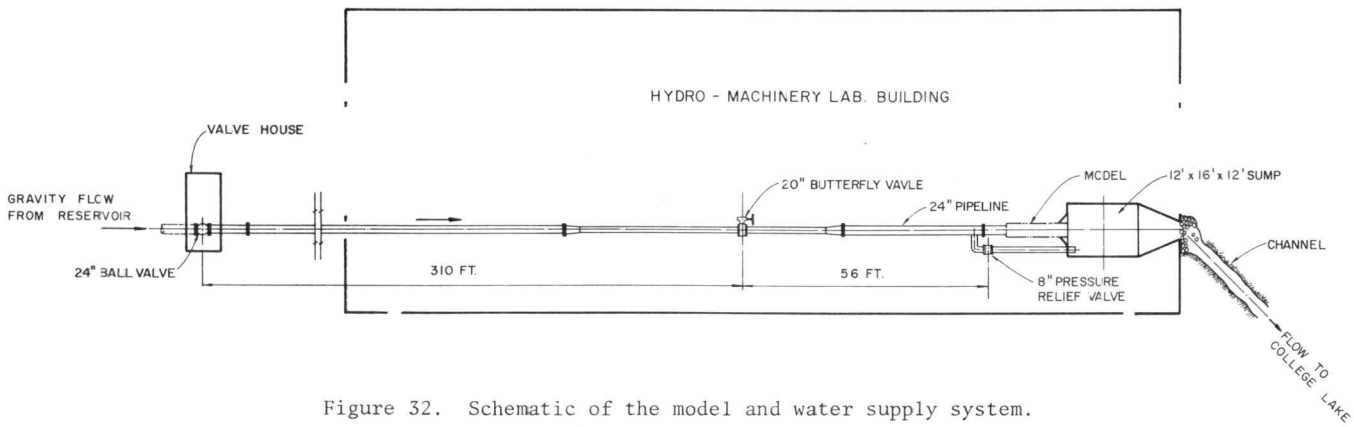

Figure 32. Schematic of the model and water supply system.

Measurement of gate movement - Seal gap width and vertical position of the gate were two important dimensions for all tests with the model. Correspondingly, tolerances in fabrication of the model were held such that gap width varied no more than ±0.005 in. from an average gap width. The gap width was calibrated with trunnion rotation with no load, then corrected for hydrostatic loading of the gate at various heads. The hydrostatic loading caused a linear downstream movement of the entire gate such that at 400 ft head, a movement of 0.025 in. (model dimension) resulted. Vertical position of the gate was determined with a point gage set on the upper cross-support of the radial arms and calibrated with a vernier height gage measuring from the floor of the transition to the bottom lip of the radial gate.

Discharge measurement - Two discharge measuring systems are available in the supply line. One an 8-in. orifice in a 12-in. line for small discharges and the other a 24-in. orifice in a 36-in. pipeline for large discharges. The pressure differential across the orifice was measured with a mercury manometer. The orifices were calibrated prior to operation of this model. Calibrations were made volumetrically in the hydraulic laboratory where the calibration system is a standard facility.

Pressure measurement - Pressure measurements, in terms of piezometric head of water, were made at 23 piezometers located on the skin plate. The piezometer locations with identifying numbers are shown in figure 33. The pressure at the midpoint in the transition was measured with a calibrated Bourdon gauge in terms of prototype feet of water. Discharge coefficients for the gate at various openings were determined with pressure heads measured at this location. The piezometers were connected by flexible tubing to a valved manifold in such a way that one pressure transducer could be used to measure all the pressures. A Pace transducer and carrier-amplifier was used. The output from the carrier-amplifier was recorded through a digital voltmeter (DVM) with a printer. Because fluctuations of pressure occurred, discrete sampling by the DVM was made at a rate of about 60 per minute. The discrete records were then converted to punched cards for appropriate analysis with a digital computer. Pressure fluctuations on the side wall were also measured with the Pace transducer and DVM-printer arrangement. A calibration system for the transducer, using a static but variable head, was used to calibrate the transducer at frequent intervals.

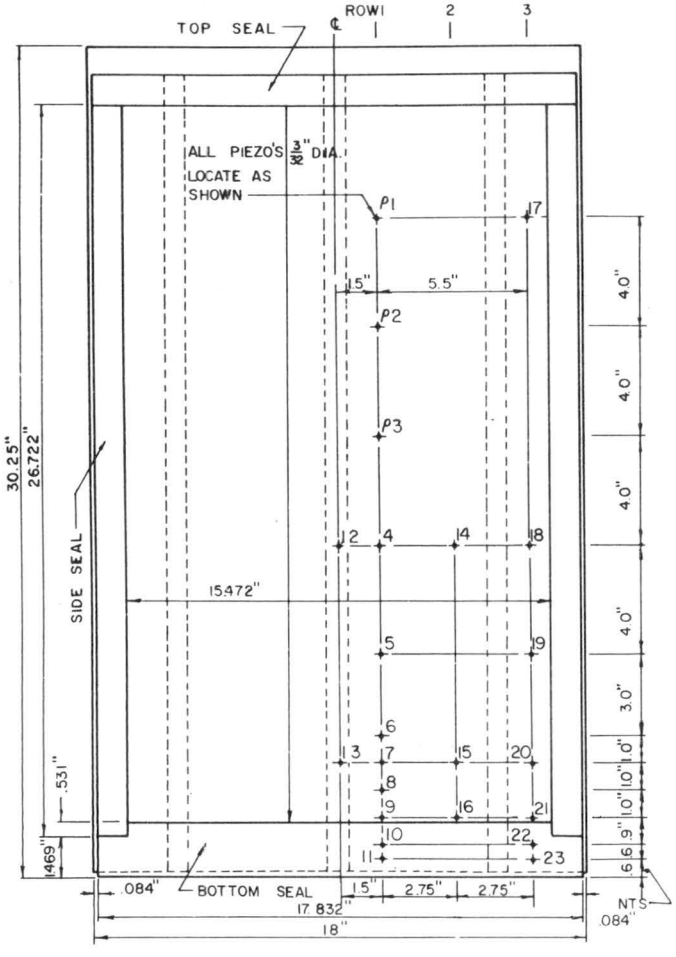

Figure 33. Location of piezometers on the skin plate of the 1:12 radial gate model.

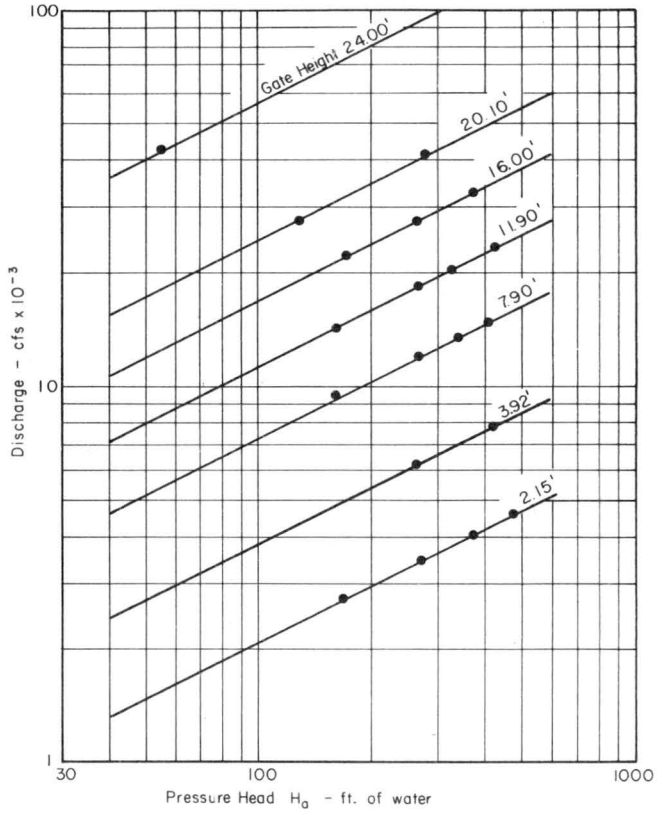

Figure 34. Discharge rating curve for the radial gate.

Model Results

Head-discharge relationship - The discharge in cubic feet per second (cfs) at various gate openings and heads, measured in the transition, are plotted on figure 34. It is noted that the curves on log-log graph paper form straight lines with slopes of one-half. Although only a few points were available at the larger gate openings, the straight lines projected through the points are reasonable in terms of the theoretical relationship of discharge to head. It will also be noted that gate openings in the model were not all set precisely to integer values. In order to make a more direct comparison to the pre-assumed rating curves for the gates, discharge coefficients are needed. The straight lines of figure 34 suggest that there is a single discharge coefficient applicable for all heads at any one gate opening. The

coefficients were, therefore, calculated and are tabulated in Table A-1 of the appendix. Discharge coefficient is usually defined in terms of total head, that is,

$$Q = C_D A\sqrt{2gH_t}$$

where

C_D = discharge coefficient

A = area of gate opening

$H_t = H_a + \frac{V^2}{2g}$

and

H_a is the piezometric head measured in the transition referenced to elevation 1117

V is the mean velocity at the location where H_a is measured.

The discharge coefficients for various gate openings are plotted on figure 35 with a smooth line joining the data. The rating curves for 2, 4, 8, and 12 feet gate positions were then calculated and are compared to the rating curves assumed for design. The latter set of curves were taken from figure 7-1 of reference 1. Both sets of curves are shown on figure 36. Significant difference is noted only for the 12-ft opening.

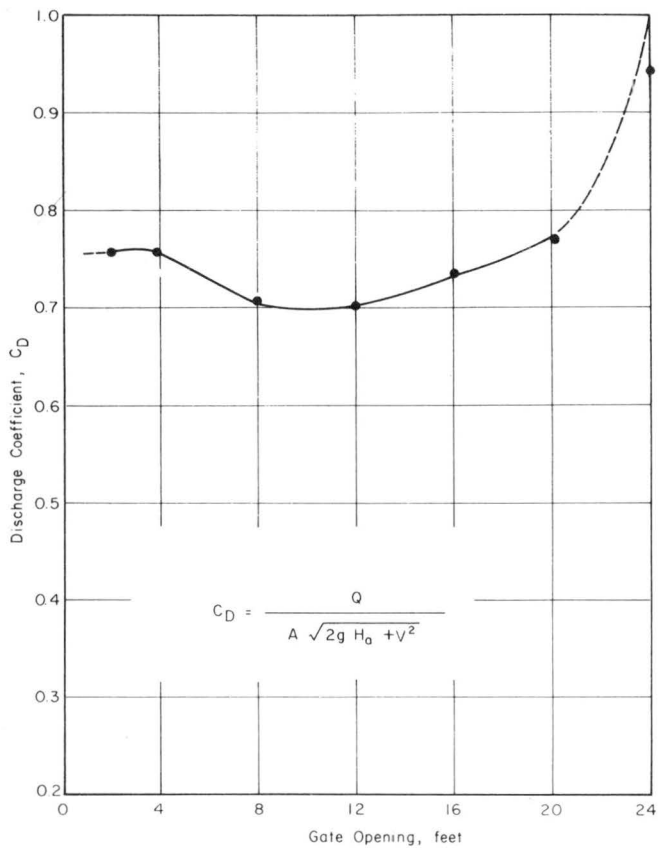

Figure 35. Computed discharge coefficients for the radial gate from figure 33.

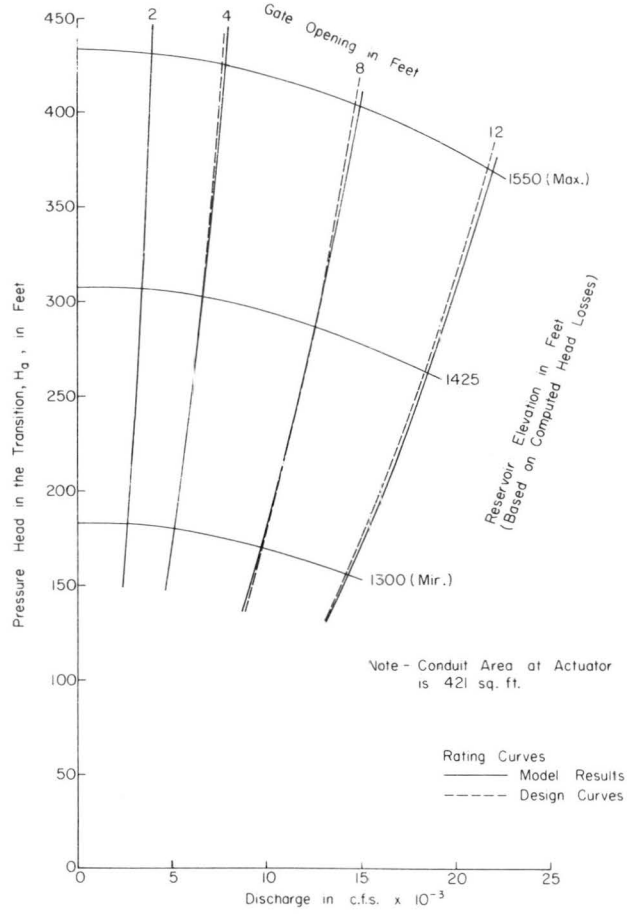

Figure 36. Discharge rating curves for various gate openings and heads. Comparison is made with model results and design calculations.

Hydraulic forces on the gate - The total hydraulic forces on the gate at various openings were calculated from the pressure heads measured by the piezometers in the skin plate. Each piezometer head reading was assumed to apply to an area of the gate defined by the median lines between the piezometers and the total force was obtained by summation over the entire cylindrical gate surface.

At openings of 12 ft and less, the hydrodynamic force on the gate varies with the pressure head and seems to be weakly dependent on gate position. The forces calculated from measured pressure heads are shown in figure 37. It should be recalled that the top jet arrestor is effective at openings below 12 feet, but not at greater openings. Thus, hydrostatic forces at least prevail over the entire surface of the skin plate at all openings less than 12 feet. The forces on the gate at 16-ft and 20-ft positions are also shown on the figure; and as a result of the jet arrestor, the forces are markedly less than those for gate openings less than 12 ft.

The data for these calculations were taken by sealing the gate with thin rubber strips so that no leakage occurred past the aluminum model seals. For 16-ft and 20-ft gate openings, a seal was placed at the location of the intermediate jet arrestor.

The sectional distribution of piezometric heads on the gates are shown by three vertical rows in figure 38. The rows are identified on figure 33. The gate was open 12 feet and the heads in the transition, H_a, (measured 60 ft upstream of the gate) are identified for the different curves. All the pressure head readings taken are tabulated in Table A-2 of the appendix.

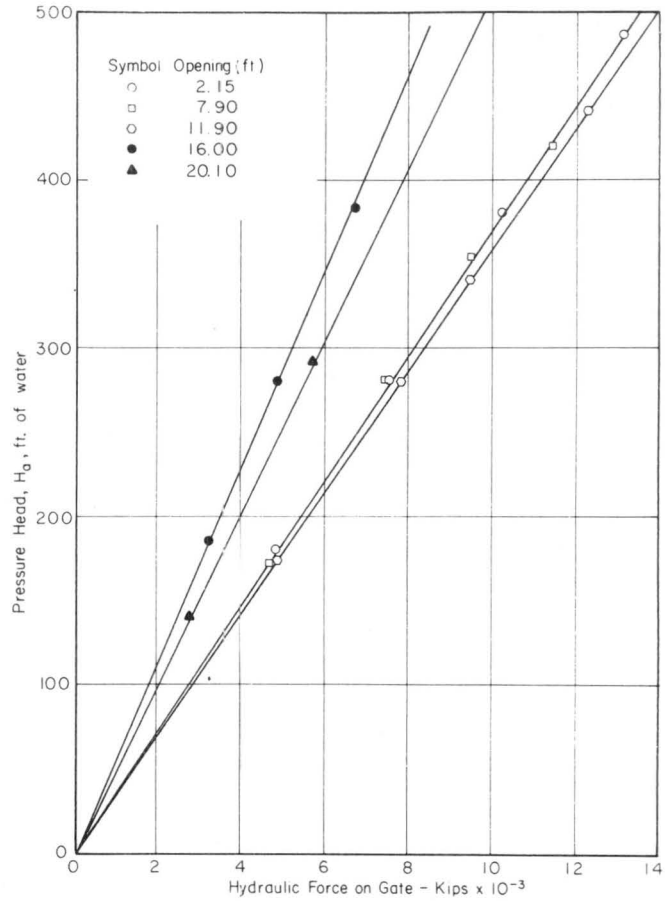

Figure 5-5 Hydraulic forces on the radial gate.

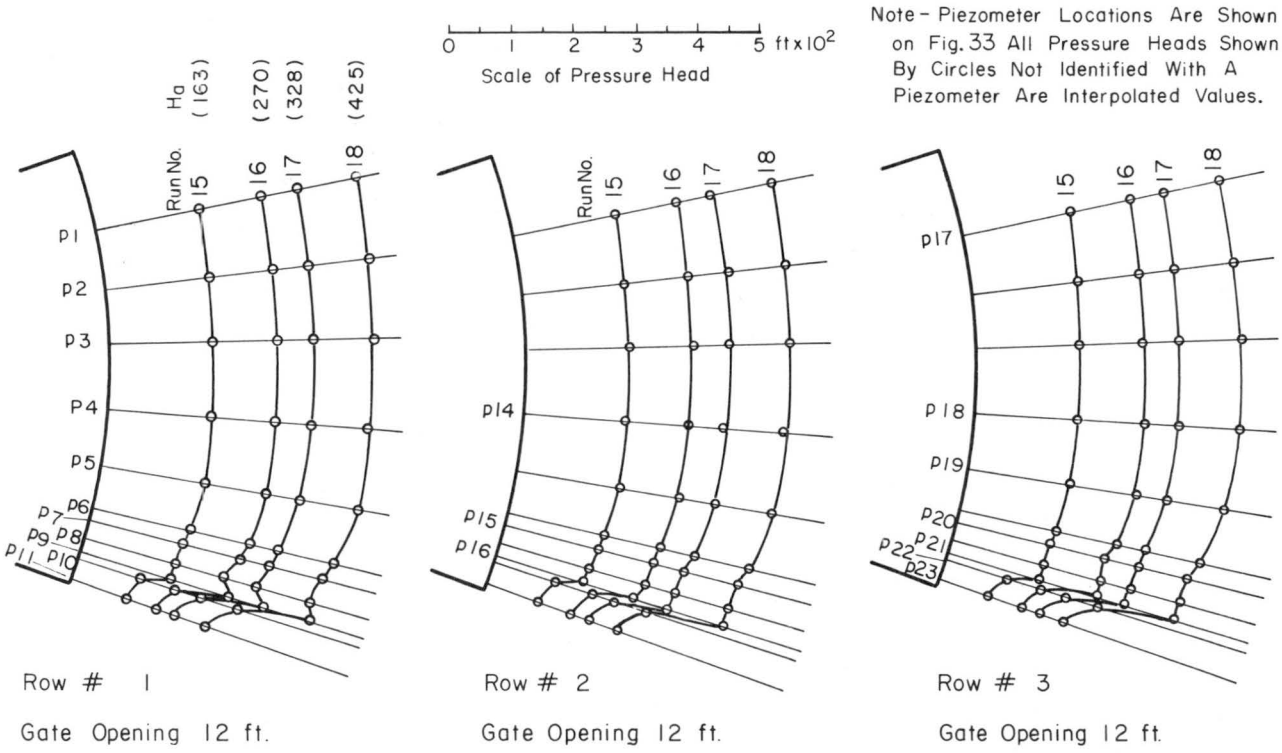

Figure 38. Pressure head distributions on the gate at 12-ft opening.

Description of the flow - The flows under the gate and through the seal gap are described for two different conditions. When the gate is set at a specific opening (up to half open) the seals will be seated, thus, no flow will occur past the seals. This will be the modus operandi for the majority of the time and is called the normal condition in this report. When the gate is retracted prior to vertical movement, there will be flow through the seal gap. This condition is referred as the retracted condition. Observations of the flow for the retracted condition were made for steady flow, i.e., the gate was held in a retracted position at a fixed opening.

The normal condition: 2-ft opening - The flow under the gate as viewed from the side wall of the model, and the resulting spray near the end of the gate structure, are shown in the photographs of figures 39 and 40. The gate was held at an opening of 2.15 ft (nominally 2 ft) and the head was 270 ft. Referring to figure 36, it will be seen that the discharge was about 3200 cfs.

The jet emerging from beneath the gate spread at the sides because of the recesses in the walls, then impinged on the walls of the side recesses near the intersection with the floor, creating a sizable "rooster tail." The spray resulting from the impingement and break-up of the rooster tail, seen in figure 40, rises to a considerable height above the wall of the gate structure. At smaller heads most of the splash was directed beneath the trunnion, filling the downstream channel with very fine spray. At larger heads a considerable amount of the splash was directed at or above the trunnion reaching heights of about 100 feet above the floor of the gate structure. The quantity and velocity of the spray on the structural members of the gate did not appear to be serious, although this was a qualitative interpretation in terms of the prototype.

Figure 39. Normal operation with triangular side-seal recess for 2.15-ft gate opening and 270-ft head.

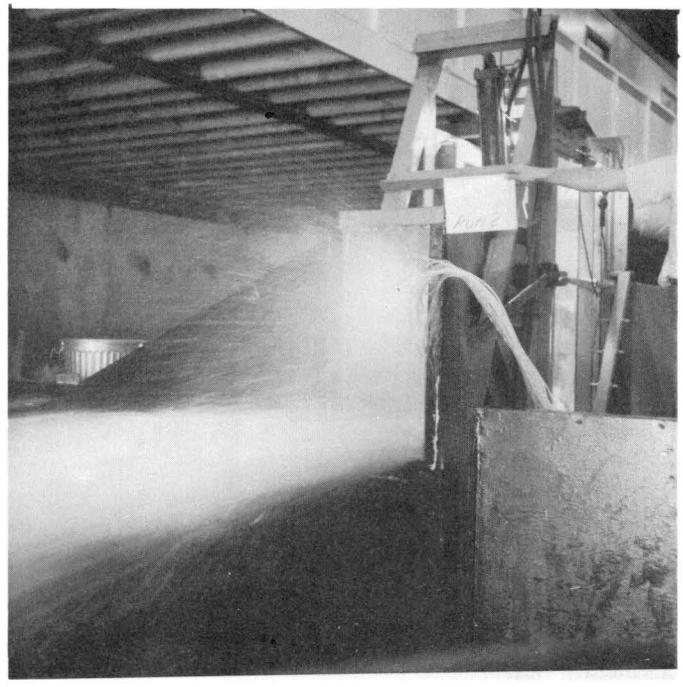

Figure 40. Note the spray created within the gate structure for the condition of figure 38.

The major hydraulic problem at this gate opening was the negative pressures on the side walls downstream from the recesses. Three rows of piezometers were placed at the locations shown in figure 41. The pressure heads measured with a manometer are shown in figure 42 for a gate opening of 2 ft and H_a of 442 ft. The head is slightly greater than that which is created by full reservoir at elevation 1550 ft (H_a should be about 431 ft in accordance with figure 36), but the difference is small. The pressure heads from piezometers P-48 to P-53 along the bottom row indicate subatmospheric pressures that reach vapor pressures, and cavitation would result. The pressure heads measured along the middle row are not particularly meaningful as the piezometers were near the water surface so that air bubbles could not be prevented from entering the manometer leads. These pressures, along with the large amounts and spray created, are suggestive of the necessity to modify the geometry of the recesses.

The primary ventilation system did not draw air into the cavity created by the drop in the floor level. Instead, water was ejected from the tube underlying the floor. The secondary ventilation system also did not draw any measurable quantities of air. If Subatmospheric pressure is developed below the nappe of the jet, a sufficient amount of air seems to be drawn from the space between the jet and the side recesses so that the ventilation systems are not measurably effective.

Normal condition: 4-ft opening - The flow condition at the wall in the vicinity of the recess for a gate opening of approximately 4 feet is shown in figure 43. The head, H_a, was 342 ft. The impact of the spreading jet with the side recesses caused a large volume of water to be directed vertically upward. The quantity of this water flow appeared to partially submerge the lower edge of the gate. The water level there was by no means steady; it varied

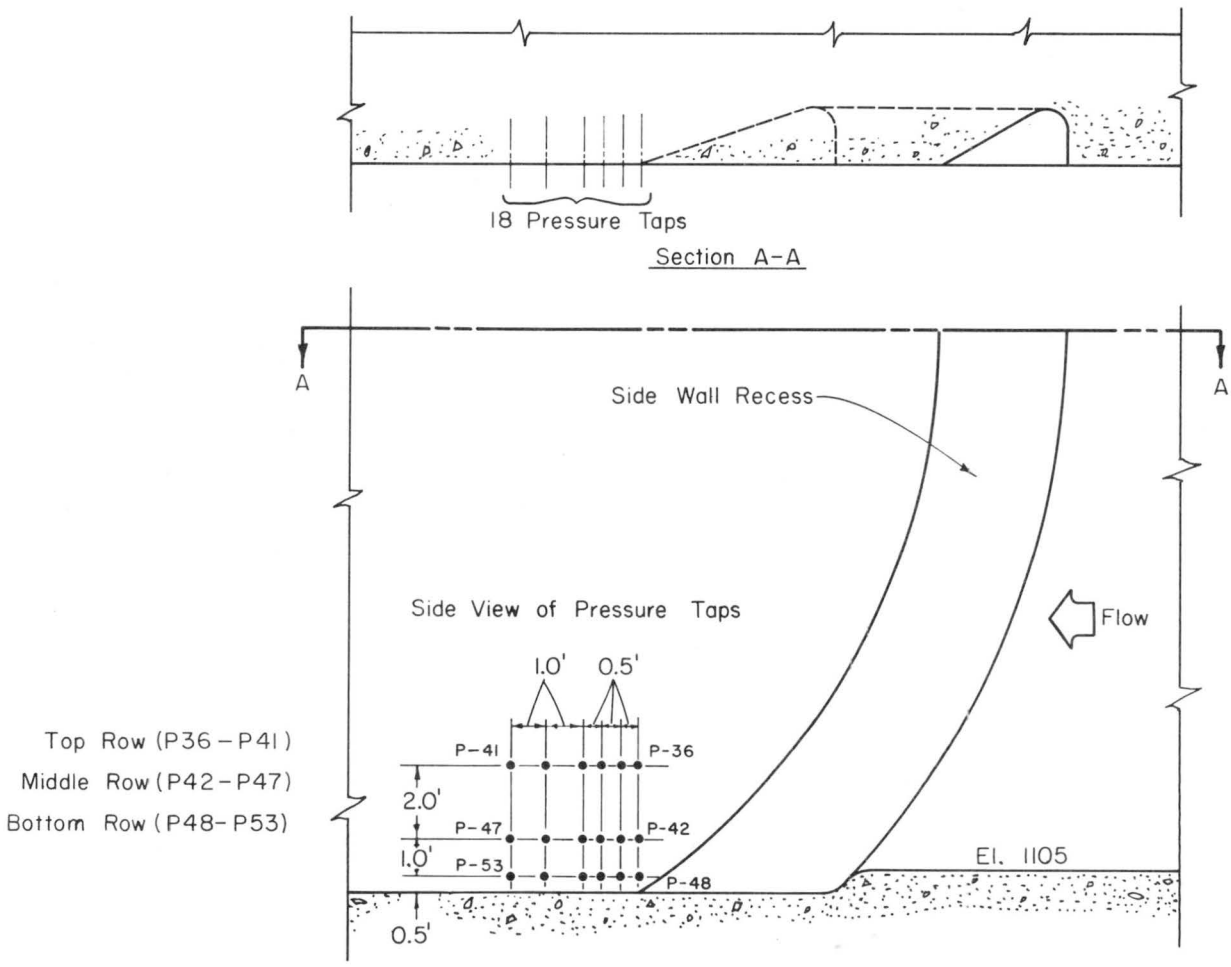

Figure 41. Location of piezometers on the side wall for 1:12 model with triangular recess.

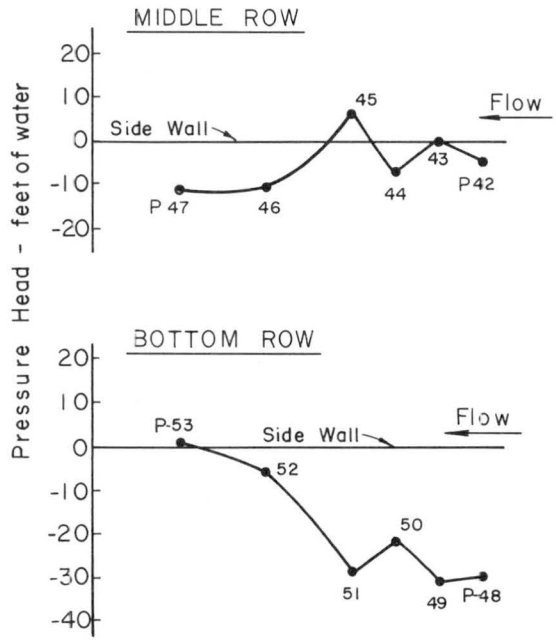

Figure 42. Side wall pressure heads: Gate opening of 2 ft and H_a of 442 ft.

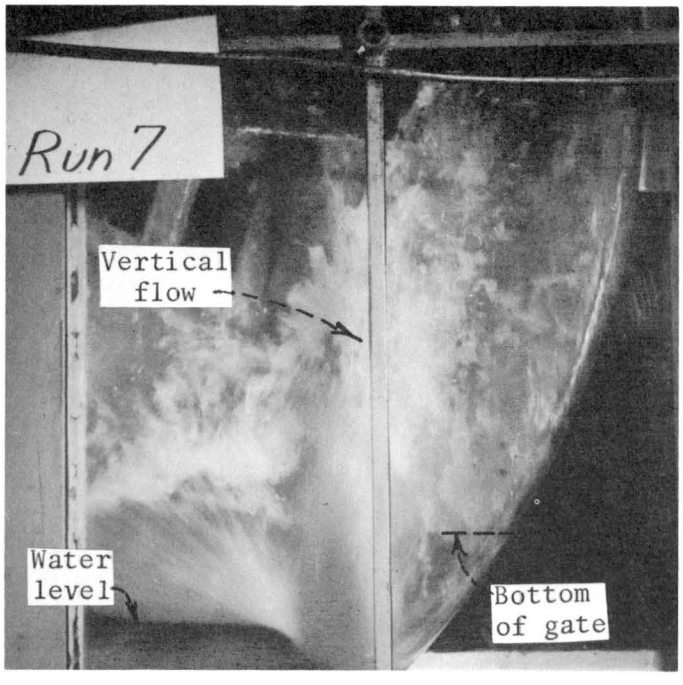

Figure 43. Normal operation with triangular side-seal recess for 3.8-ft gate opening and 342-ft head.

up and down irregularly. This might be suggestive of some vibrational problems on the prototype gate, but there was no evidence of oscillating forces on the gate registered by the piezometers on the skin plate.

The amount of spray within the gate structure was large, although the height to which the spray reached was less than for the 2-ft gate opening. This is attributable partly to the greater flow depth downstream of the gate and partly to the vertical flow mentioned in the previous paragraph. The difference can be better seen by comparing figures 39 and 43.

The pressures on the side walls for a head, H_a, of 444 feet in the transition are shown in figure 44 in ft of water. Cavitation will result along the corner formed by the wall and the floor downstream of the recess. Subatmospheric pressures were also encountered at the other two rows of piezometers although they did not reach vapor pressure.

Air was not drawn through the primary ventilation system. At heads above 150 feet, the secondary system did draw air, though not in measurable amounts. Subatmospheric pressures developed below the nappe of the jet at the floor recess because the jet which deflected upward at the wall partially restricted the air supply from the side recesses.

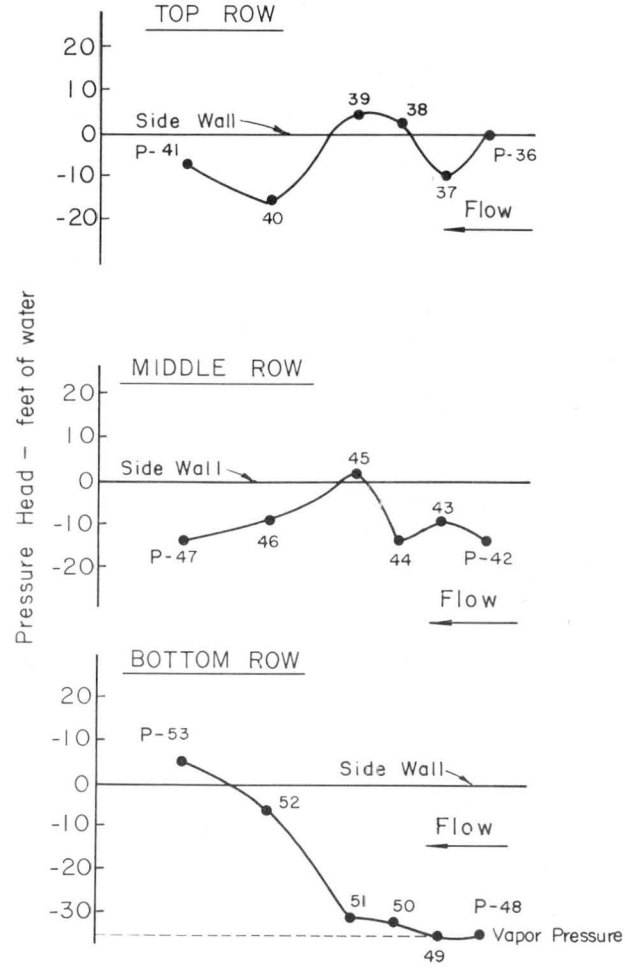

Figure 44. Side wall pressure heads: Gate opening of 4 ft and H_a of 444 ft.

Normal condition: 8-ft opening - The deflection of the jet onto the arms of the radial gate is shown in the photograph of figure 45. The spray created at the wall was directed toward the trunnion and ascended to a height of about 150 ft above the gate structure floor level. Most of this spray would be contained within the confines of the downstream chute and stilling basin, although some of the spray would surely extend laterally beyond the walls of the chute. The head in the transition, H_a, was 342 ft for the flow shown in figure 45.

Vortices were formed within the grooves of the side recesses which spiraled inward toward the center of the gate structure floor. These vortices drew in large amounts of air and appear white in the photograph in figure 45. Although these vortices contain very large velocities, no serious damage should result as the whole vortex is well aerated. The vortices formed for all heads tested which ranged from 161 ft 407 ft.

The primary ventilation pipeline was full of water, but air was drawn into the secondary system although not in great quantities. The nappe of the jet at the step in the floor appeared to be well ventilated.

Normal condition: other gate openings - The conditions for flow at gate openings greater than 8 feet were similar to that described above. Spray was created by the jet impact with the side recesses at all gate positions except for the fully-open condition. The vortices in the side recesses were evident for all heads and openings, and the primary ventilation system was always ineffective. Photographs of the flow for the various gate positions are shown in figures 46 through 49 for 12-ft, 16-ft, 20-ft, and full-open positions, respectively. Pressures at the side walls for 8-ft and 12-ft gate positions are shown in figures 50 and 51, respectively.

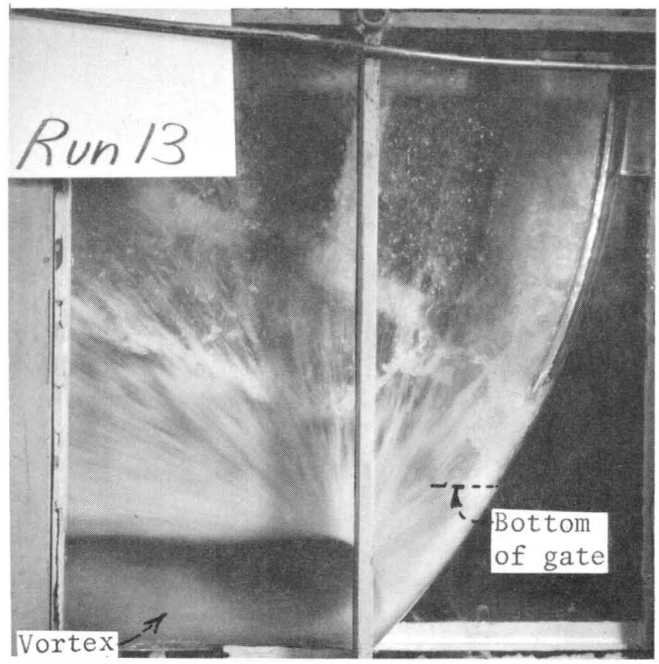

Figure 45. Gate open 8 ft at 342-ft head.

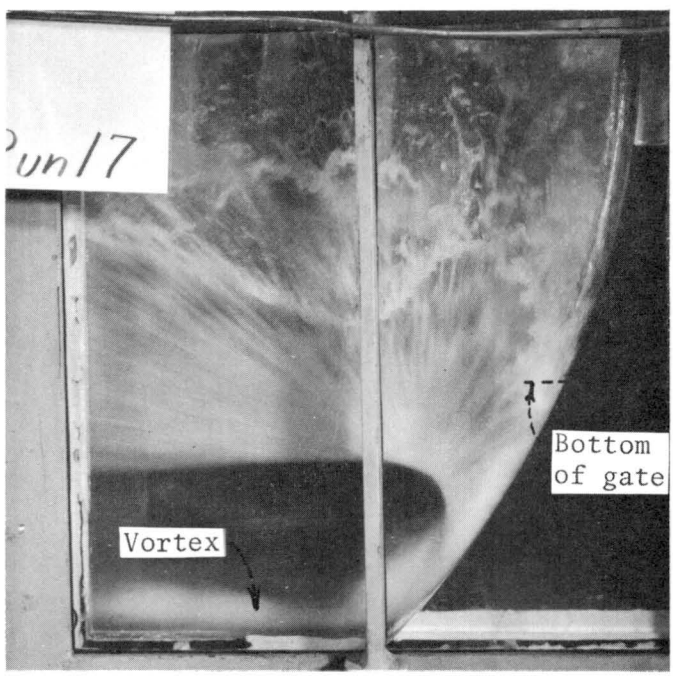

Figure 46. Gate open 12 ft at 328-ft head.

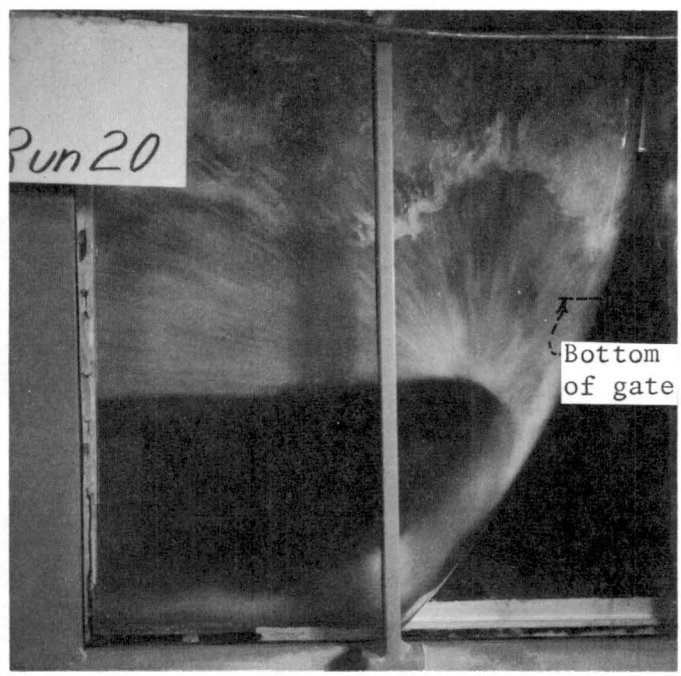

Figure 47. Gate open 16 ft at 268-ft head.

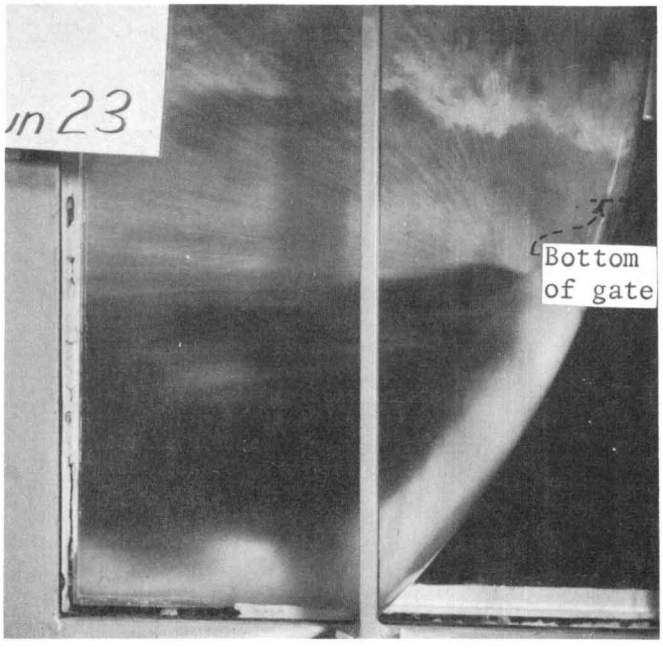

Figure 48. Gate open 20 ft at 281-ft head.

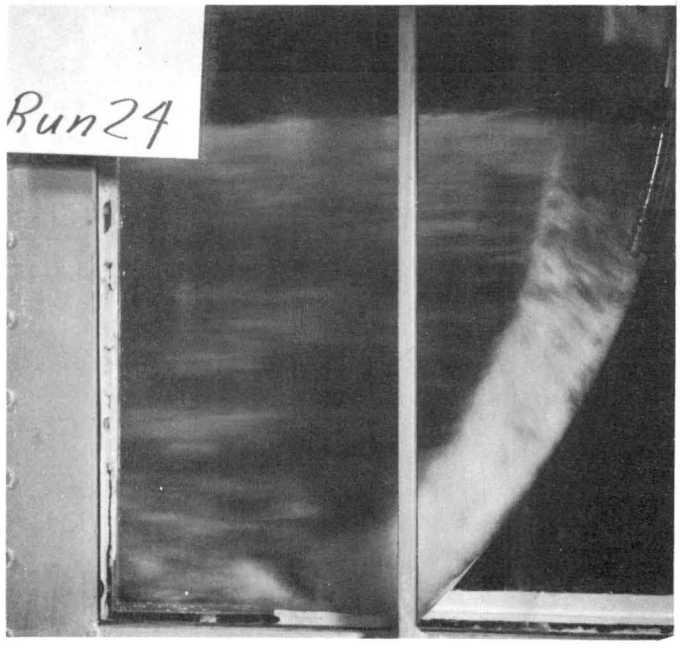

Figure 49. Gate full open. Measured head was 56 ft.

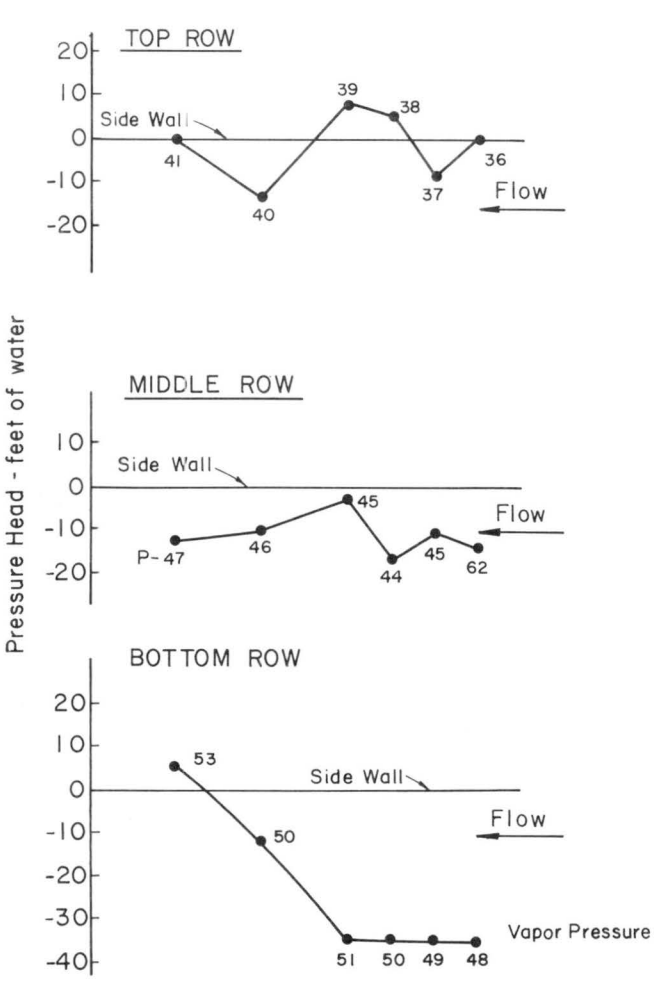

Figure 50. Side wall pressure heads: Gate opening of 8 ft and H_a of 433 ft.

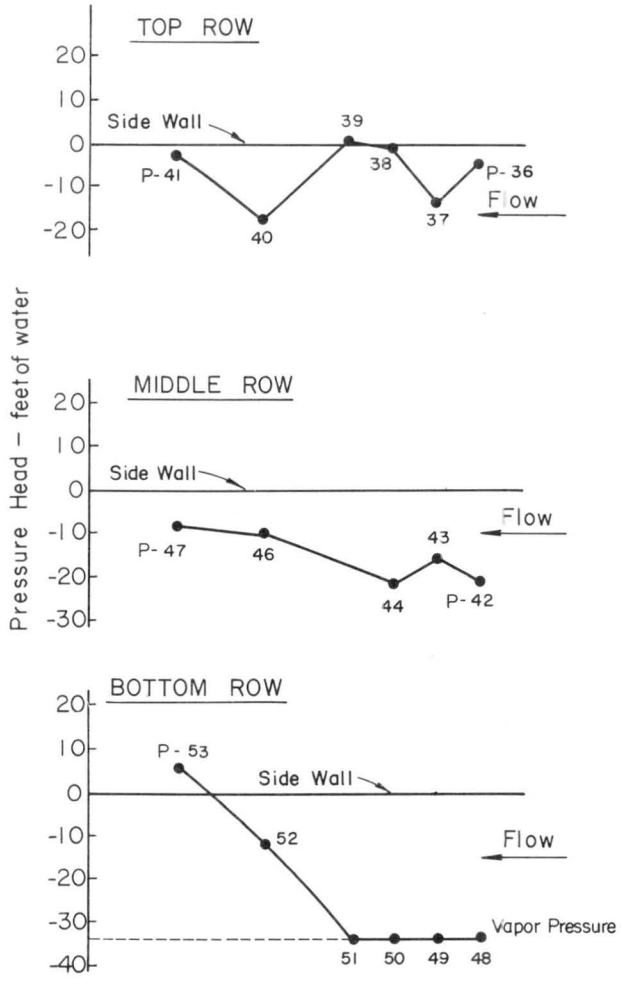

Figure 51. Side wall pressure heads: Gate opening of 12 ft and H_a of 418 ft.

Retracted gate condition - There were two sets of conditions tested: (1) flow with jet arrestors removed, (2) flow with the jet arrestors simulated. For the first condition the gate was closed, but the gap width and head were varied. For the second condition the gap width was nominally constant near maximum (0.8 in.) and gate position and heads were varied.

The flow through a narrow gap of 0.26 in. (prototype dimension), and a wider gap of 0.67 in. at low heads of 155 and 175 ft, respectively, are shown in figures 52 and 53. The difference is principally in the quantity of water which impinges against the arms of the gate. Although it is difficult to see from the photographs, there will obviously be greater amounts of flow against the arms with the wider gap. At these low heads, the water jet past the upper seal did not have sufficient energy to reach the deflector hood to be directed into the collector-energy dissipator basin. Consequently, the water flowed into the gate chamber or fell back onto the arms of the radial gate. The streaks in the jet along the face of the plexiglas wall are turbulent instability streaks and are not all attributable to minor imperfections (roughnesses) along the edge of the gate. The frictional drag along the wall is greater in the model than for the prototype.

At low heads nearly all the water is contained within the gate structure. Only minor amounts of spray were noted outside the gate structure.

At larger heads the majority of flow past the upper seal was deflected into the collector-dissipator basin. The upward jet was difficult to photograph from the side wall because of the foreground spray, but a view of the flow into the basin is shown from the top in figure 54 and from the end of the basin in figure 55. The gap width for this test was 0.59 in. with a head of 425 ft. It is evident from these photographs that a basin length of about 30.5 ft measured from the leading edge of the deflector to the end wall was adequate (see figure 31). The jet plunges into the pool and the energy is adequately dissipated by the turbulence created within the pool. A view of the flow into the basin at a lower head of 300 ft and gap width of 0.77 in. is shown in figure 56. The dimensions of the basin shown in these photographs are drawn on figure 31. A small change in the shape of the deflector hood (at the exist end) materially assisted in directing the jet into the plunge pool.

The flow past the seals at the upper corners of the "picture frame" resulted in a jet which missed the deflector altogether. A view of the jet on one side is shown in figure 57 for a seal gap of 0.59 in. and head of 425 ft. The jets of water ascended to about elevation 1250 ft, which is 150 feet above the floor of the gate structure. The resulting spray and impact of a portion of the jet on the gate hoist assembly would clearly be undesirable.

The jets from the sides of the gate intersected about 30 ft downstream from the skin plate of the gate. Some of the jet impinged on the gate arms with consequent development of spray. Part of the flow which continued past the gate arms impinged against the side wall of the gate structure and continued downstream. A small but significant portion of the jet from the upper part of the gate intersected above the gate arms, continued past the trunnion, and laterally beyond the bounds of the gate structure onto the surrounding terrain.

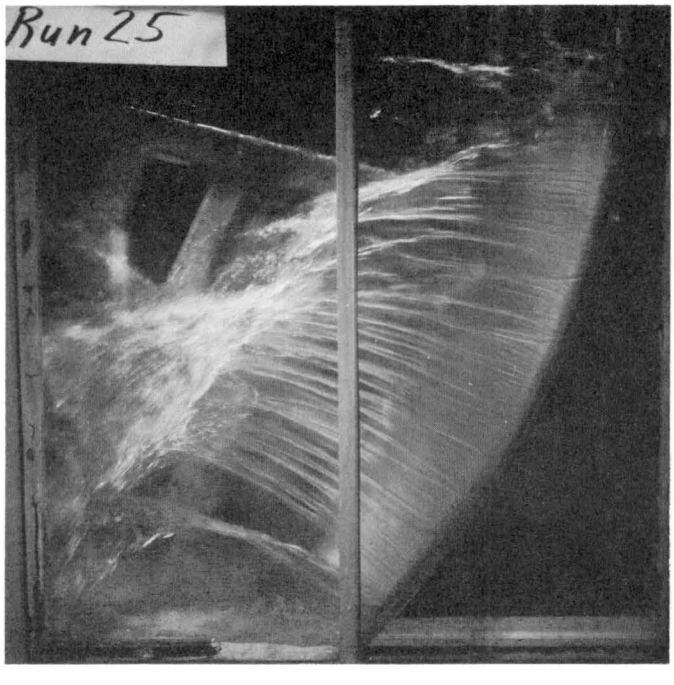

Figure 52. Retracted condition with gap width of 0.264 in. and H_a of 155 ft, without jet arrestor. Gate is closed.

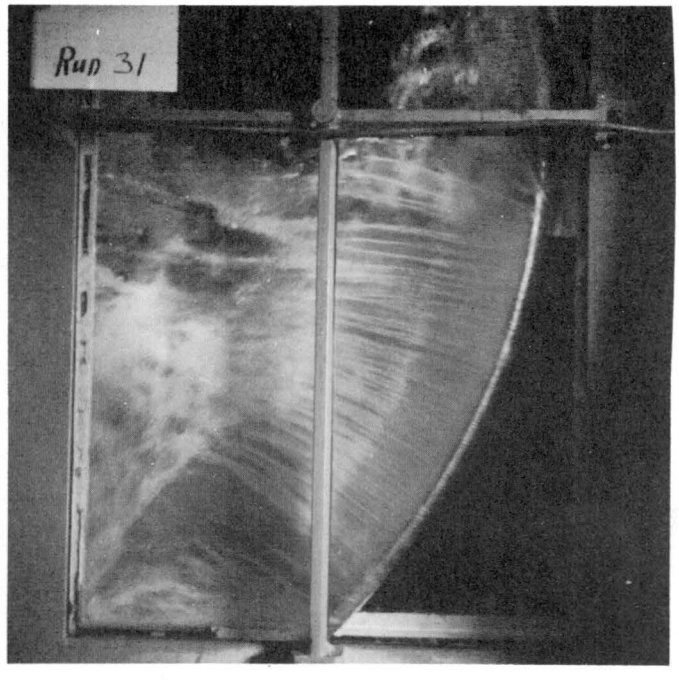

Figure 53. Retracted condition with gap width of 0.67 in. and H_a of 175 ft. Gate is closed.

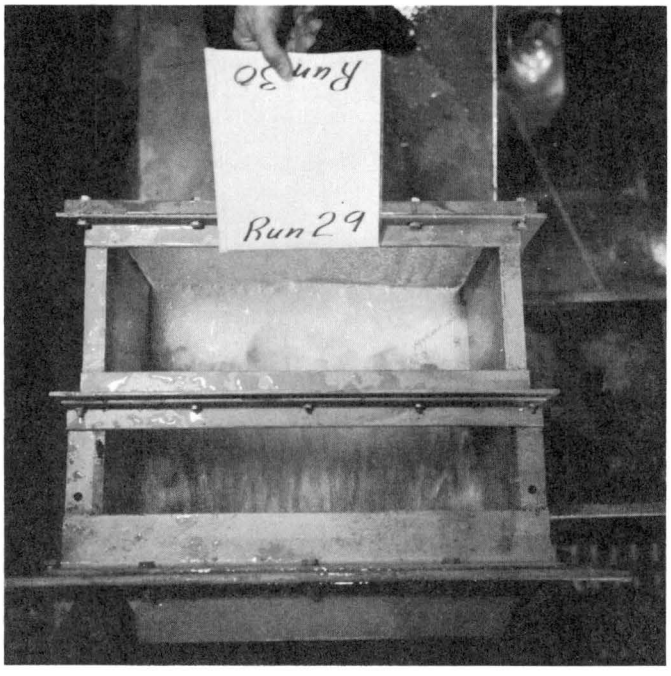

Figure 54. Flow of water past the top seal into the basin - top view. Gap width is 0.59 in. and H_a is 425 ft. Gate is closed.

Figure 55. End view of the same flow as in figure 54.

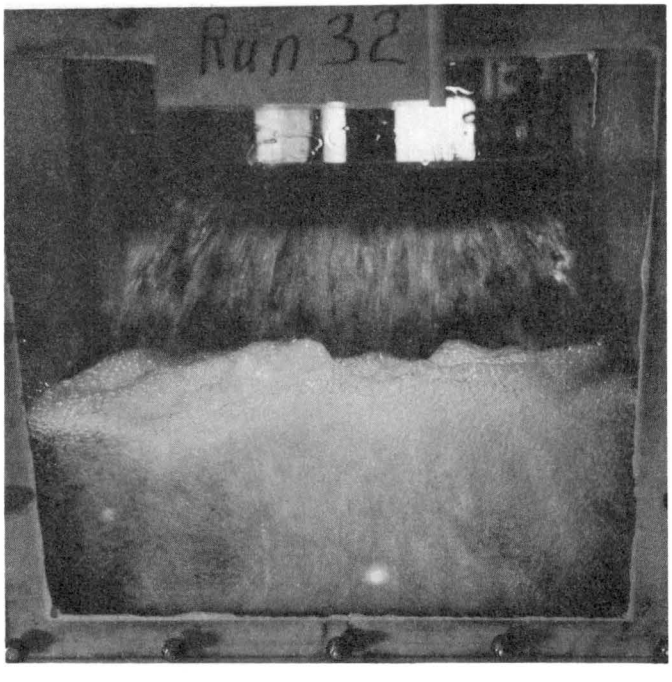

Figure 56. End view of flow into the basin with gap width of 0.77 in. and H_a of 300 ft.

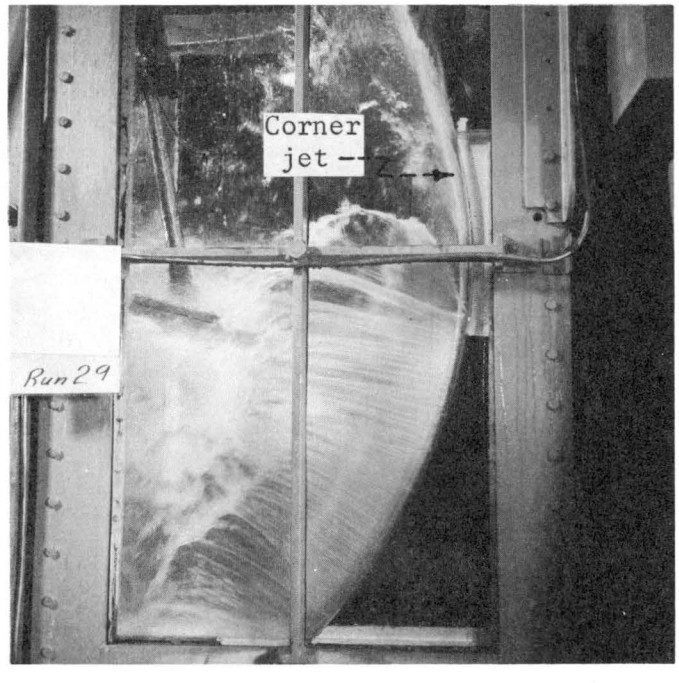

Figure 57. Retracted condition for gate at 0 ft with gap width of 0.588 in. and H_a of 425 ft without jet arrestor.

The upper jet arrestor was simulated in the model with a thick foam rubber weather stripping. The tests with the jet arrestor are depicted in the photographs of figures 58 and 59 for gate closed, gap width of 0.86 in. and head of 430 ft. It is to be noted that the "corner" jet was eliminated and, of course, no flow existed upward from the top seal. The problem associated with the flow past the upper part of the gate, around the sides, was still the same as before, namely that the spray proceeded past the trunnion and laterally beyond the walls of the gate structure.

The flow of water in the gate structure for partial gate openings and with the gate retracted, compounds the conditions which exist separately into a chaotic mixture of jets and spray within the gate structure. The photograph of figure 60 might be helpful in picturing the conditions of the flow. The gate is open 12 ft, the seal gap is 0.82 in. and the head is 375 ft. A considerable amount of spray extended upward to heights of 100 ft or so, and some of the spray extended laterally beyond the walls.

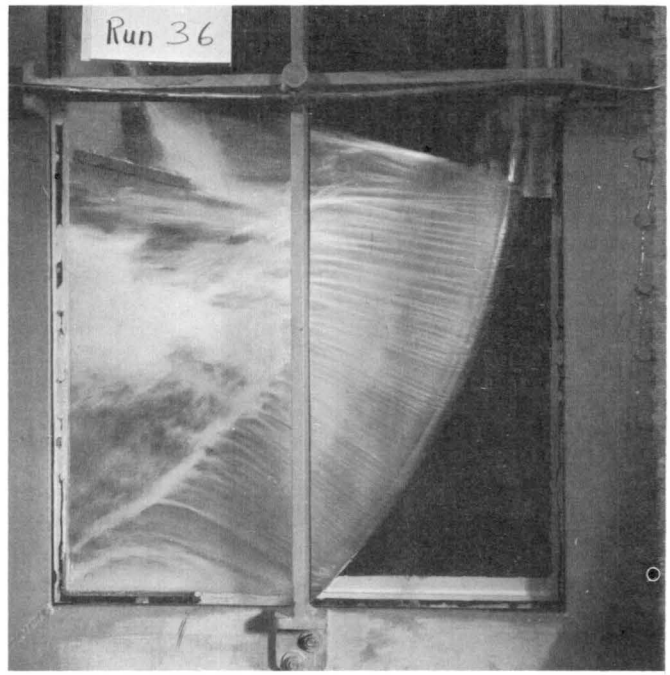

Figure 58. Retracted condition for gate at 0 ft, gap width of 0.863 in. and H_a of 430 ft with top jet arrestor.

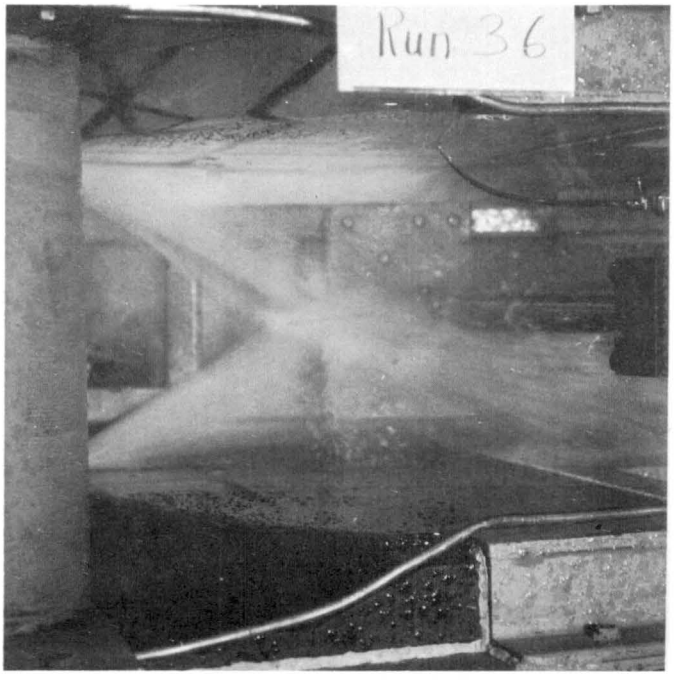

Figure 59. Retracted condition for gate at 0 ft, gap width of 0.863 in. and H_a of 430 ft with top jet arrestor.

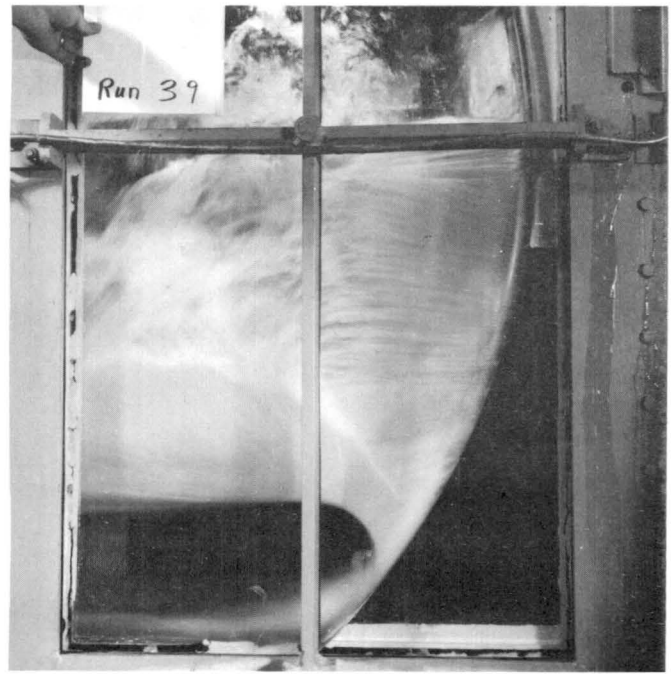

Figure 60. The gate is nominally half open, retracted with seal gap width of 0.82 in. and H_a of 375 ft.

Recommendations

The triangular side wall recesses in the original design were not properly shaped. There are several possible solutions to the problem of a proper side-wall recess geometry which were investigated in a small model (1:70 scale) and will be discussed in the next section. The spray and jet impingement on the arms of the gate should be reduced, and the large amounts of spray which extend high above and laterally beyond the gate structure walls should be contained. The potential is great for cavitation damage to the walls of the gate structure downstream from the recesses.

The jet discharge coefficients assumed for design were not significantly different from the model results as shown by the comparison of rating curves. The total hydraulic force on the gate was determined with the model for various gate openings and heads.

It is recommended that the secondary ventilation system be utilized in the prototype. The primary system was not effective in ventilating the region below the nappe of the jet caused by the offset in the floor.

IV. RADIAL GATE MODEL - 1:70 SCALE

General

From the results of the tests on the 1:12 scale model, it was evident that a gate-recess geometry was required which would produce less spray and would not be subject to cavitation; but to investigate several different geometries in the 1:12 scale model would have been expensive and would have required much more time than was available. It was decided, therefore, to use a 1:70 scale model of the radial gate which had been built for an earlier study of the Tarbela tunnels (see reference 2). This model had a side-wall offset at the gate seals equivalent to 33 inches in the prototype. As a result, the walls of the gate chamber were 21.5 ft apart compared to the 16 ft width of the transition just upstream of the gate. It was a simple matter to install inserts to fill in this offset and obtain any type of gate slot desired. This model was expected to reproduce in a gross way the character of flow in the gate structure.

Description of the Model

The layout of the 1:70 model is shown in figure 61. The head box from the earlier study was still available and was used for these tests. A flexible hose, 4 inches in diameter, was used to connect the head box to the gate model. The flexible hose was connected directly to the plexiglas model of the transition section which, in the prototype, connects the radial gate to the upstream tunnel bifurcation. The bifurcation was not included in the model. The plexiglas model of the transition has an upstream diameter of 4.13 inches, providing a reasonably consistent connection with the 4-in. flexible hose. The previous model of the chute downstream of the gate was made of wood and had been discarded; hence, to save time and expense, the discharge from the gate structure was allowed to plunge directly into a calibrated weir box. The chute would have had no effect on the flow in the gate structure in any event. The head on the model was measured by the piezometer tap located midway along the transition, shown in figures 61 and 62.

Tests on the Triangular Gate Recess

The triangular gate recess geometry was the first one tested in the 1:70 scale model. This was done to verify that the small model would reproduce the flow characterisitcs observed in the 1:12 model. Specially shaped inserts, shown in figure 63(b), were fastened to the offset walls of the gate chamber to reproduce the triangular gate recesses. This insert did not reproduce the concave surface at the inside of the slot, but it did model correctly the convex area where the critical jet impingement occurred. Inasmuch as these were only pilot studies, few direct measurements of the flow were made and most of the observations were visual. The small model did, in fact, reproduce the flow observed in the larger model very well, and because it was made entirely of plexiglas and because it was easy to manipulate, clear observations were possible over a wide range of flow conditions.

The small model was also able to reproduce some of the finer details of the flow with a considerable amount of similarity to the larger model. The flow in the model with the gate open 2 feet and with 395 ft of head is shown in figure 64. This condition is comparable to that shown in figure 39, reproduced here again for convenience. The rooster tail is well reproduced, as is the spray which is very pronounced at this condition. At a gate opening of 8 feet with 370-ft head, the flow appears as in figure 65, a condition somewhat comparable to that shown in figure 45. The spray is very well reproduced, although the amount of air entrainment in the flow, judged visually, is not as great as in the 1:12 model. The vortices that originate in the gate slots and extend along the floor of the gate structure are also shown clearly. The flow with the gate positioned at 12-ft opening with 295-ft head is shown in figure 66, a flow condition roughly comparable to figure 46 in the 1:12 scale model. The spray patterns and the vortices were very similar in the two models. These tests show that the 1:70 scale model can be relied upon to represent the qualitative nature of the flow including some of the detailed flow conditions as well.

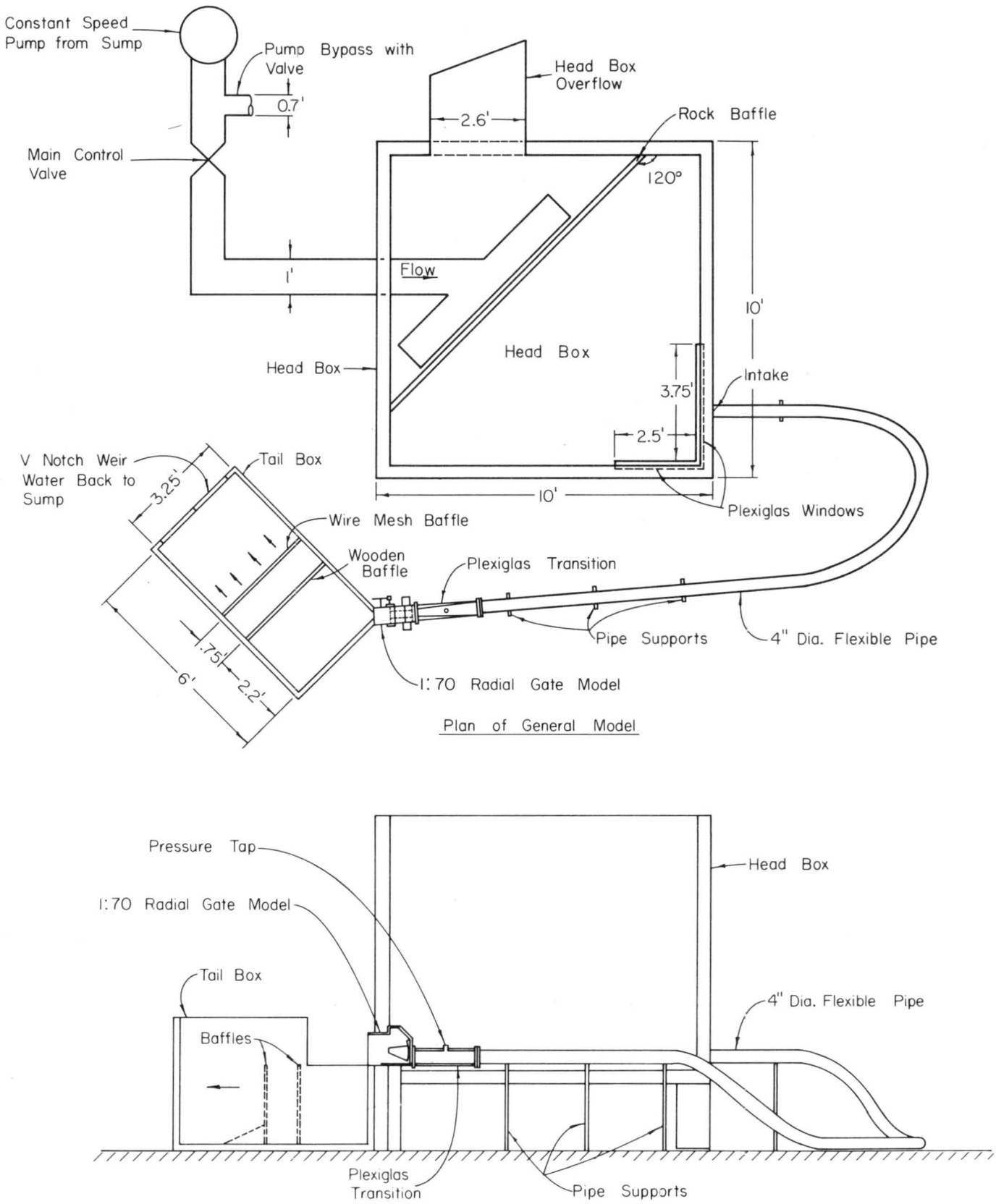

Figure 61. Schematic drawing of 1:70-scale model.

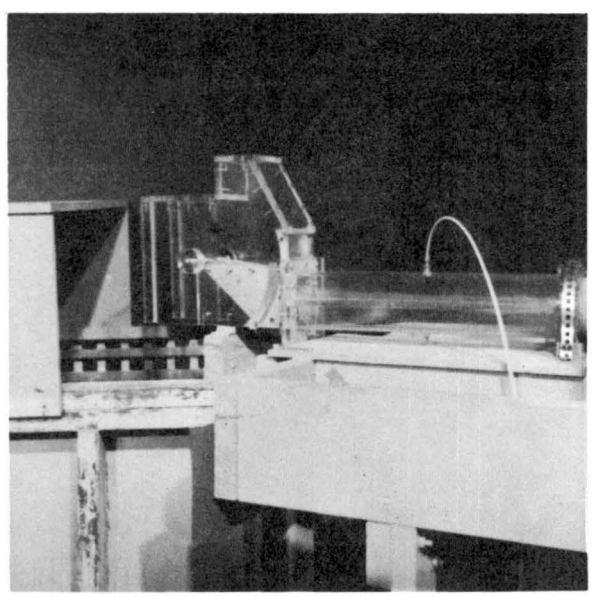

Figure 62. 1:70-scale model of the gate structure and the upstream transition.

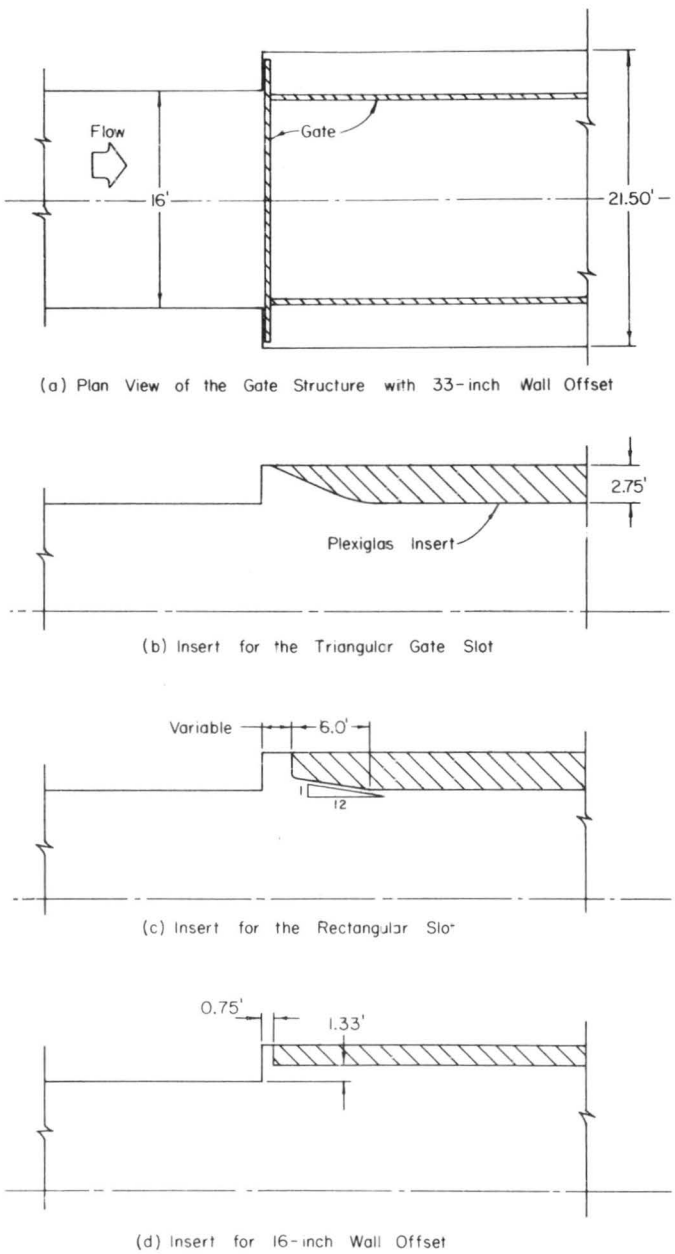

Figure 63. Wall inserts for the 1:70-scale model.

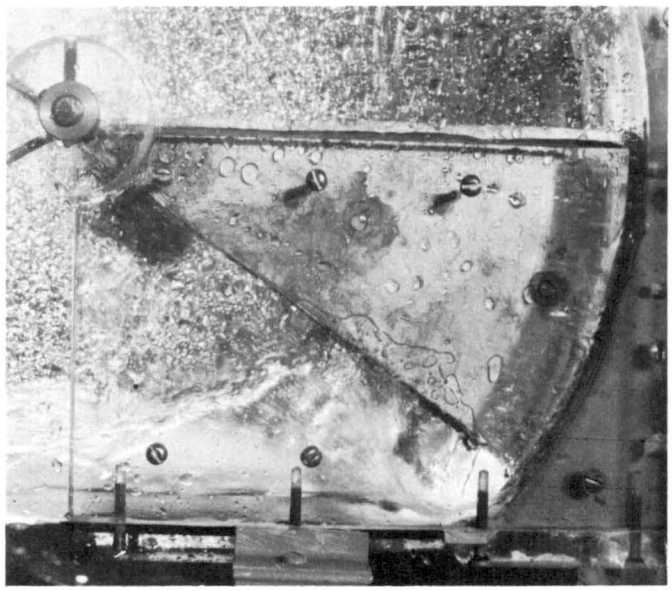

Figure 64. 1:70-scale model with the triangular gate slot geometry with flow for opening of 2 ft and 395-ft head.

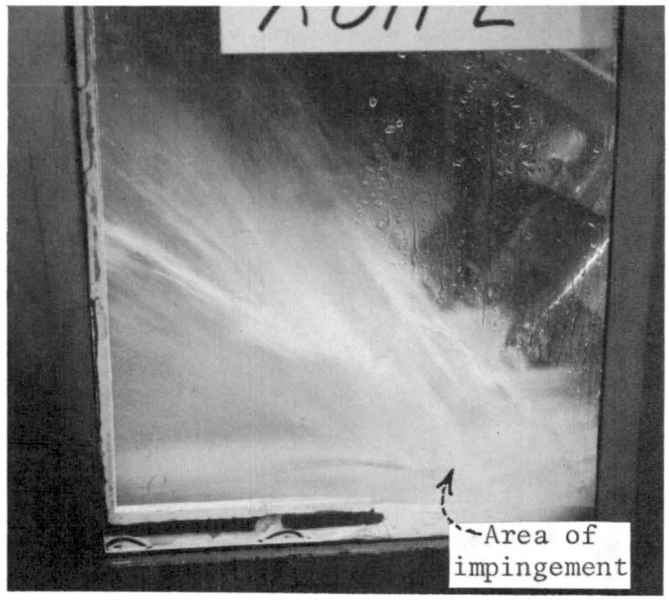

Figure 39. Normal operation with triangular side-seal recess for 2.15-ft gate opening and 270-ft head.

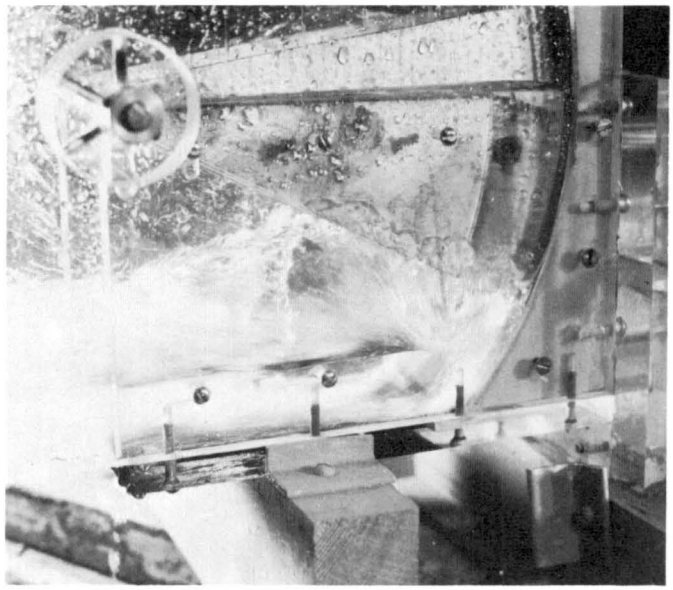

Figure 65. 1:70-scale model with the triangular gate slot geometry with flow for opening of 8 ft and 370-ft head.

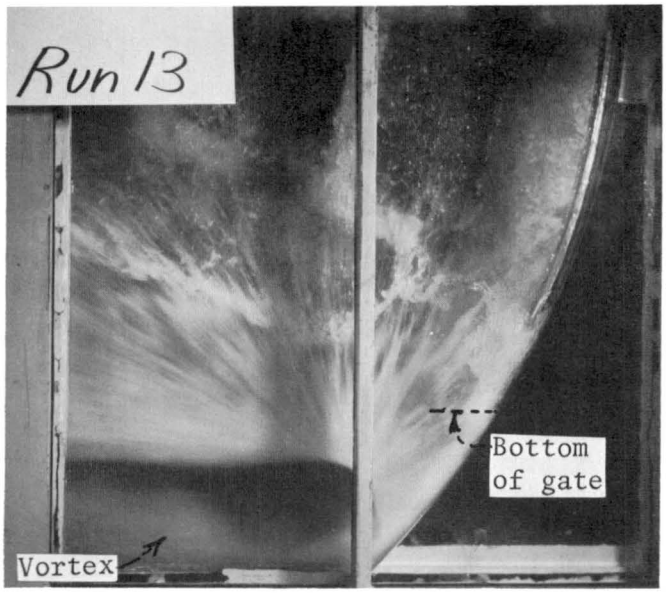

Figure 45. Gate open 8 ft at 342-ft head.

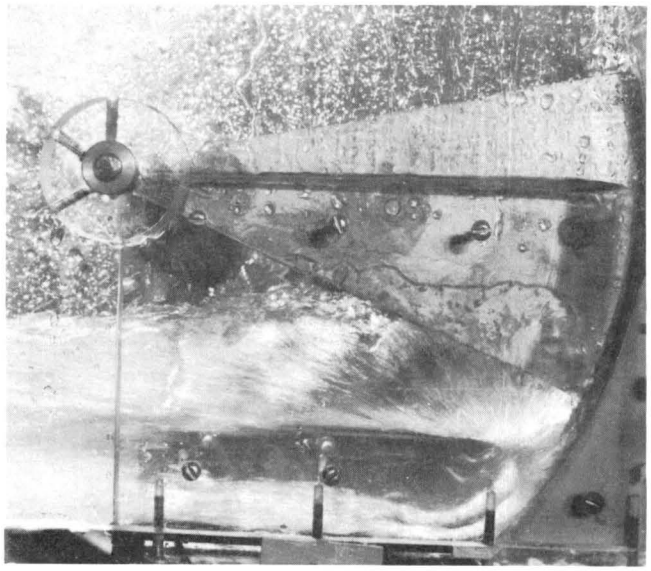

Figure 66. 1:70-scale model with the triangular gate slot geometry with flow for opening of 12 ft and 295-ft head.

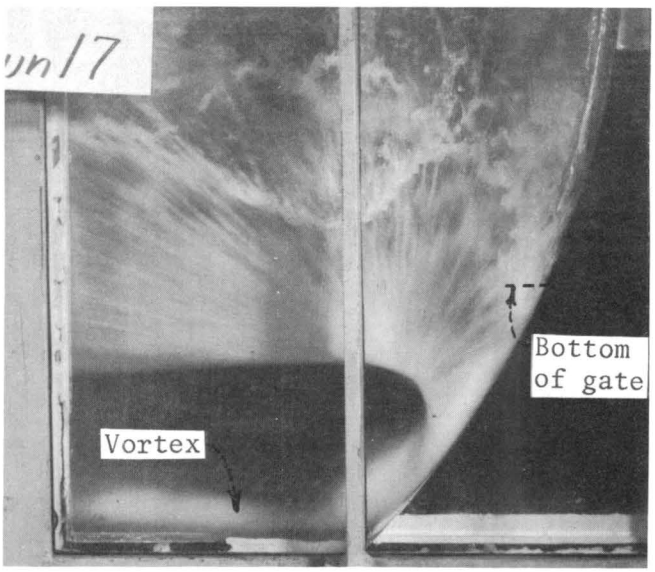

Figure 46. Gate open 12 ft at 328-ft head.

Tests on Rectangular Gate Recesses

The various wall inserts used in the model to test different gate recess geometries are shown in figure 63. The insert pieces shown as part (c), used to form a rectangular gate recess, were tested in two positions, representing 2.5-ft and 4-ft wide recesses. With a gate recess of 4 feet, the arc of the insert was not exactly concentric with the arc of the gate so that the width varied, albeit slightly, from the top to the bottom of the gate. This was considered unimportant for the observations with this model. The rectangular gate recess geometry reduced the spray considerably but increased the problem of localized negative pressures on the wall and the problem of the flow past the seal when the gate was retracted.

The width of the gate recess had very little effect on the nature of the flow. The flow with a 2.5-ft gate recess with the gate open 4, 12, and 24 feet is shown in figures 67, 68, and 69, respectively. The greatest surface disturbance was created by the condition shown in figure 68. A rooster tail is created along each wall that extends about half way up to the trunnion. This condition could be tolerated if all other conditions were satisfactory. Vortices near the bottom of the gate slot can also be seen, indicating the presence of strong localized velocity disturbances in that area. Very little surface disturbance for full gate opening is evidenced in figure 69, a condition that holds for all gate recess geometries tested.

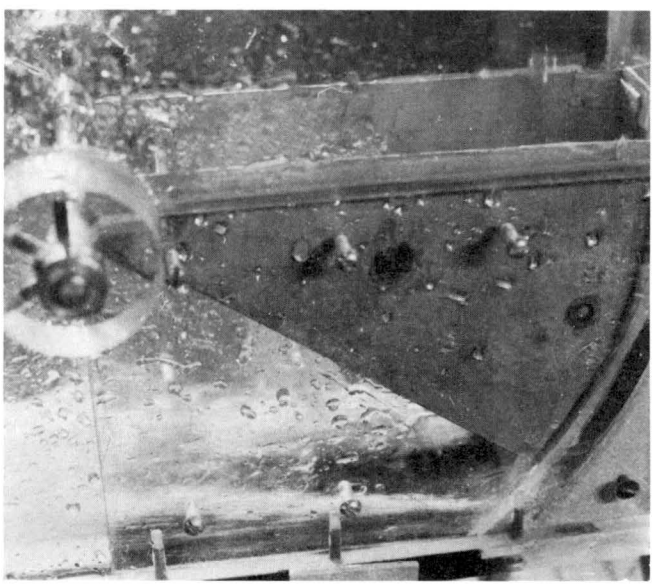

Figure 67. 1:70-scale model with a 2.5-ft wide rectangular gate slot with flow for gate at 4 ft and 375-ft head.

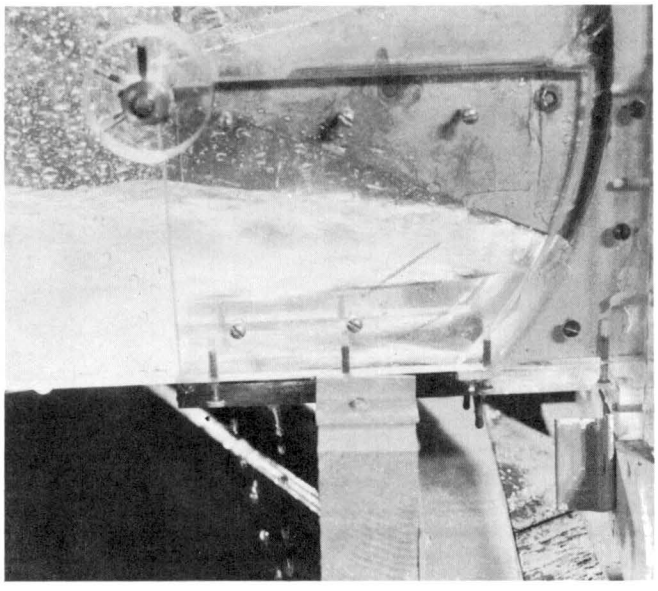

Figure 68. 1:70-scale model with a 2.5-ft wide gate slot for gate at 12-ft opening and 340-ft head.

Gate recesses characteristically create low pressures along the wall immediately downstream of the recess. To measure these pressures, six piezometer taps were located in the wall along a horizontal line 2 feet above the floor. The results of the piezometer measurements are shown in figures 70, 71, and 72. The pressure heads for the 2.5- and 4-ft wide recesses are shown in figures 70 and 71, respectively. The heads were influenced only slightly by recess width with the wider recess generally showing the lowest pressures. The variation of heads at selected piezometers with different gate openings are shown in figure 72 for the 2.5-ft recess. The lowest pressures occur at a gate opening of 12 feet. Subatmospheric pressures existed for a wide range of conditions for both recess widths. At the large velocities occurring in this region, a

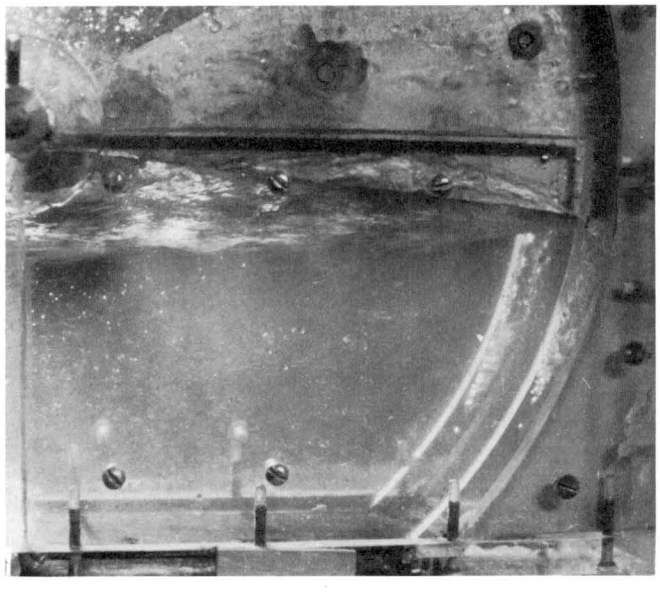

Figure 69. 1:70-scale model with a 2.5-ft wide gate slot for gate full open and 50-ft head.

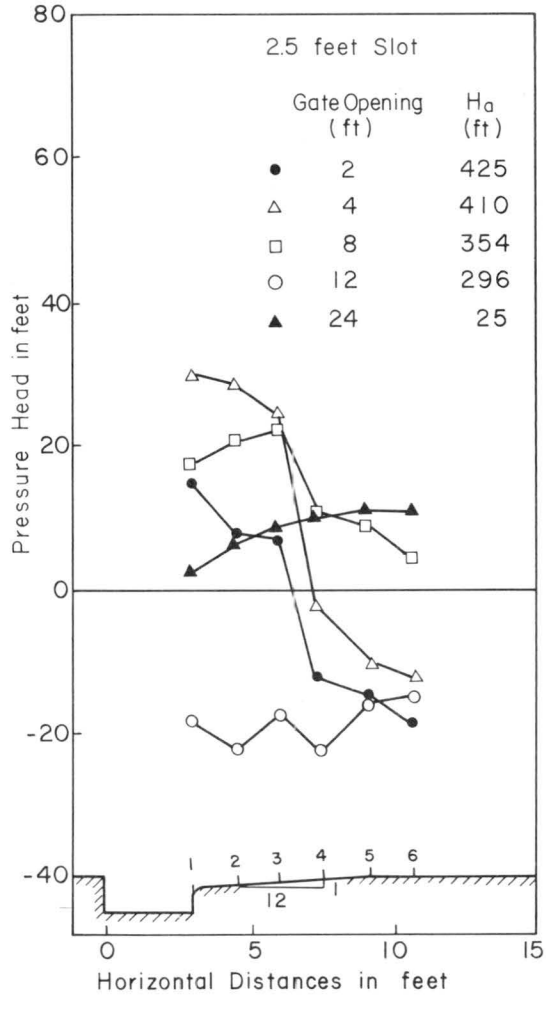

Figure 70. Piezometer pressure heads obtained from 1:70-scale model with 2.5-ft wide rectangular gate slot. Piezometers located 2 feet above the floor level.

pressure head of 20 feet of water below atmospheric represents a cavitation number of the order of 0.02, which would indicate severe cavitation potential even for steel. Also, it is very unlikely that any of the six piezometers used are located exactly at the point of lowest pressure, hence, lower pressure heads than those shown are quite likely to exist elsewhere on the side walls. Because of the low pressures associated with the gate recesses and because the recesses would cause the flow past the seals, with the gate retracted, to be deflected back directly onto the gate frame, it was decided to see if a geometry utilizing a simple wall offset would be acceptable. A simple offset wall would not have a re-entrant corner that would cause negative pressures and would not direct the retracted flow back onto the gate frame.

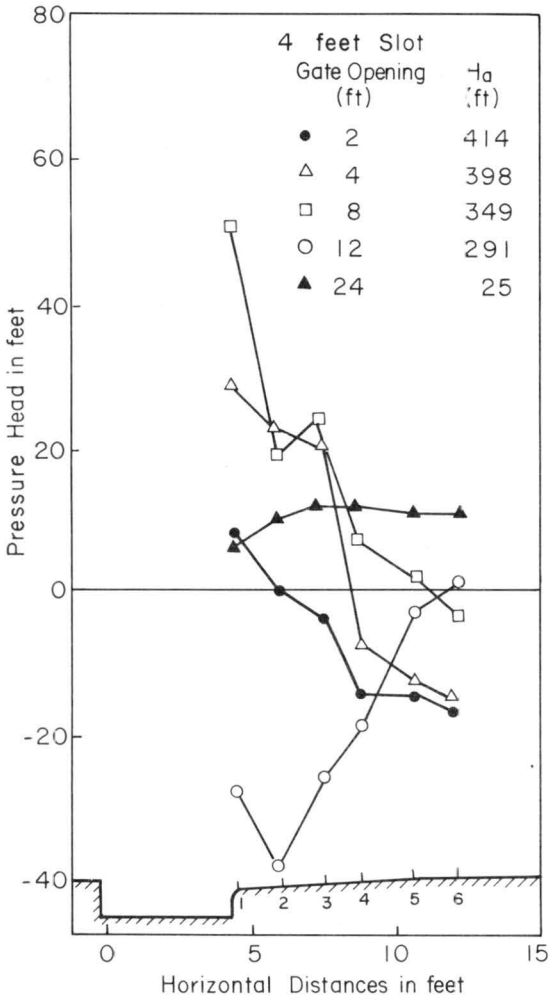

Figure 71. Piezometer pressure heads obtained from 1:70-scale model with 4.0-ft wide rectangular gate slot. Piezometers located 2 feet above the floor level.

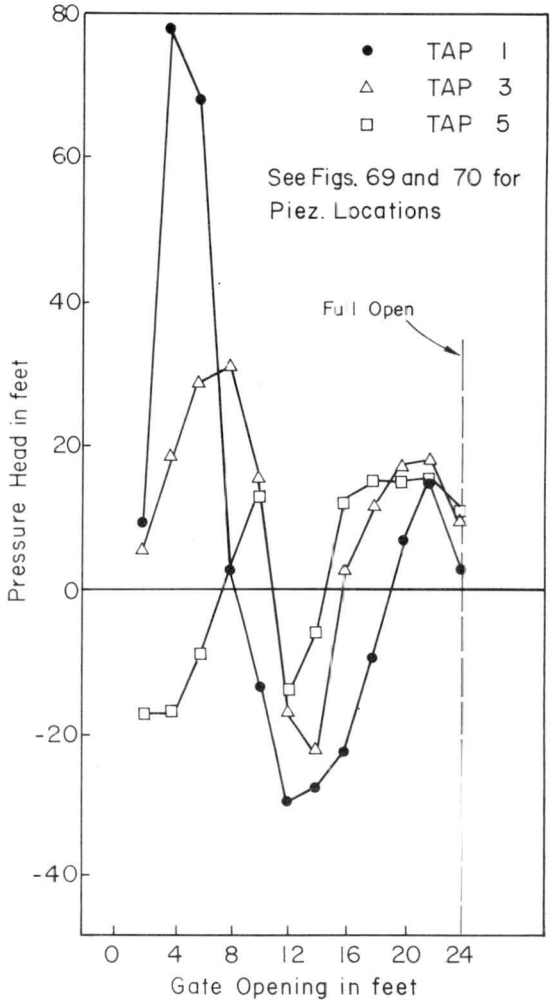

Figure 72. Effect of gate opening on piezometer pressure heads for 1:70-scale model with 2.5-ft wide rectangular gate slot.

The 33-Inch Wall Offset

The model configuration without an insert represented a 33-inch wall offset as shown in figure 63(a). This arrangement was tested in the earlier tunnel study (Ref. 2). As was found before, the effect of the offset was to create a large rooster tail at the point where the laterally expanding flow made contact with the offset wall. The flow for the gate 12 feet open is shown in figure 73. The solid part of the rooster tail almost touches the trunnion and considerable spray arches much higher. It would be necessary to reduce this effect, thus, a smaller 16-in. offset was tested.

The 16-Inch Wall Offset

The 16-in. wall offset, reproduced by the insert shown in figure 63(d), performed well in the 1:70 scale model and was finally selected for testing in the 1:12 scale model. The smaller offset produced a smaller rooster tail, which appeared to be acceptable from the point of view of spray and gate-wall height. The flow with gate openings of 4 ft, 8 ft, 12 ft, and full open are shown in figures 74 through 77, respectively. The rooster tail is highest at a gate opening of about 8 feet but it is approximately half as high as for the 33-inch offset (compare with figure 73). It is also not measurably larger than for the rectangular gate recesses (compare with figure 68).

The conditions with the 16-in. offset appeared to be as satisfactory as any gate recess geometry tested and had several advantages. First, the side seal flow with the gate retracted should remain close to the wall and not impinge on the gate frame. This, of course, could not be tested on the small model. Second, the wall surface was flat in the area of impingement of the widening flow from the gate so that there should not be localized subatmospheric pressures. Last, the geometry would be more easily adapted for construction in the prototype than any of the others. It should be mentioned here that the 16-in. offset was the smallest that could be used because of gate clearance requirements.

Recommendation

The significant result of those presented in this section is that a 16-in. offset should be modeled in the 1:12 scale model. This appeared to be the simplest and best arrangement from a hydraulic standpoint.

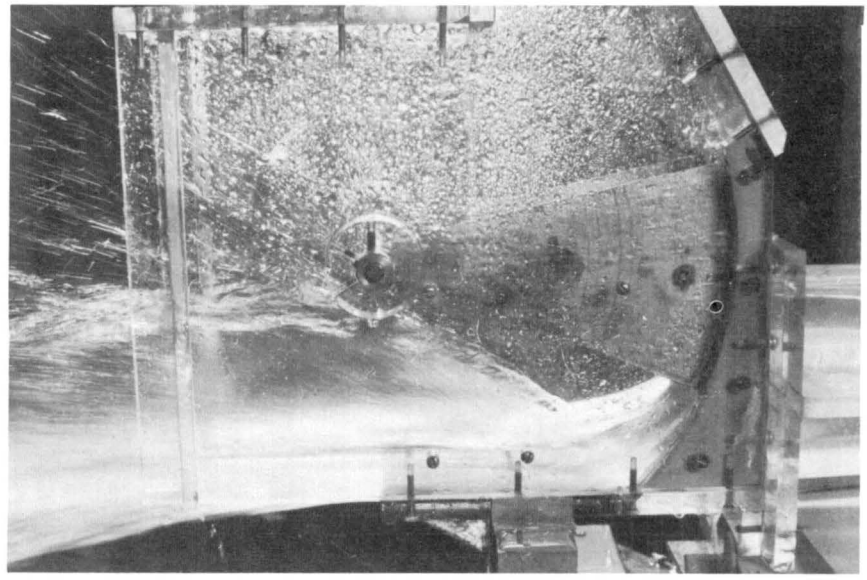

Figure 73. 1:70-scale model with a 33-in. offset for 12-ft gate opening and 290-ft head.

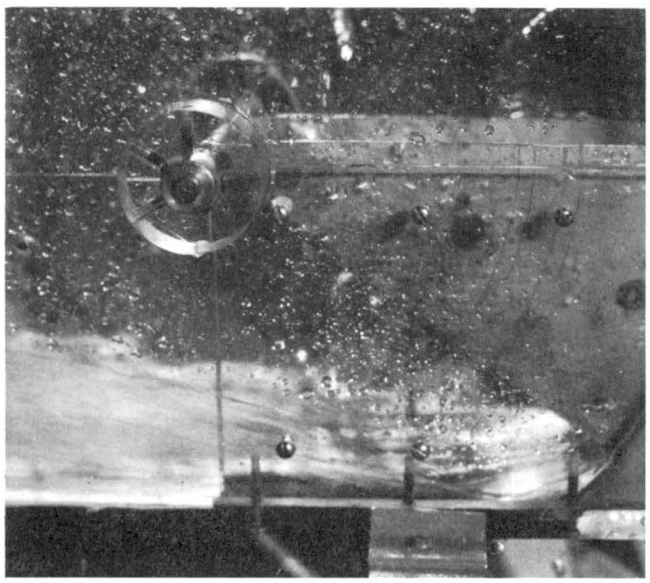

Figure 74. 1:70-scale model with a 16-in. wall offset for 4-ft gate opening and 415-ft head.

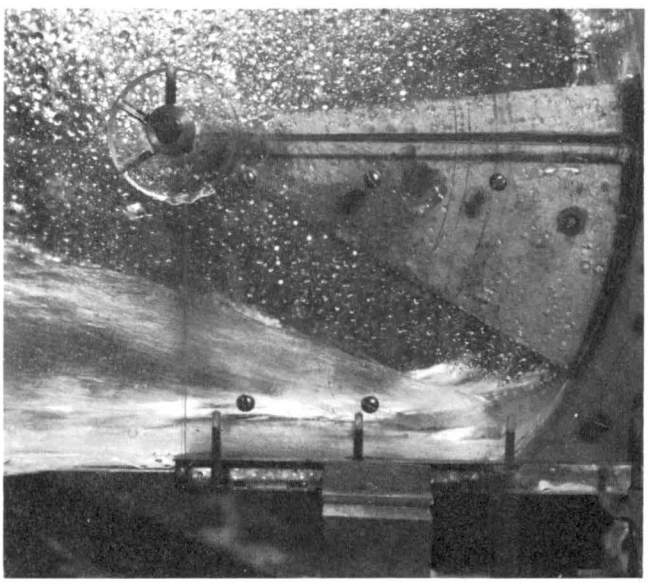

Figure 75. 1:70-scale model with a 16-in. wall offset for 8-ft gate opening and 360-ft head.

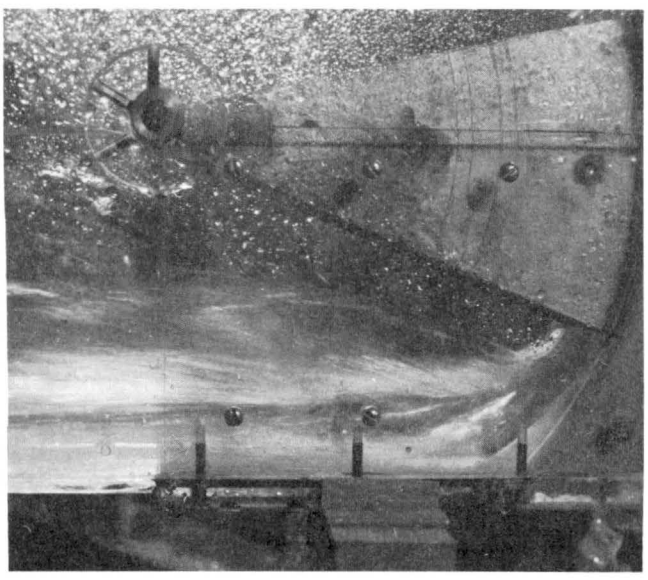

Figure 76. 1:70-scale model with a 16-in. wall offset for 12-ft gate opening and 260-ft head.

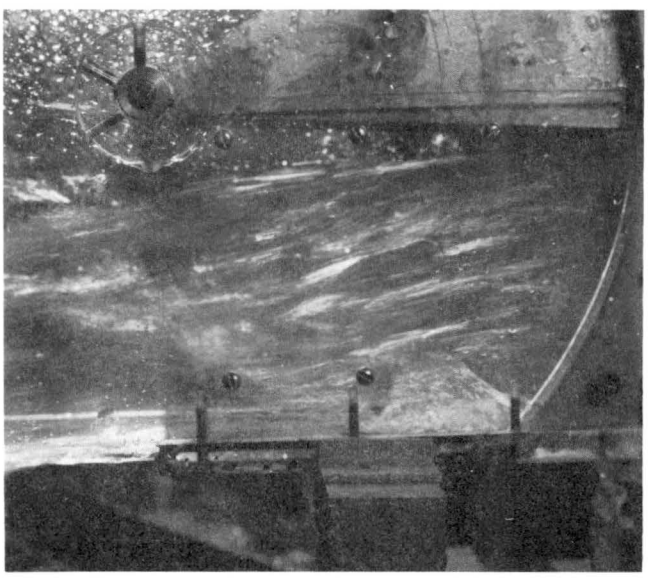

Figure 77. 1:70 scale model with a 16-in. wall offset for gate full open and 50-ft head.

V. 1:12 RADIAL GATE MODEL - MODIFICATIONS

The Model

Modifications were made to the 1:12 model of the radial gate. The first was the change to 16-in. wall offsets of the gate structure, as shown in figure 78. New plastic walls were machined and installed. A second modification was the addition of 160 feet of chute downstream from the gate structure. The deflector hood was raised so that the leading edge was at elevation 1158. Although previous study had indicated a lower position would be equally acceptable, greater space was needed in the gate chamber for mechanical or maintenance reasons. The changes are shown schematically on figure 79. The upstream piping was changed so that the 20-in. butterfly valve was located approximately 150 ft upstream of the gate and 135 feet of 24-in. diameter pipe preceded the transition. This was done to facilitate construction of an adjacent flume, not because the prior location of the valve was unsatisfactory.

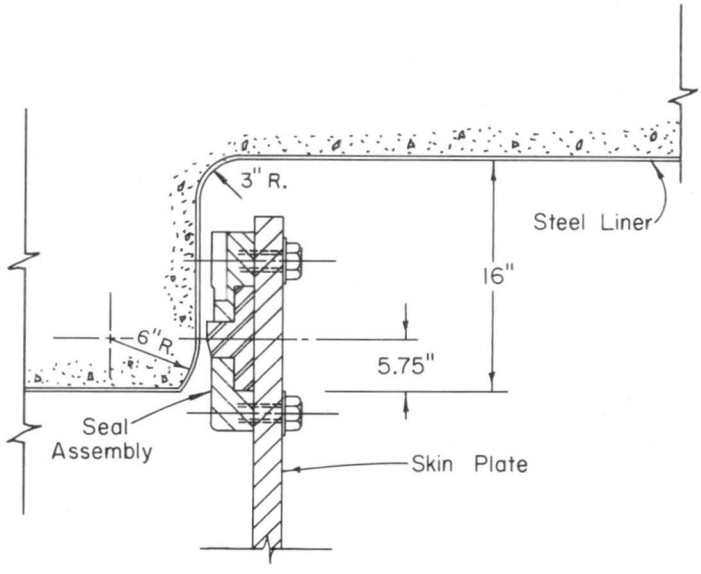

Figure 78. Cross-section of the wall offset geometry.

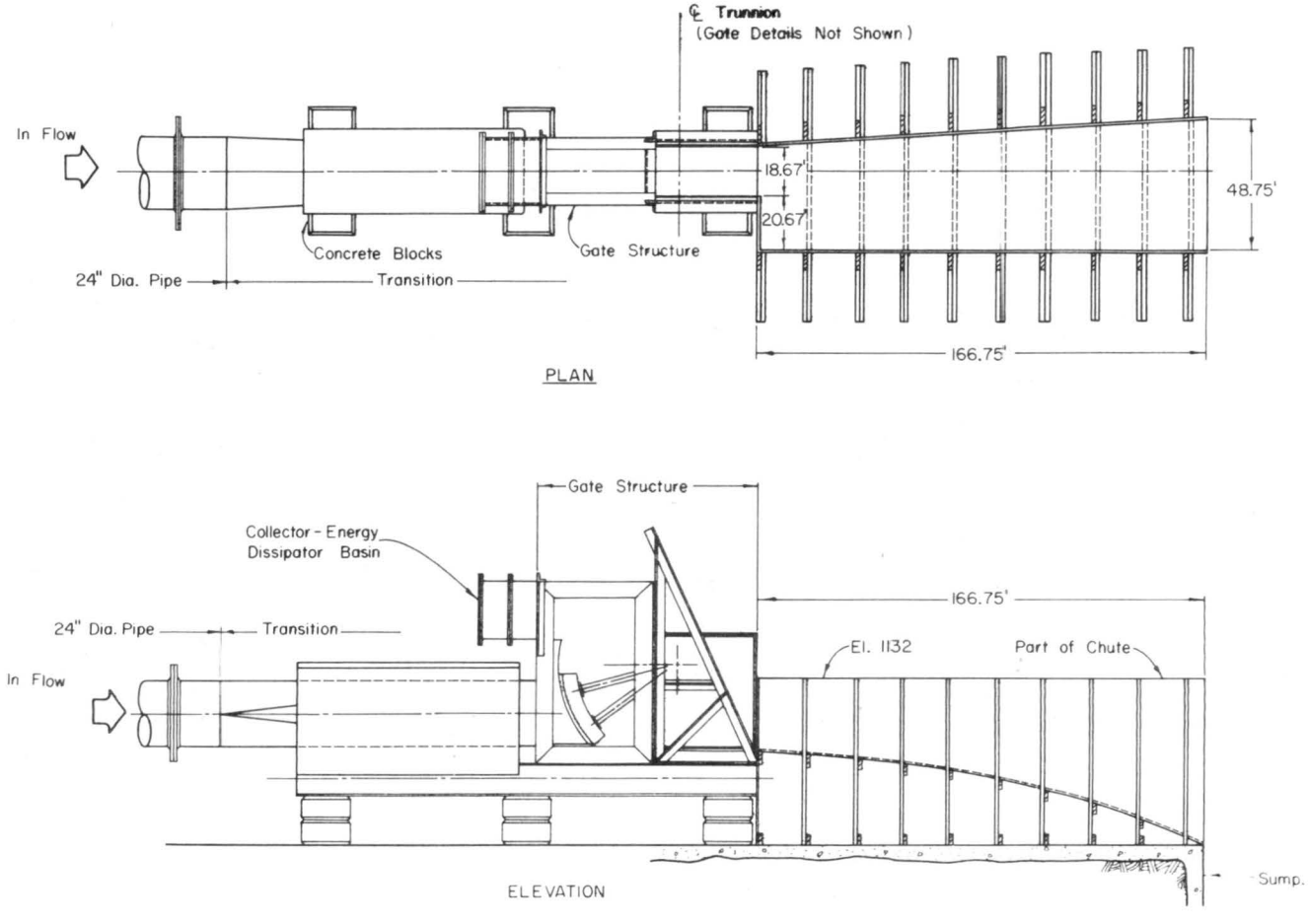

Figure 79. 1:12-scale general model of the radial gate with modifications.

Results

The major modification to the model was the 16-in. offset of the side walls of the gate structure. The discharge rating curves for the gate at various openings, the forces on the gate and performance of the collector-energy dissipator basin would not be affected by the modification. Thus, only flow features downstream from the radial gate were examined and are reported in this section.

Flow with gate retracted - The initial tests were made with the radial gate closed and retracted. The flow in the gate structure with a seal gap width of 0.28 in. and heads of 150 and 450 feet are shown in figures 80 and 81. Jet arrestors were obviously not installed in these tests. The flow picture seen in figure 80 is comparable with figure 52 for the triangular gate slots. The jets along the side walls pass below the trunnion and at low heads they are contained within the walls of the chute. At large heads, however, the water sprays to considerable heights above the chute walls as shown in figure 82. Some of the spray extends laterally beyond the wall as well. When the gap width was increased to 0.8 in. with a head of 450 ft, the resulting flow along the wall and beyond the gate structure can be seen in figures 83 and 84. Clearly, the spray must be contained; the jets of water seen in figures 82 and 84 would probably create mountainous clouds of mist in addition to "solid" spray in the prototype.

The jets of water past the top seal are directed adequately by the deflector into the basin. Of course at low heads, as in figure 80, the water falls onto the arms of the radial gate or into the gate chamber as discussed in section II. Without the jet arrestor, the upper corner flows past the gate seal, seen in figures 80, 81, and 83, miss the deflector and continues upward past the gate hoist assembly in a great arch. The corner flows contain radial and upward velocity components with the result that the combined vector velocity jets the flow so that it misses the deflector hood.

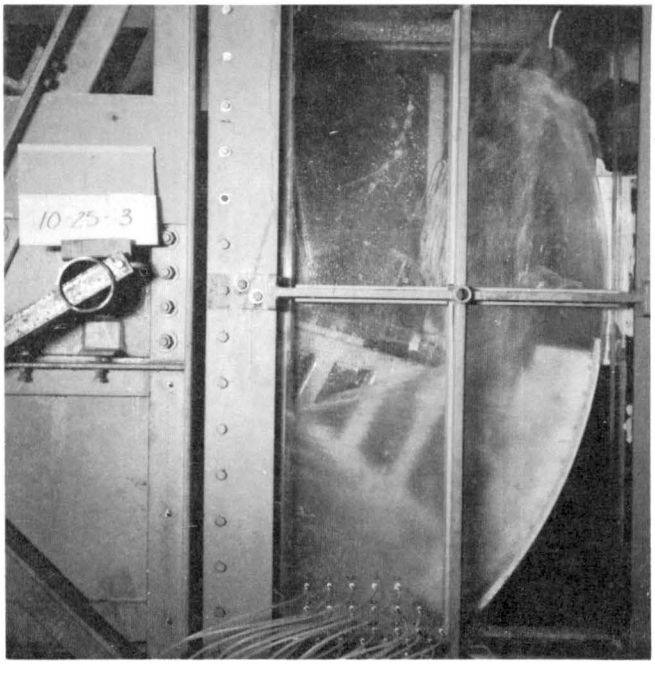

Figure 80. Gap width is 0.28 in. and H_a is 150 ft. Gate is closed.

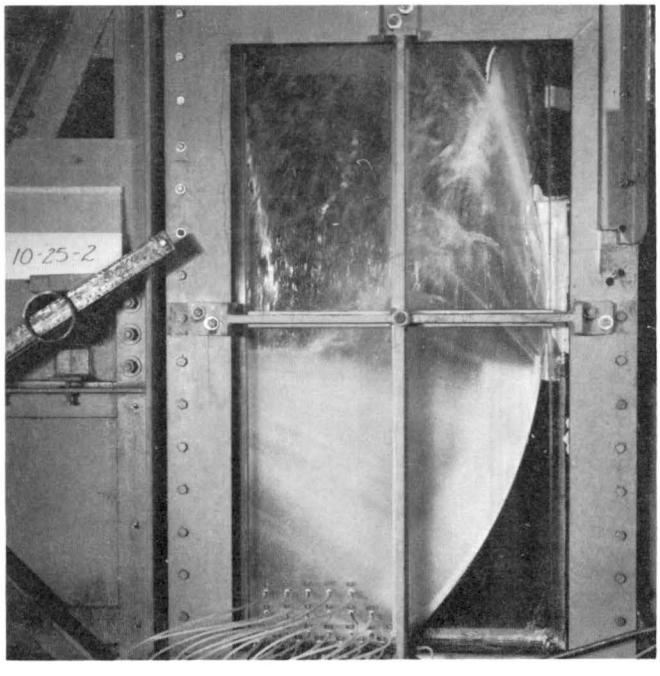

Figure 81. Gap width is 0.29 in. and head is 450 ft. Gate is closed.

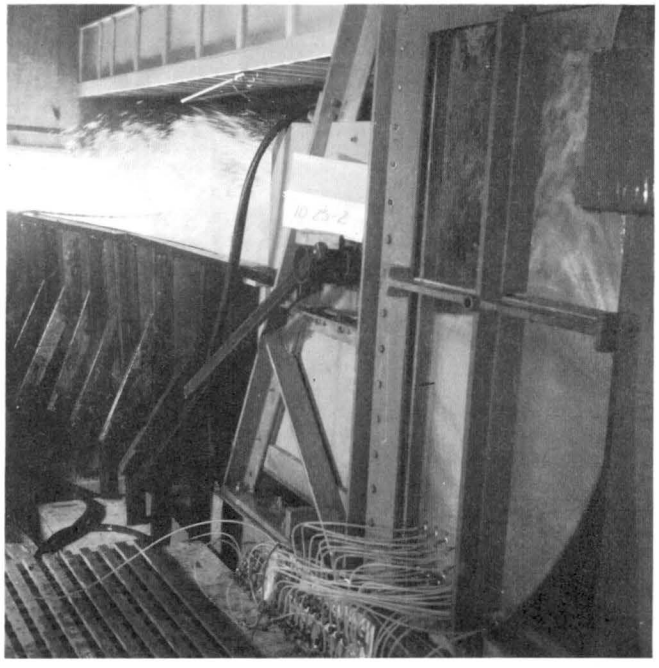

Figure 82. The jet along the side wall sprays high above and laterally beyond the chute wall. Condition is same as in figure 81.

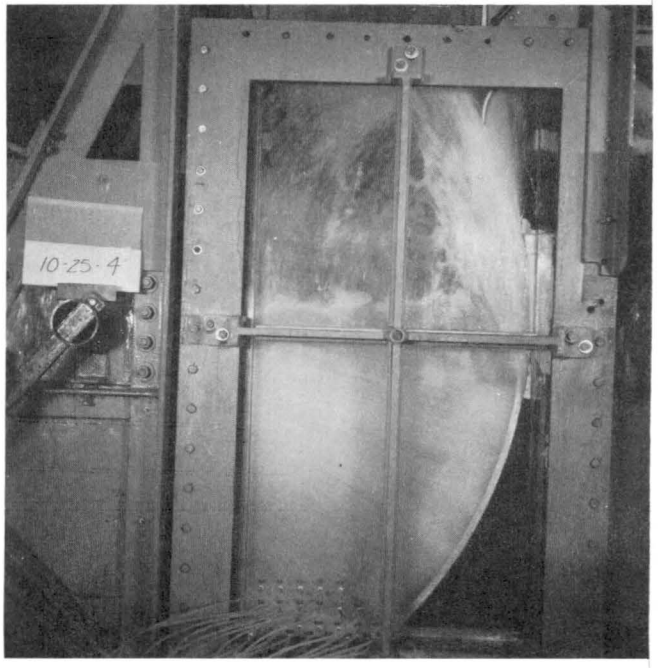

Figure 83. Gap width is 0.8 in. and head is 450 ft. Gate is closed.

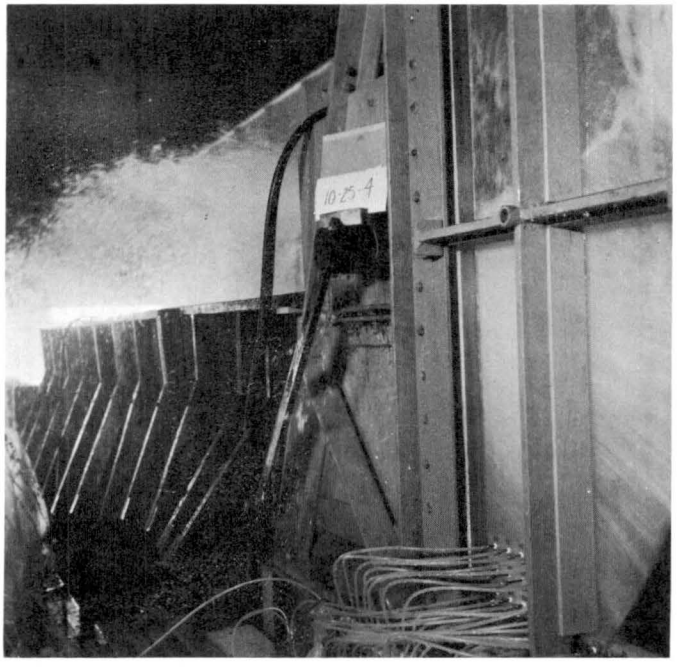

Figure 84. The spray from the side seals extends high above and laterally beyond the chute wall.

With the gate partially open and retracted, the jets become even more accentuated. In fact, when viewed in terms of the prototype, they might be termed spectacular. The flow resulting from a gate opening of 11.2 ft, gap width of 0.8 in. and head of 400 ft is shown in figures 85, 86, and 87. The spray would be even higher if it were not for the ceiling placed above the gate structure in the model to deflect the corner jets.

It is evident that at least two features of the flow must be controlled. First, the jet past the side seals must be deflected back and contained within the gate structure and chute; and second, the corner jets must be stopped. From previous tests it was evident that the jet arrestor above the top seal would eliminate the corner jet. Control of the wall jets was effected by a deflector with the shape and arrangement shown in figure 88. The shape (longitudinal radius) was established in such a way that deflection would always be downward and away from the oncoming flow.

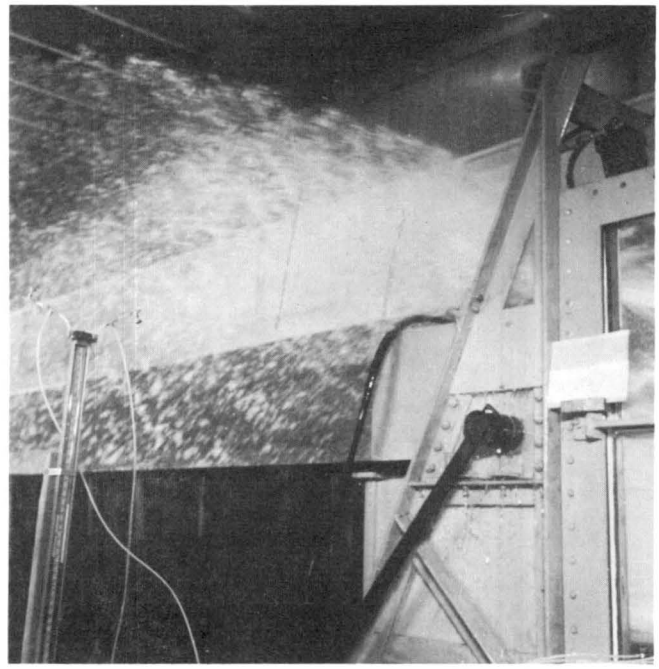

Figure 85. Jet beyond the gate structure. Gate is open 11.2 ft, head is 440 ft and gap width is 0.8 in.

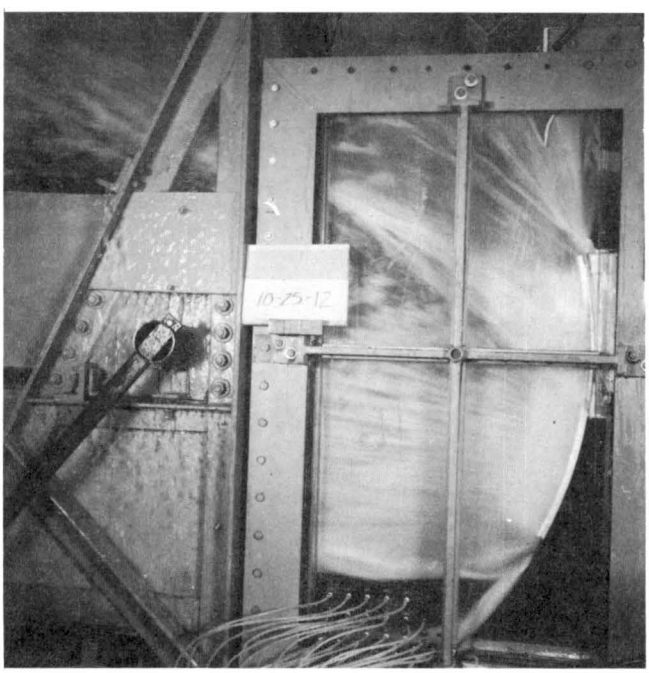

Figure 86. Flow in the gate structure for the gate and head conditions for figure 85.

Figure 87. View of the flow of figure 85 as seen from above.

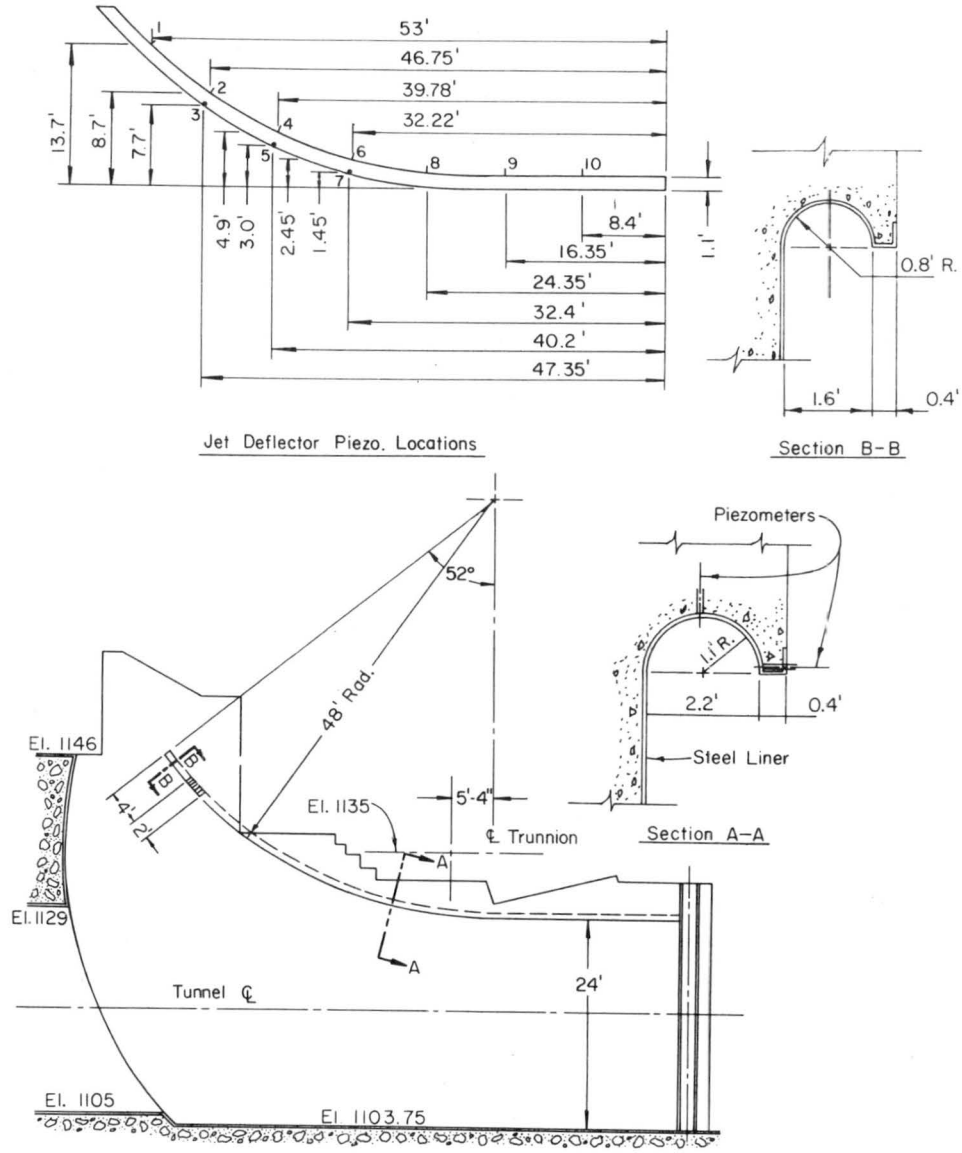

Figure 88. The side-wall deflector - placement and details.

With the deflectors in place, all the flow around the periphery of the gate was well contained within the waterway channel for the entire range of heads and gap widths with the gate closed. The conditions of flow for a gap of 0.8 in. (which were most severe) and head, H_a, measured in the transition of 150 ft are shown in figures 89 and 90. The entire side-wall jet is deflected effectively back into the channel. The side-wall deflectors functioned as well when the head was increased to 450 feet, as shown in figures 91 and 92. The corner jet which appears in figure 91 resulted from a faulty rubber seal which simulated the jet arrestor. At a head of 450 ft, to which the rubber seal was subjected with a gap of 0.8 in., the pressure deformed the rubber seal and some of the flow passed by. That this was a manifestation of model workmanship and inferior material is verified by figure 93, where the seal gap width was reduced to 0.28 in. and the head maintained at 450 ft. No corner flow resulted in that test.

The side-wall deflectors, which extend to elevation 1146, appeared to be adequate. The flow resulting from a gate opening of 12.35 ft, retracted to 0.8 in. gap width with a head of 350 ft is shown in figures 94 and 95. It is evident that the deflectors functioned satisfactorily.

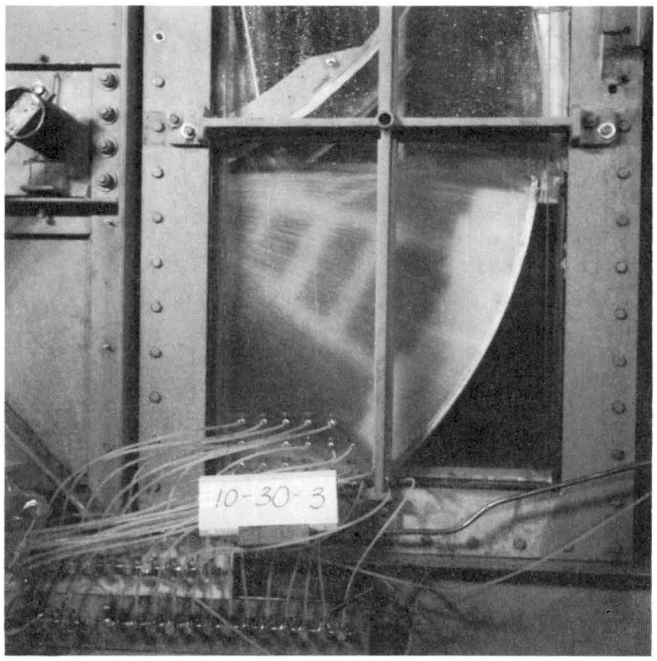

Figure 89. Side-wall deflectors and jet arrestor were installed. Gate is closed, gap is 0.8 in. and head is 150 ft.

Figure 90. The effectiveness of the side-wall deflectors is seen for the condition of figure 89.

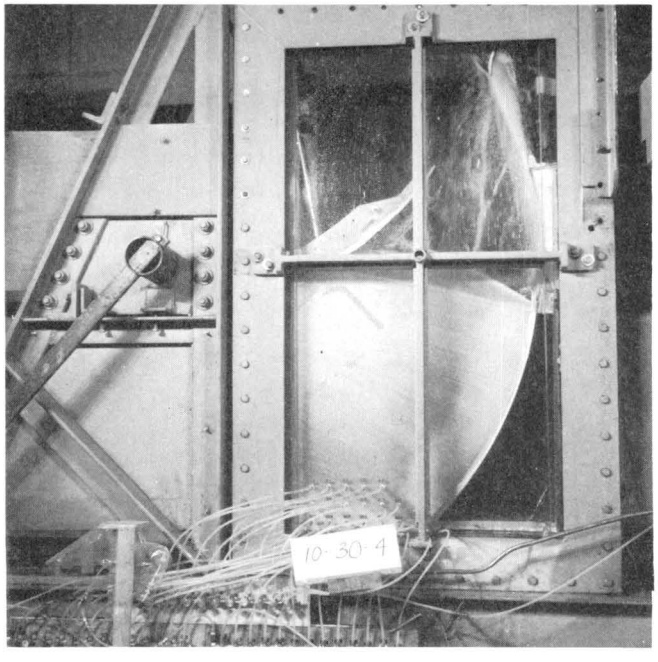

Figure 91. Head is 450 ft, gap width is 0.8 in. and gate is closed. The corner jet is a result of an inferior rubber seal which simulated the jet arrestor.

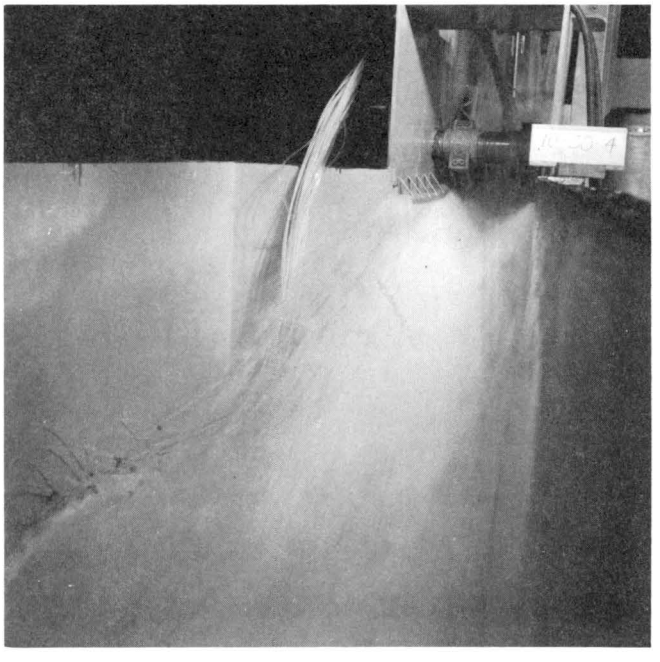

Figure 92. The effectiveness of the side-wall deflectors is clearly evidenced.

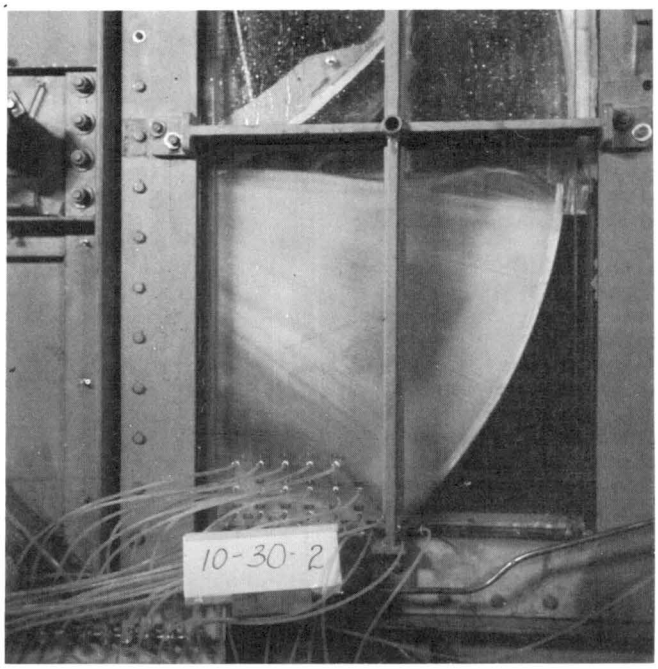

Figure 93. Seal gap is 0.28 in., head is 450 ft and the gate is closed. No corner flow is evident here.

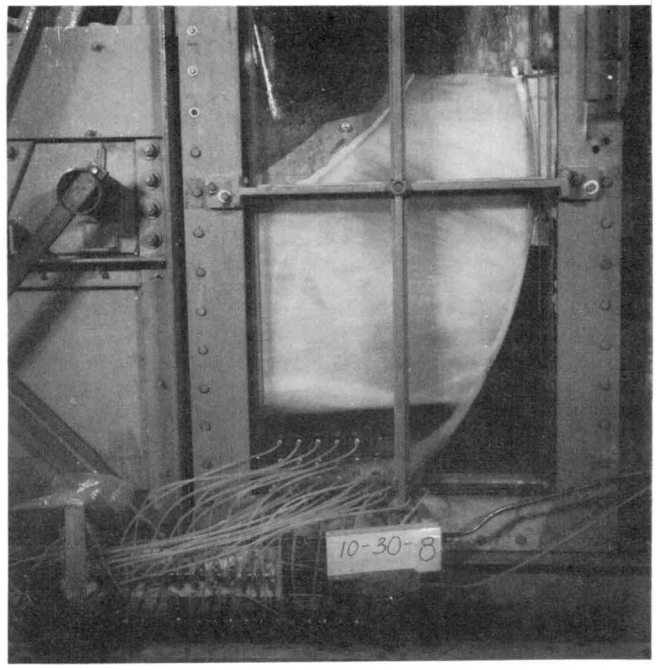

Figure 94. Gate is open 12.35 ft, gap width is 0.8 in. and head is 350 ft.

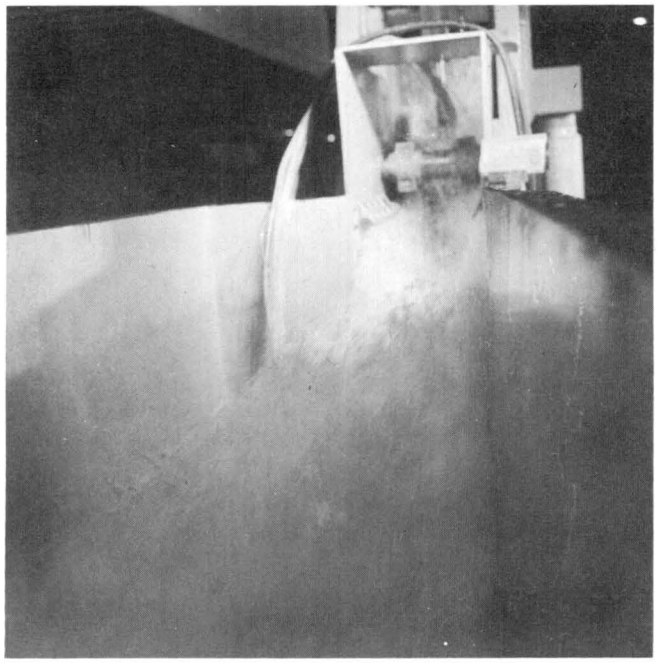

Figure 95. Flow in the channel for the condition in figure 94 as viewed from the chute. The side-wall jets are well contained by the deflectors.

Flow with gate seated - The flow beneath the gate and in the channel for nominal gate positions of 4-, 8-, and 12-ft openings are shown in the series of photographs, figures 96 through 101. The offset of the walls cause rooster tails to form where the expanding jet from the 16-ft wide transition impacts with the wider channel of the gate structure. The rooster tailing was greatest at the 8-ft gate opening, although this is not entirely clear from the photographs. This was also the case with the 1:70 model reported in section IV and can be seen by comparing figures 74, 75, and 76. Although the heads do not match exactly, there is considerable similarity in details of the flow in figures 96, 98, and 100 with comparable flows in the 1:70 model. This fact was mentioned earlier in section IV. In addition to the height of the rooster tail, the vortices formed at the offsets have remarkable similarities.

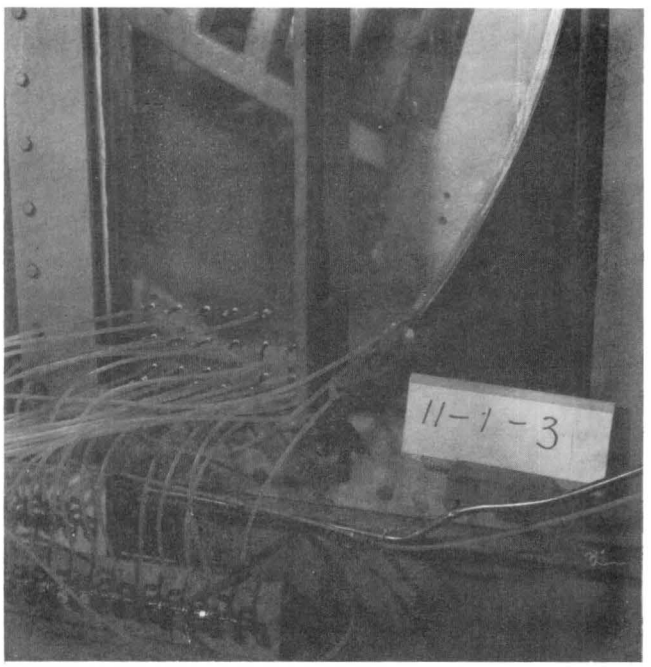

Figure 96. The gate is open 4.1 ft with a head of 450 ft.

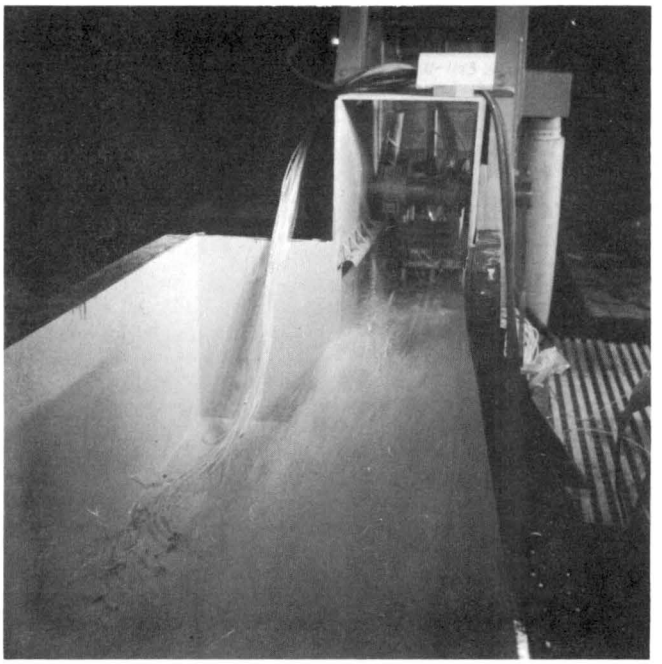

Figure 97. The rooster tail at the walls created by the expanding flow causes some spray which extends above the wall.

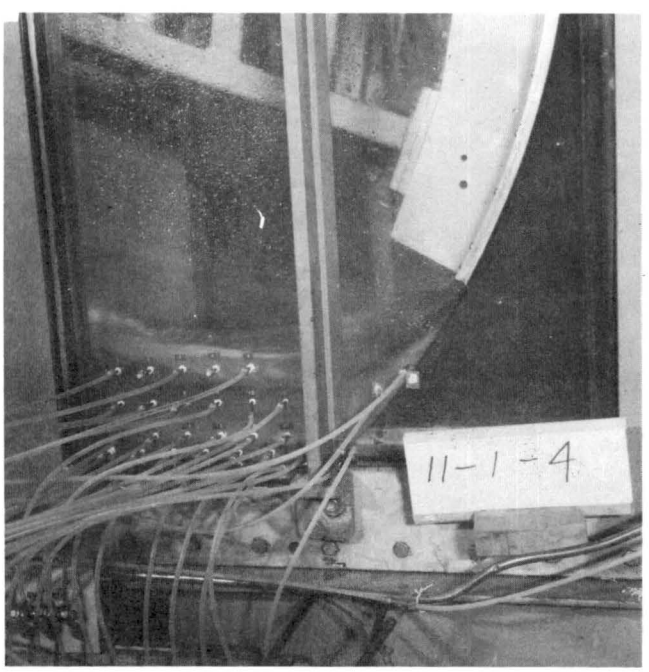

Figure 98. The gate is open 8.25 ft with a head of 150 ft.

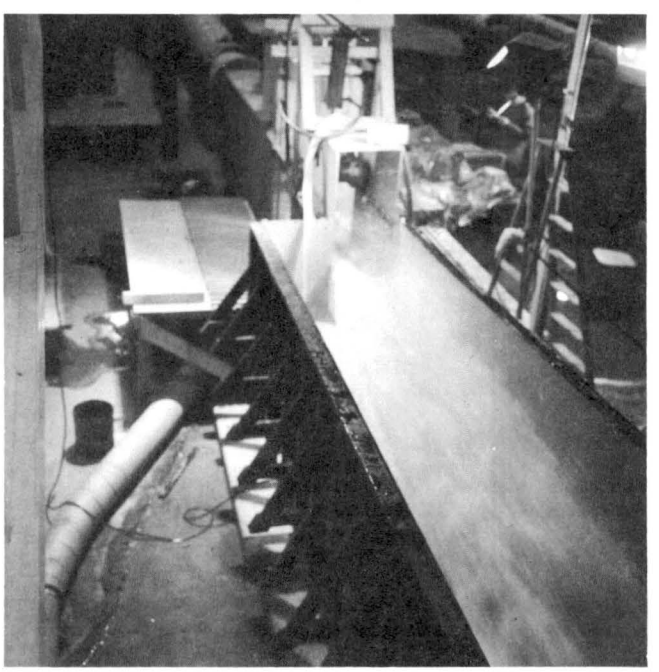

Figure 99. There is some spray along the chute wall created by the rooster tails for the conditions given for figure 98.

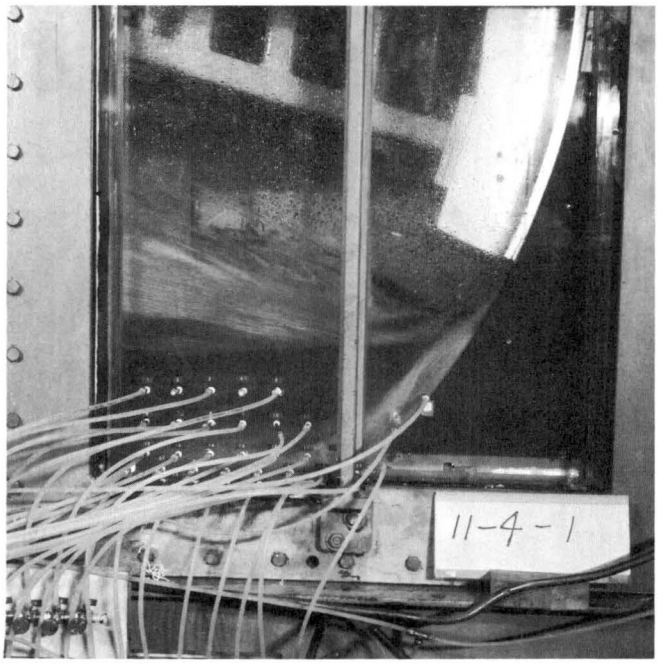

Figure 100. Gate opening is 12.25 ft and head is 200 ft. Origin of the rooster tails is clearly seen.

Figure 101. The spray resulting from the rooster tails extends above the chute walls.

There was some concern with the quantity of water which splashed laterally beyond the chute wall. Although in the model only a few drops, akin to light rainfall, fell beyond the walls, perhaps protection of the terrain surrounding the chute would be in order for the prototype. A closer view of the spray created with a gate opening of 8 ft and head of 400 ft is seen in figure 102. The string gridwork on the right of the figure and the dark backdrop on the left were set up in an attempt to photograph the trajectories of the spray droplets in time exposure so that the envelope of the droplets could be identified. Unfortunately, the photographs taken from the side did not show the desired result. A visual sketch of the envelope was therefore made, using the grid as reference. The sketch is shown in figure 103. A description of the "more solid" jet is rather difficult; but with reference to figure 102, the region below the all-white portion of the jet in the photograph is the "more solid" jet. The trajectories of isolated droplets appear as separate streaks and the highest trajectories of identifiable isolated drops is confined within the "upper envelope of droplet spray." Attention should be focused on the portion of the droplet spray which goes beyond the lateral confines of the channel. Visually, it is seen in figure 102 that the proportion is small.

The flow with the gate fully open is shown in figures 104 and 105. There is no problem with spray or rooster tailing when the gate is fully open. Note in the photograph that the water surface is below the deflectors.

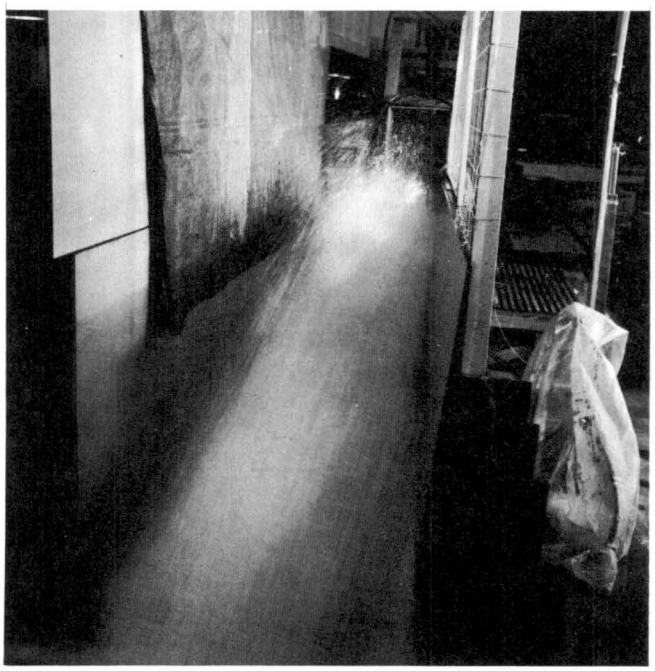

Figure 102. Gate is open 8 ft and H_a is 400 ft. Note the trajectories of the droplet spray.

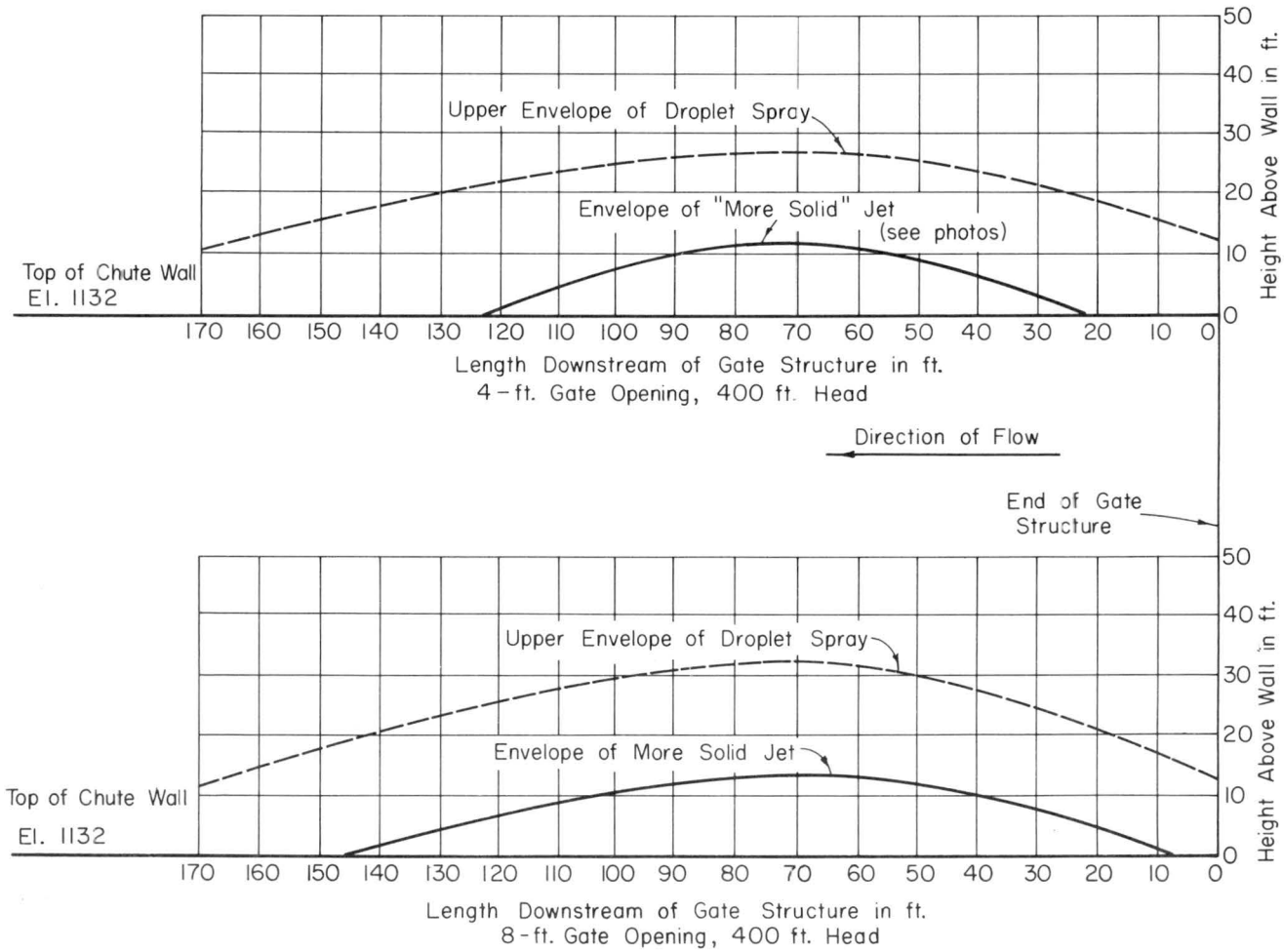

Figure 103. Trajectories of the spray which extend above the chute walls.

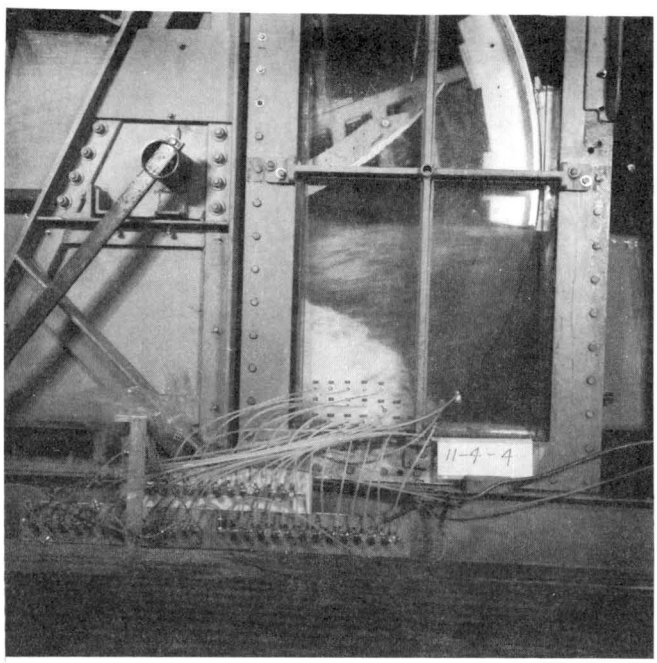

Figure 104. Gate is fully open.

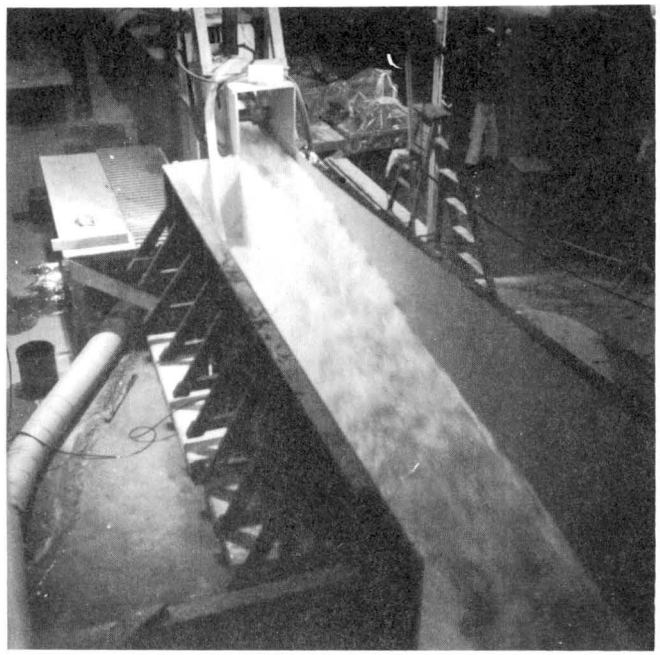

Figure 105. There is no problem with rooster tailing when the gate is fully open. The water surface is below the level of the deflectors.

There will undoubtedly be considerable mist developed in the region of the outlet works for tunnels 3 and 4 from the combined effects of the flow through the gate structure and the hydraulic jump in the stilling basin. The mist will keep the terrain wet, and if there is sufficient accumulation of moisture, erosion protection may be required. It may be helpful, therefore, from a view point of erosion protection, to prevent even small amounts of water from escaping the bounds of the channel. One way to contain the spray is to construct a roof across the chute walls. Tests were made to determine how far the roof must extend downstream from the gate structure to contain all of the spray within the channel. The arrangement in the model is shown in figure 106. The box girder was placed downstream of the trunnion and the roof was extended downstream from the girder at the level of the channel walls.

Tests were made only with a gate opening of 8 ft at 400 ft head, representing the worst spray conditions in the model. It was found that in order to contain all the spray within the channel the roof must extend approximately 24 feet downstream from the stop-log slots. If there is no roof between the stop-log slots and the girder, some spray from the walls will terminate outside the wall of the chute. Since the stop-log slot must be open and the roof must extend to the girder within the gate structure, one way to arrange both needs is to construct the roof at a lower elevation within the gate structure at, say, elevation 1130.5 slightly above the level of the wall deflectors, leaving the slot open for the stop logs and continuing the roof downstream at elevation 1132.

Wall pressures - The piezometers in the wall and the floor of the gate structure are numerically identified and the locations are shown in figure 107. Pressure fluctuations were recorded with a transducer and analog FM tape recorder. The data were analyzed digitally to determine means and standard deviations of the fluctuating pressures. The mean pressures are tabulated in the appendix in Table A-3.

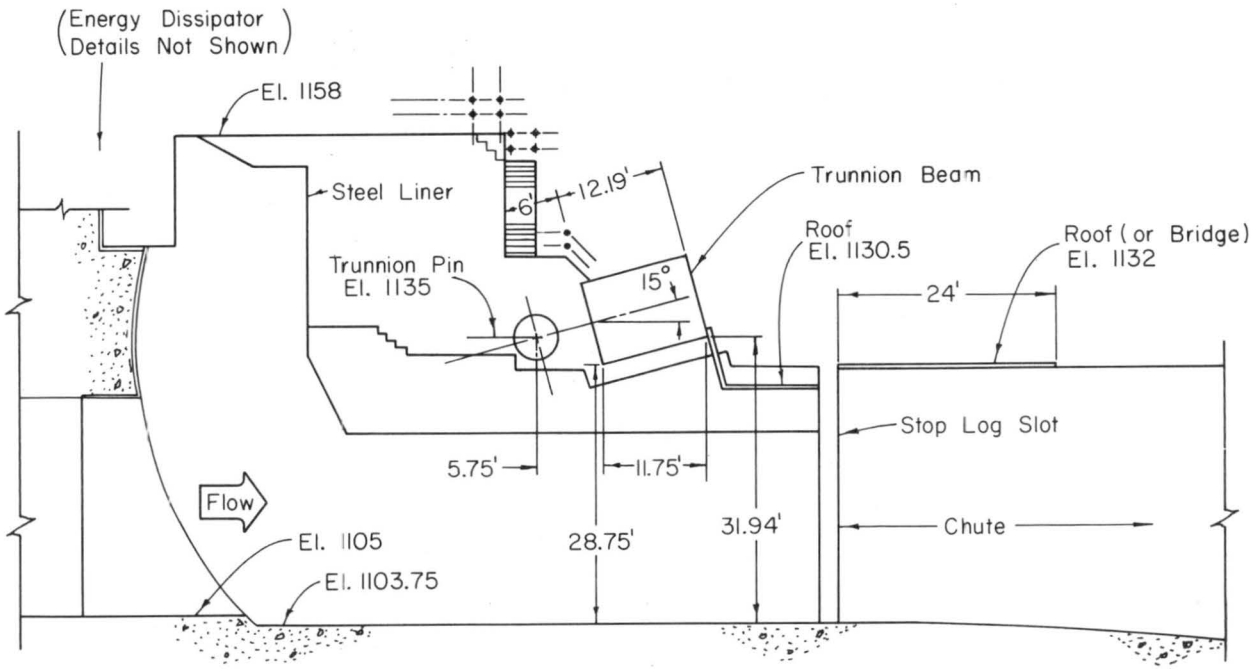

Figure 106. Suggested roof arrangement and dimensions to contain spray.

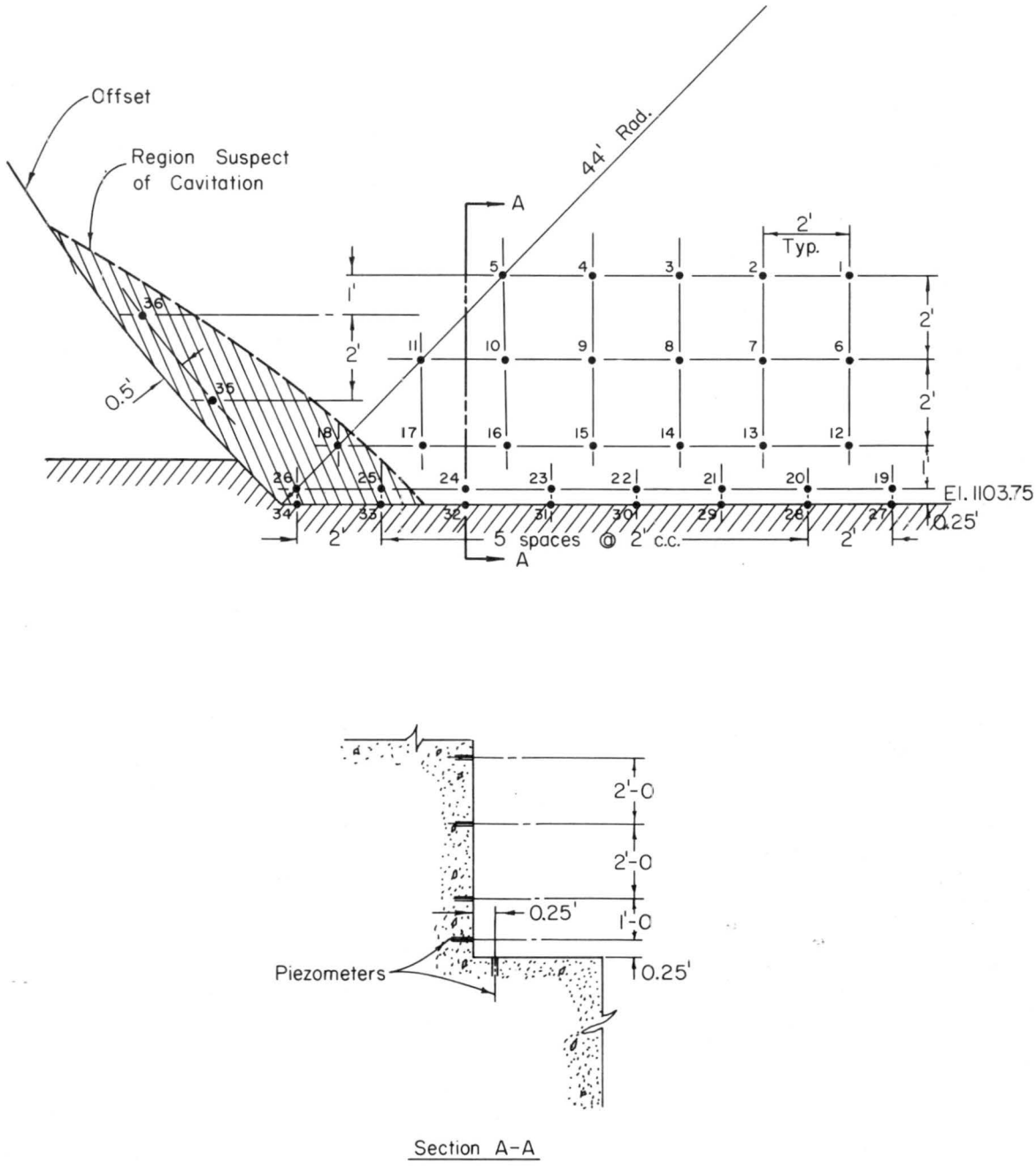

Figure 107. Piezometer locations in the 16-in. offset wall, 1:12 model.

There is a small region of the wall containing piezometers 18, 25, 26, and part of the floor of the gate structure near piezometers 33 and 34 which are subject to low pressures. Although the mean pressures are positive, relative to atmospheric pressure, the standard deviations of the pressure fluctuations are about the same order of magnitude as the means. For instance, with a gate opening of 4.1 ft and head of 150 ft, the mean head at piezometer 33 was 16.0 ft with standard deviation of 11.2 ft. In another instance, at a gate opening of 8.25 ft with a head of 400 ft, the mean head at piezometer 34 was 69.1 ft while the standard deviation of head was 42.6 ft. In order to determine the nature of the pressure fluctuations at these and other piezometers, probability density functions and cumulative distributions were calculated from the recorded signals. Three of these calculations are plotted in figures 108, 109, and 110. Evidently negative pressures exist for a small portion of the time even though the mean pressures are positive everywhere on the wall (with the exception of piezometer 36 for the 12.25 ft gate opening at H_a = 275 ft where the mean pressure head was -2.74 ft). The area under the probability density curve gives the probability of encountering a given pressure head within a chosen range and the cummulative distribution function indicates the percentage of the fluctuations less than a particular pressure head. Thus, the probability of pressure heads, at piezometer 33 for gate opening of 4.1 ft and H_a of 150 ft (see figure 108), in the range from 0 to 10 ft would be given by the area under the curve. The total area under the probability density curve must necessarily be unity. Also from figure 108, it is seen that the probability of pressure heads less than say -10 ft is about 0.002 from the cumulative distribution curve.

These example calculations are given to indicate that there is cavitation potential along the wall near the floor of the gate structure, just downstream from the offset. The area which may be subject to cavitation is crosshatched on figure 107, which is within the area that is planned to be provided with steel liners. It should also be recalled that this is a region where the flow is well aerated because of the offset.

Pressures on the side-wall deflector - Pressure heads on the side-wall deflectors, caused by the flow when the gate is retracted, were measured with 10 piezometers located as shown on figure 88. Two conditions were selected for measurement. The first was with the gate closed, retracted 0.8 in. with a head in the transition, H_a, of 450 ft. The second was with the gate half open (11.55 ft), retracted 0.8 in. with H_a of 420 ft. These conditions were selected because they represent the extreme conditions of operation. The results are shown in the table below.

TABLE OF PRESSURE HEADS (IN FT)
ON THE SIDE-WALL DEFLECTOR

Piezo. No.	Gate Closed	Gate Half Open
1	0.6	124.0
2	1.2	0.2
3	-0.2	13.0
4	28.2	2.3
5	2.1	4.4
6	38.2	1.9
7	63.9	0.8
8	-10.7	2.0
9	1.4	2.0
10	1.4	1.6

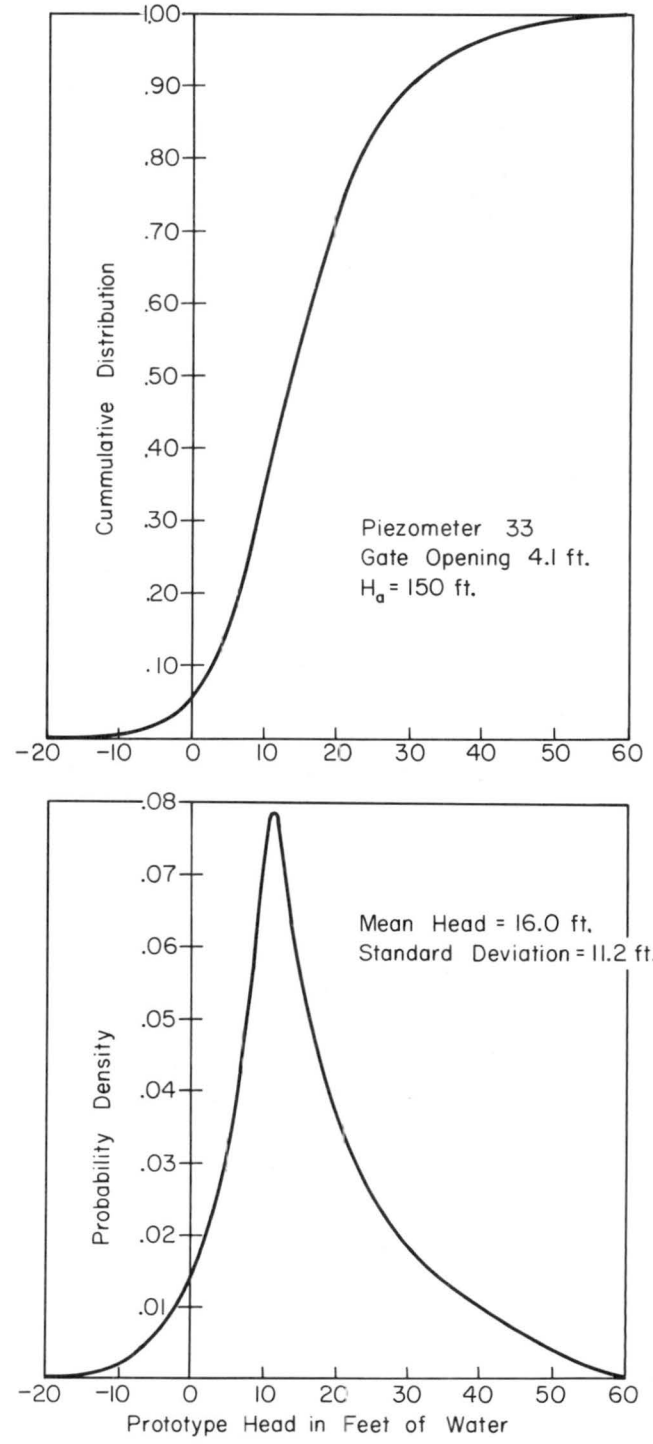

Figure 108. Probability density and cumulative distribution functions for floor piezometer 33 (see figure 107 for location). Test conditions were gate opening of 4.1 ft and H_a of 150 ft.

The negative head of -11 ft at piezometer 8 was caused by the tendency of the flow to spring free at the point of tangency of the circular curve. The subject flow is that which accumulates and tends to flow longitudinally down the length of the deflector. The majority of the flow is deflected by the circular cross-sectional shape of the deflector back into the channel. Because the gate-retracted condition is a transient operational mode, and the total time for this particular gate position is expected to be of very short duration, no problem with cavitation is expected.

Recommendations

The 16-in. offset of each wall of the gate structure from the transition wall is an acceptable arrangement from a hydraulic viewpoint. Side-wall deflectors will be necessary to deflect the jets (downward) created by gate retraction. The spray was reduced considerably when compared to the triangular gate recess geometry. A small amount of spray in droplet form still arches beyond the chute walls. If this is to be contained, a roof over the chute for a distance of approximately 24 feet beyond the gate structure will be needed.

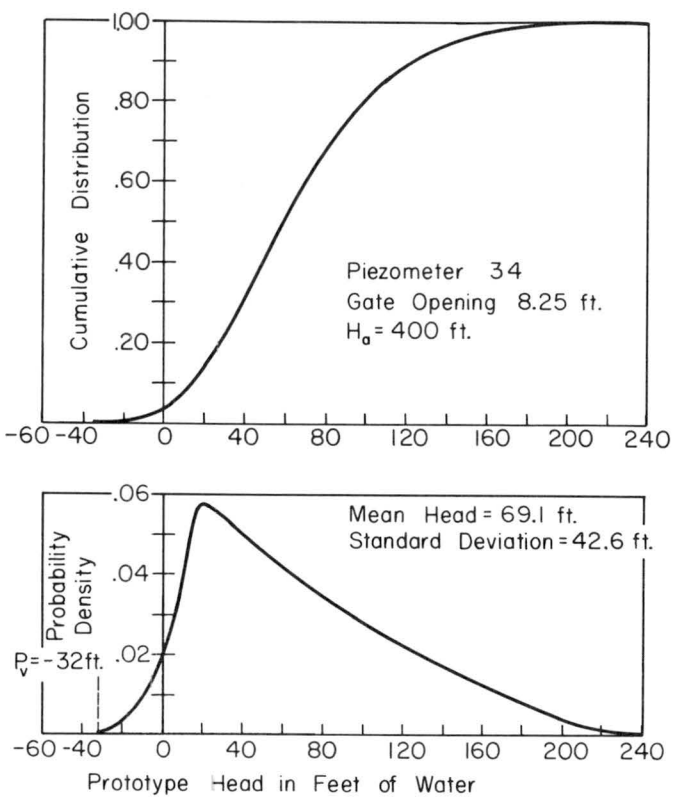

Figure 109. Probability density and cumulative distribution functions for floor piezometer 34. Test conditions were gate opening of 8.25 ft and H_a of 400 ft.

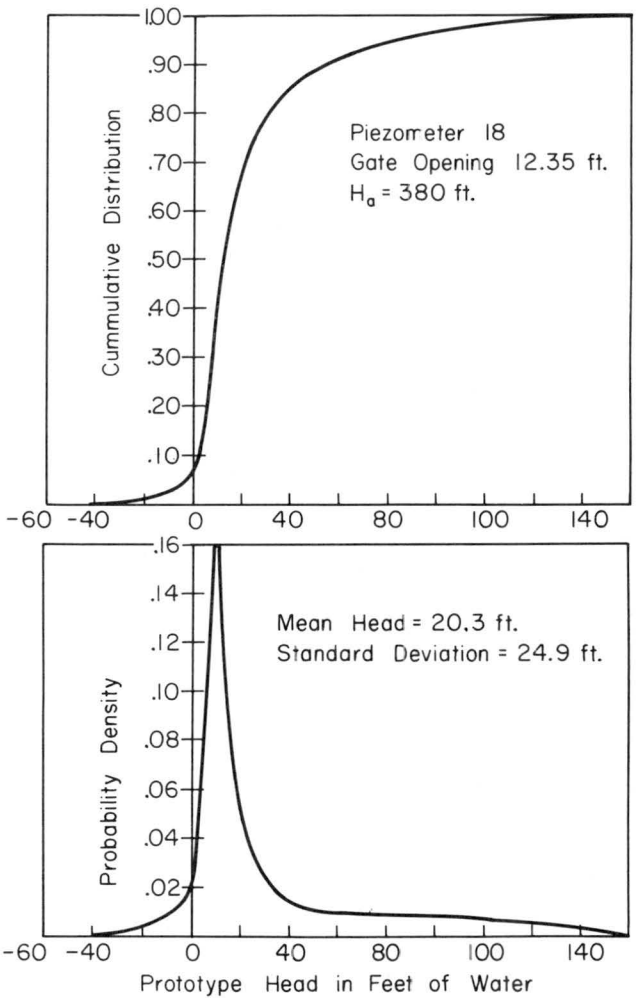

Figure 110. Probability density and cumulative distribution functions for wall piezometer 18. Test conditions were gate opening of 12.35 ft and H_a of 380 ft.

VI. CONCLUSIONS AND RECOMMENDATIONS

The radial gates at the outlets of tunnels 3 and 4 of the Tarbela project can be made to perform satisfactorily at the conditions for which they were designed. The major questions which were outlined in section I under Scope of the Model Study may now be answered in order:

(a) The large velocity flow past the seals, which occurs when the gate is retracted prior to movement, will not cause cavitation of the seal clamp bars or the gate seat. There were conditions encountered in the 1:4 scale model when ventilation was inadequate, but these conditions are generally outside the expected range of operation for the prototype. Although ventilation slots on the clamp bars were tested in the model, they are not recommended for the prototype.

(b) In the event that the jet arrestor does not function as intended, the deflector hood at elevation 1158 will adequately deflect the upward jet when pressure heads measured at the midpoint of the conduit transition are greater than 200 ft. If the seal gap is small and heads are less than 200 ft, the jet of water does not contain sufficient energy to be deflected into the collector-energy dissipator basin. The water then falls into the gate chamber and onto the arms of the radial gate. It does not appear that this condition will materially affect mechanical operation of the gate, nor cause material disruption of the flow beneath the gate. The recommended dimensions of the basin, into which the jet is deflected, are shown in figure 31. It is to be noted that in this figure the leading edge of the deflector hood is at elevation 1155 and at elevation 1158. The deflector will function equally well at both locations.

(c) With the triangular recess geometry, negative (subatmospheric) heads to equivalent prototype vapor pressure were measured in the model for all gate openings, indicating that a change in the geometry of the side walls was necessary to avoid cavitation.

(d) The side-wall jets, created when the gate is retracted, were directed by the triangular recess geometry directly onto the structural members of the radial gate arms. The jets spread out and created objectionable spray. It appeared that a change in the wall recess geometry offered the best prospect for improving the jet action.

(e) Side walls which were offset 16 inches from the transition walls were found to be hydraulically satisfactory for all normal and retracted gate positions. Side-wall deflectors were found to be necessary to keep the jets of water contained within the channel. Some spray in the form of droplets land outside the lateral boundaries of the chute walls for normal gate positions. The spray was most noticeable for a gate opening of 8 feet with maximum head. If it is desired to contain this spray within the channel, a roof above the deflectors in the gate structure and downstream of the stop-log slot on the channel wall will be required.

Pressure fluctuations at the walls were largest in a small region downstream from the offsets near the floor. The mean pressures of these fluctuations were greater than atmospheric pressures although a small percentage of the fluctuations were found to be subatmospheric. The region of the expected subatmospheric pressures is within the area of the wall where steel lining is planned. There was marked improvement over the effect of the original triangular recess geometry.

(f) The forces on the gate were determined in the model by integrating (summing) the measured pressure force over the gate surface. The model forces were larger than those predicted in design and seemed to be independent of gate position (up to half-open position). The forces on the gate determined in this study are presented on figure 37.

(g) The discharge coefficients for the gate at various openings were determined by the model and are presented in figure 35 with a continuous curve joining the data points. The coefficients for the gate were independent of head. They were not materially different from those used in design.

(h) The ventilation system originally planned, which is referred to as the primary ventilation system in this report, was not materially effective. Water was ejected from the system during each test rather than drawing air. Adequate amounts of air are drawn into the region below the nappe from the offset space. The secondary ventilation system which vents on the face of the sloping step in the floor should be provided. The vents must be located below the seating surface of the bottom seal when the gate is closed.

REFERENCES

1. Tippetts-Abbett-McCarthy-Stratton, Civil Engineering Works Design Report, Vol. 7 X-Tunnels. Tarbela Dam Project, Supplement No. 2, Tunnels 3 and 4 Outlet Gates and Hoists, July 1968. Issued by Tippetts-Abbett-McCarthy-Stratton-International Corp., New York, New York.

2. Karaki, S. and Ruff, James F., Diversion, Power and Irrigation Tunnels, Hydraulic Model Study. Engineering Research Center, Colorado State University, Fort Collins, Colorado, CER65SSK-JFR6, January 1965.

APPENDIX

TABLE A-1. DISCHARGE AND FORCE DATA

Run No.	Gate feet	Discharge cfs	Force on Gate KIPS	H_a feet	Discharge
1	2.15	2732	4910	168	.763
2	2.15	3427	7660	270	.754
3	2.15	4000	10360	367	.755
4	2.15	4532	13280	474	.753
11	7.90	9481	4730	161	.719
12	7.90	11985	7610	267	.707
13	7.90	13374	9630	342	.698
14	7.90	14694	11620	407	.703
15	11.90	14375	4960	163	.700
16	11.90	18442	7940	270	.698
17	11.90	20421	9590	328	.701
18	11.90	23224	12380	425	.701
19	16.00	22141	3310	174	.734
20	16.00	27533	4980	268	.734
21	16.00	32531	6850	373	.735
22	20.10	27482	2830	129	.763
23	20.10	41125	5800	281	.771
24	24.00	42324	0	56	.945
25	20.10	41316	0	283	.772
26	24.00	42444	0	57	.943
27	3.92	7784	11615	421	.750
28	3.92	6224	7480	266	.754

TABLE A-2. PRESSURE-HEAD DISTRIBUTION ON GATE

Piezo. No.	Pres. Head feet	Piezo. No.	Pres. Head feet	Piezo. No.	Pres. Head feet	Piezo. No.	Pres. Head feet	Piezo. No.	Pres. Head feet	Piezo. No.	Pres. Head feet
Run No. 1 Opening - 2.15 ft Head - 168 ft											
1	181.0	5	177.6	9	168.6	13	171.2	17	181.0	21	166.3
2	181.1	6	173.2	10	136.3	14	179.9	18	179.8	22	134.0
3	180.6	7	170.9	11	121.8	15	171.0	19	177.5	23	118.0
4	179.9	8	168.4	12	179.5	16	168.3	20	169.7		
Run No. 2 Opening - 2.15 ft Head - 270 ft											
1	282.5	5	276.8	9	263.8	13	266.4	17	282.8	21	260.2
2	282.7	6	270.0	10	202.9	14	280.0	18	280.0	22	209.7
3	281.9	7	267.6	11	191.1	15	266.0	19	276.8	23	185.3
4	280.2	8	262.9	12	280.3	16	262.7	20	265.2		
Run No. 3 Opening - 2.15 ft Head - 367 ft											
1	382.0	5	373.4	9	356.6	13	360.1	17	382.0	21	351.8
2	383.3	6	364.9	10	289.5	14	378.7	18	378.9	22	284.2
3	380.2	7	359.8	11	258.4	15	359.8	19	373.7	23	249.6
4	378.1	8	355.4	12	378.1	16	354.9	20	358.7		
Run No. 4 Opening - 2.15 ft Head - 474 ft											
1	486.0	5	476.5	9	453.7	13	464.5	17	486.4	21	462.6
2	486.2	6	465.6	10	369.0	14	482.7	18	483.4	22	411.6
3	485.4	7	459.5	11	329.1	15	464.0	19	479.6	23	391.7
4	482.3	8	452.0	12	482.5	16	457.9	20	466.9		
Run No. 11 Opening - 7.90 ft Head - 161 ft											
1	179.0	5	171.7	9	158.4	13	157.6	17	179.1	21	154.1
2	177.7	6	161,8	10	126.2	14	177.5	18	175.8	22	101.1
3	177.7	7	155.4	11	93.6	15	153.8	19	170.3	23	85.9
4	179.0	8	152.5	12	179.8	16	157.2	20	153.9		
Run No. 12 Opening - 7.90 ft Head - 267 ft											
1	288.0	5	277.8	9	256.8	13	253.3	17	286.8	21	250.5
2	286.8	6	259.8	10	173.8	14	284.0	18	285.3	22	161.3
3	285.5	7	252.4	11	151.6	15	249.9	19	275.1	23	139.2
4	288.5	8	245.7	12	287.4	16	253.1	20	247.5		
Run No. 13 Opening - 7.90 ft Head - 342 ft											
1	361.9	5	350.3	9	326.0	13	320.7	17	365.5	21	317.3
2	362.2	6	327.4	10	216.6	14	361.7	18	359.1	22	203.2
3	365.8	7	318.7	11	189.9	15	315.7	19	347.9	23	175.1
4	363.3	8	310.7	12	364.2	16	322.1	20	314.1		
Run No. 14 Opening - 7.90 ft Head - 407 ft											
1	437.9	5	422.7	9	395.5	13	387.1	17	439.7	21	382.9
2	439.1	6	396.5	10	263.2	14	438.3	18	435.1	22	247.9
3	435.2	7	384.2	11	230.1	15	383.6	19	418.7	23	211.0
4	436.3	8	374.6	12	436.7	16	389.9	20	378.6		
Run No. 15 Opening - 11.90 ft Head - 163 ft											
1	185.5	5	185.8	9	169.2	13	168.4	17	185.7	21	165.3
2	185.9	6	176.2	10	119.0	14	181.1	18	182.8	22	111.3
3	184.9	7	169.8	11	103.7	15	168.6	19	181.8	23	94.5
4	181.8	8	164.1	12	182.5	16	167.0	20	166.0		
Run No. 16 Opening - 11.90 ft Head - 270 ft											
1	296.2	5	295.7	9	276.2	13	270.5	17	295.5	21	264.4
2	296.6	6	282.2	10	186.6	14	292.4	18	293.9	22	174.3
3	296.9	7	272.3	11	165.7	15	269.6	19	292.6	23	149.3
4	291.6	8	263.2	12	293.7	16	266.2	20	266.5		

TABLE A-2. PRESSURE HEAD DISTRIBUTION ON GATE - continued

Piezo. No.	Pres. Head feet	Piezo. No.	Pres. Head feet	Piezo. No.	Pres. Head feet	Piezo. No.	Pres. Head feet	Piezo. No.	Pres. Head feet	Piezo. No.	Pres. Head feet
Run No. 17 Opening - 11.90 ft Head - 328 ft											
1	359.5	5	354.8	9	333.1	13	326.9	17	356.9	21	320.8
2	359.5	6	337.8	10	223.9	14	352.6	18	354.9	22	214.0
3	359.4	7	328.0	11	197.4	15	326.8	19	352.4	23	182.0
4	353.4	8	317.2	12	352.1	16	324.9	20	322.6		
Run No. 18 Opening - 11.90 ft Head - 425 ft											
1	462.1	5	460.9	9	426.9	13	426.9	17	464.1	21	411.4
2	462.3	6	438.9	10	293.7	14	454.2	18	458.1	22	273.4
3	462.0	7	422.9	11	253.8	15	422.0	19	452.3	23	231.5
4	456.4	8	408.9	12	457.2	16	422.3	20	415.1		
Run No. 19 Opening - 16.00 ft Head - 174 ft											
1	0	5	206.9	9	205.2	13	207.2	17	0	21	194.4
2	0	6	210.3	10	157.8	14	208.4	18	208.7	22	146.9
3	0	7	203.1	11	139.3	15	203.8	19	203.7	23	123.8
4	209.2	8	208.4	12	208.6	16	204.6	20	199.5		
Run No. 20 Opening - 16.00 ft Head - 268 ft											
1	0	5	311.7	9	303.4	13	311.3	17	0	21	291.5
2	0	6	316.0	10	234.8	14	312.3	18	318.9	22	219.3
3	0	7	312.1	11	202.5	15	307.5	19	307.8	23	184.0
4	313.7	8	300.5	12	313.2	16	304.7	20	305.0		
Run No. 21 Opening - 16.00 ft Head - 373 ft											
1	0	5	424.6	9	358.9	13	428.4	17	0	21	423.0
2	0	6	418.8	10	343.4	14	433.3	18	435.0	22	327.7
3	0	7	429.0	11	281.1	15	431.0	19	427.5	23	257.3
4	429.2	8	420.9	12	428.3	16	425.5	20	422.5		
Run No. 22 Opening - 20.10 ft Head - 129 ft											
1	0	5	173.9	9	171.9	13	169.5	17	0	21	163.7
2	0	6	173.0	10	170.5	14	176.2	18	174.5	22	147.7
3	0	7	167.0	11	155.9	15	164.9	19	177.1	23	127.1
4	175.5	8	166.3	12	177.7	16	174.5	20	165.2		
Run No. 23 Opening - 20.10 ft Head - 281 ft											
1	0	5	358.3	9	368.4	13	350.8	17	0	21	334.0
2	0	6	332.8	10	343.0	14	362.8	18	367.2	22	289.0
3	0	7	345.0	11	305.1	15	342.6	19	359.9	23	252.2
4	363.5	8	353.7	12	365.3	16	355.7	20	340.3		
Run No. 27 Opening - 3.92 ft Head - 421 ft											
1	435.4	5	419.0	9	397.2	13	394.2	17	434.6	21	388.4
2	434.4	6	400.7	10	287.8	14	429.5	18	429.7	22	277.2
3	436.5	7	392.6	11	254.6	15	391.8	19	417.8	23	241.3
4	431.3	8	385.6	12	431.3	16	392.9	20	388.7		
Run No. 28 Opening - 3.92 ft Head - 266 ft											
1	281.1	5	269.7	9	253.0	13	254.3	17	280.6	21	249.2
2	280.2	6	258.8	10	185.3	14	276.6	18	276.7	22	178.1
3	280.5	7	253.3	11	163.5	15	251.8	19	268.1	23	155.5
4	276.4	8	247.8	12	277.1	16	250.9	20	250.2		

TABLE A-3. PRESSURE HEADS AT THE WALL

Piezo. No.	Pressure Head feet	Standard Deviation feet	Piezo. No.	Pressure Head feet	Standard Deviation feet	Piezo. Nc.	Pressure Head feet	Standard Deviation feet
Gate Opening - 4.10 ft Head - 150 ft								
12	12.5	3.2	23	43.8	12.0	32	41.6	10.8
14	19.6	6.4	24	28.3	7.8	33	16.0	11.2
16	12.8	5.1	25	9.1	9.2	34	18.1	10.1
18	1.2	1.9	26	4.5	3.4	35	0	1.1
19	13.0	2.9	28	16.4	2.3			
21	19.9	4.0	30	42.0	8.7			
Gate Opening - 4.10 ft Head - 275 ft								
16	16.5	10.6	23	73.0	19.6	26	8.4	5.6
17	25.4	8.2	24	56.0	9.8	32	80.2	13.6
18	3.3	3.7	25	29.8	16.0	34	43.6	16.3
Gate Opening - 4.10 ft Head - 450 ft								
12	34.8	9.4	23	110.0	28.3	30	102.0	20.0
14	51.3	22.6	24	83.0	12.0	32	121.0	19.9
16	34.4	12.0	25	51.9	25.9	33	71.8	30.4
18	5.4	6.5	26	17.0	12.9	34	81.6	32.0
19	36.8	6.4	27	38.8	4.7	35	0	
21	54.1	11.9	28	43.4	6.4			
Gate Opening - 8.25 ft Head - 150 ft								
7	19.1	2.1	18	3.2	1.6	30	49.6	4.2
9	15.5	2.8	19	20.2	2.0	32	85.9	20.9
11	26.8	3.4	21	31.8	3.1	33	72.2	28.7
12	18.2	1.7	23	63.8	8.2	34	90.5	16.0
14	31.2	2.0	25	47.1	10.9	35	3.7	5.6
16	50.4	5.2	26	13.2	10.1	36	-1.8	2.2
Gate Opening - 8.25 ft Head - 275 ft								
11	40.0	4.7	22	68.6	8.8	26	16.4	14.7
16	94.2	9.0	24	105.0	17.7			
18	4.2	1.8	25	70.7	19.2			
Gate Opening - 8.25 ft Head - 400 ft								
7	37.0	4.1	19	39.2	*	30	116.0	10.8
8	44.6	*	21	65.7	*	31	17.8	*
9	56.4	*	23	143.0	17.9	32	183.0	47.3
10	56.0	*	24	139.0	*	33	160.0	*
11	56.0	6.4	25	95.6	28.8	34	69.1	42.6
12	33.4	*	26	23.4	*	35	-6.6	5.3
14	66.8	*	27	39.4	*	36	9.0	*
16	97.5	*	28	51.0	*			
18	6.1	2.6	29	73.2	*			
Gate Opening - 12.25 ft Head - 150 ft								
1	16.0	2.3	15	54.2	*	27	28.3	*
3	22.4	3.0	16	63.8	*	28	34.1	*
5	25.6	*	17	44.6	*	29	44.7	*
6	16.8	*	18	10.3	*	30	52.1	*
7	18.3	*	19	28.2	*	31	92.8	*
8	24.2	*	20	28.2	*	32	116.0	*
9	30.4	*	21	42.0	*	33	51.2	*
10	35.2	*	22	55.1	*	34	93.4	*
11	39.8	*	23	78.5	*	35	2.8	*
12	25.9	*	24	95.6	*	36	0.1	2.06
13	30.7	*	25	63.5	*			
14	41.1	*	26	65.7	*			

*Standard deviation not calculated because mean digital voltmeter readings only were recorded.

TABLE A-3. PRESSURE HEADS AT THE WALL - continued

Piezo. No.	Pressure Head feet	Standard Deviation feet	Piezo. No.	Pressure Head feet	Standard Deviation feet	Piezo. No.	Pressure Head feet	Standard Deviation feet
Gate Opening - 12.25 ft Head - 275 ft								
1	23.1	*	15	80.5	*	27	44.3	*
3	31.6	*	16	101.0	*	28	54.5	*
5	38.2	*	17	48.2	*	29	72.7	*
6	24.4	*	18	22.9	*	30	105.5	*
7	29.4	*	19	43.8	*	31	169.4	*
8	40.2	*	20	53.4	*	32	172.0	*
9	49.5	*	21	69.3	*	33	85.5	*
10	57.0	*	22	94.1	*	34	18.4	*
11	63.3	*	23	135.1	*	35	3.0	*
12	54.5	*	24	144.5	*	36	-2.7	*
13	45.8	*	25	80.6	*			
14	60.4	*	26	95.4	*			
Gate Opening - 12.35 ft Head - 380 ft								
1	28.8	3.1	16	117.1	18.1	24	176.0	30.6
3	40.8	3.3	17	56.6	27.5	25	133.9	33.8
5	59.1	5.0	18	20.3	24.9	26	138.8	30.1
7	46.1	4.0	19	54.5	5.0	28	71.7	6.2
9	71.5	5.7	20	66.2	4.7	30	135.0	19.3
11	96.9	14.5	21	84.0	8.4	32	213.0	50.3
12	27.0	4.2	22	112.0	15.4	33	155.7	54.2
14	86.0	8.4	23	151.0	29.5	34	213.0	45.2
Gate Fully Open Head - 40 ft								
1	9.5	*	13	8.3	*	23	2.0	*
3	0.0	*	14	4.4	*	25	0.1	*
5	1.2	*	15	1.7	*	26	1.8	*
6	16.3	*	16	0.7	*	27	44.9	*
7	7.9	*	17	0.0	*	29	9.4	*
8	3.5	*	18	0.2	*	31	2.3	*
9	1.6	*	19	45.2	*	33	1.3	*
10	1.2	*	20	28.4	*	34	2.4	*
11	0.4	*	21	11.5	*	35	1.9	*
12	27.2	*	22	3.7	*	36	0.8	*

*Standard deviation not calculated because mean digital voltmeter readings only were recorded.